**UNIVERSIDADE DE LISBOA**

**FACULDADE DE FARMÁCIA**

# Development of a small library of bioactive compounds through isolation and molecular derivatization

João Nuno da Silva Gomes

Dissertação orientada pela Professora Doutora Maria José Umbelino Ferreira e coorientada pela Professora Doutora Noélia Maria da Silva Dias Duarte

**Mestrado em Química Farmacêutica e Terapêutica**

**Lisboa**

**2017**

**UNIVERSIDADE DE LISBOA**

**FACULDADE DE FARMÁCIA**

# Development of a small library of bioactive compounds through isolation and molecular derivatization

João Nuno da Silva Gomes

Dissertação orientada pela Professora Doutora Maria José Umbelino Ferreira e coorientada pela Professora Doutora Noélia Maria da Silva Dias Duarte

**Mestrado em Química Farmacêutica e Terapêutica**

**Lisboa**

**2017**

The studies presented in this dissertation were carried out at the Natural Products Chemistry Group of the Institute for Medicines and Pharmaceutical Sciences (iMed.ULisboa), Faculdade de Farmácia da Universidade de Lisboa. The Project was financed by Fundação pela Ciência e Tecnologia (FCT), Portugal (Projects: PTDC/QEQ-MED/0905/2012, UID/DTP/04138/2013.

# Abstract

The present dissertation focuses on the phytochemical study of *Euphorbia boetica* Boiss. and *Euphorbia pubescens* Vahl (Euphorbiaceae) aerial parts in an attempt to find effective modulators for P-glycoprotein (P-gp) mediated multidrug resistance (MDR) in tumour cells.

The methanol extracts of both plants were fractioned by chromatographic techniques such as column chromatography, preparative thin layer chromatography and high-performance liquid chromatography (HPLC). From the methanol extract of *E. boetica*, one new premyrsinane-type diterpene with the unusual 5:7:6:3 fused ring system and a new acylation pattern, named euphomyrsinane A, two new tigliane-type diterpenes with new acylation patterns, named phorboboetirane A and phorboboetirane B along with four known macrocyclic diterpenes, premyrsinol-3-propanoate-5-benzoate-7,13,17-triacetate, euphoboetirane A, epoxyboetirane A and epoxyboetirane K were isolated. A known triterpene with the cycloartane skeleton, 24-methylenecycloartanol, and a phenolic compound, methyl gallate were also isolated. From the methanol extracts of *E. pubescens*, were obtained a known macrocyclic diterpene, euphopubescenol, and a known diterpenic lactone, helioscopinolide A.

Due to its biological activity and simple structure paired with the fact that it was isolated in large amounts, methyl gallate was derivatized, aiming at generating a small set of bioactive derivatives. In this way, taking into account that lipophilicity and the presence of nitrogen atoms are described to improve the ability to reverse MDR, three main steps were considered: i) methylation of the hydroxyl groups on the aromatic ring by reaction with dimethylsulfate, yielding methyl 3,4,5-trimethoxebenzoate; ii) reaction of methyl 3,4,5-trimethoxybenzoate with hydrazine yielding 3,4,5-trimethoxybenzohydrazide; iii) condensation of 3,4,5-trimethoxybenzohydrazide with aromatic aldehydes to obtain three derivatives bearing an imine moiety.

The chemical structures of the compounds were deduced from their physical and spectroscopic data, which included infrared spectroscopy, mass spectrometry and extensive one- ($^{1}$H-NMR, $^{13}$C-NMR, DEPT) and two-dimensional ($^{1}$H-$^{1}$H-COSY, HMQC, HMBC, and NOESY) Nuclear Magnetic Resonance studies and by comparison with literature data.

**Keywords:** *Euphorbia boetica, Euphorbia pubescens,* macrocyclic diterpenes, lathyrane, multidrug resistance, P-glycoprotein.

# Resumo

A presente dissertação descreve o estudo fitoquímico de algumas frações dos extratos metanólicos das partes aéreas da *Euphorbia boetica* Boiss. e *Euphorbia pubescens* Vahl (Euphorbiaceae) com o intuito de encontrar moduladores eficientes na multirresistência farmacológica mediada pela glicoproteína-P, em células tumorais.

O fracionamento dos extratos metanólicos foi realizado através de varias técnicas, nomeadamente cromatografia em coluna, cromatografia preparativa em camada fina e cromatografia líquida de alta eficiência (HPLC). Do extrato metanólico da *E. boetica*, foram isolados e caracterizados um novo diterpeno com o esqueleto do premirsinano apresentando um sistema de anéis 5:7:6:3 fundidos, com um novo rearranjo e um novo padrão de acilação, nomeado euphomyrsinane A e dois diterpenos com o esqueleto do tigliano com novos padrões de acilação, designados phorboboetirane A e phorboboetirane B. Foram ainda isolados: quatro diterpenos macrocíclicos já conhecidos, premirsinol-3-propanoato-5-benzoato-7,13,17-triacetato, eufoboetirano A, epoxiboetirano A e epoxiboetirano K; um triterpeno conhecido com o esqueleto do cicloartano, 24-metilenocicloartanol; e um composto fenólico, o galhato de metilo. Dos extratos metanólicos da *E. pubescens*, foram isolados e identificados um diterpeno macrocíclico conhecido, euphopubescenol, e uma lactona diterpénica conhecida, helioscopinolido A.

Dada a sua atividade biológica e estrutura simples, associado ao facto de ter sido isolado em grande quantidade, o galhato de metilo foi derivatizado, com o objetivo de criar um pequeno conjunto de derivados bioativos. Desta forma, e tendo em conta que a lipofilia e presença de átomos de azoto aumentam as propriedades moduladoras dos compostos, foram considerados três passos: i) metilação dos grupos hidroxilo do anel benzénico através de reação com dimetilsulfato, obtendo 3,4,5-trimetoxibenzoato de metilo; ii) reação do 3,4,5-trimetoxibenzoato de metilo com hidrazina para obter a 3,4,5-trimetoxibenzo-hidrazida; iii) condensação da 3,4,5-trimetoxibenzo-hidrazida com aldeídos aromáticos para obter derivados com a função imina.

A estrutura química de todos os compostos foi deduzida com base as suas características físicas e espetroscópicas, incluindo espetroscopia de infravermelho (IV), espetrometria de massa, RMN unidimensional ($^{1}$H-RMN, $^{13}$C-RMN, DEPT) e bidimensional ($^{1}$H-$^{1}$H-COSY, HMQC, HMBC e NOESY), e comparação com a literatura.

**Palavras-Chave:** *Euphorbia boetica*, *Euphorbia pubescens*, diterpenos macrocíclicos, latiranos, multirresistência, glicoproteína-P.

# Acknowledgments

First of all, I would like to express my sincerest gratitude to Professor Maria José Umbelino for her constant scientific guidance and support and for always believing in me and for keeping me motivated along the way.

I would also like to express my deepest gratitude to Professor Noélia Duarte, not only for her scientific guidance, patience while teaching and supervising all my work, but also for her friendliness, geniality and encouragement that got me through to the end, even during the toughest moments.

I would also like to thank Ricardo Ferreira, a PhD student turned Professor during the elaboration of this dissertation, for his kindness and companionship and, oft-times, invaluable help during laboratory work.

I would also like to thank Professor Rita Capela for her invaluable support and encouragement along the way.

I sincerely acknowledge Fundação para a Ciência e Tecnologia for financing this project.

I would like to thank my laboratory partners for all their help, support and for always keeping a good working environment.

My extended thanks go to Professor Ana Paula Francisco, Professor Emilia Valente, Professor Maria de Jesus Perry and Professor Ana Margarida Madureira, not only for all their help, support and encouragement, but also for the knowledge they imparted on me during all my work.

I would like to take this opportunity to show my appreciation to my friends and colleagues, especially Luis Sobral, Pedro Gonçalves and Claudia Braga for their companionship and supportive and understanding demeanours.

I am deeply grateful to my parents, Maria João and José Luis, for their unconditional love, friendship, support and patience, for being my role models and for always encouraging me to go further. I will never forget the sacrifices both had to make in order to provide me the education and greatest opportunities I had in life.

I want to thank my brother, Pedro, who I truly love and cherish, for all his help and support whenever I needed the most.

I am deeply grateful to my grandparents, especially my grandmother, Maria Antonieta, for a lifetime of love, support, patience and sacrifice.

I would also like to show my deepest and sincerest appreciation to my friend and colleague Cristina Silva who, despite our love-hate relationship, has been one of my strongest pillar throughout this whole ordeal by patiently listening and supporting me in some of my darkest moments and for the great moments we spent inside and outside the laboratory.

To all my friends and family, named and unnamed here, my deepest thanks. Without you, I would never have finished this long and arduous task.

# Table of Contents

Chapter III
*Experimental Section*



Chapter IV

# Tables Index

# Schemes index

# Figures index

# Abbreviations and Symbols

| | |
|---|---|
| $[M]^+$ | Molecular ion |
| $^{13}$C-NMR | $^{13}$C Nuclear Magnetic Resonance |
| $^{1}$H-NMR | $^{1}$H Nuclear Magnetic Resonance |
| 2,3-dMB | 2,3-diMethylButane |
| ABC | ATP Binding Cassette |
| Ac | Acetyl |
| Acetyl-CoA | Acetyl-Coenzyme A |
| ADP | Adenosine DiPhosphate |
| ATP | Adenosine TriPhosphate |
| BCRP | Breast Cancer Resistance Protein |
| br s | broad singlet |
| Bz | Benzoyl |
| CC | Column Chromatography |
| $CDCl_3$ | Deuterated chloroform |
| CDP-ME | 4-diphosphocytidyl-2C-methyl-D-erythritol |
| COSY | Correlation SpectroscopY |
| CTP | Cytosine TriPhosphate |
| d | doublet |
| dd | Doublet of Doublet |
| ddd | Doublet of Doublet of Doublet |
| DEPT | Distortionless Enhancement by Polarization Transfer |
| DMAPP | DiMethylAllyl diPhosphate |
| DMSO-$d_6$ | Deuterated DiMethylSulfOxide |
| $DMSO_4$ | Dimethyl Sulphate |
| dt | Doublet of Triplets |
| DXP | Deoxy Xylulose Phosphate Pathway |
| ESI-MS | ElectroSpray Ionization Mass Spectrometry |
| EtOAc | Ethyl Acetate |
| FDP | Farnesyl DiPhosphate |
| GC-MS | Gas Chromatography Mass Spectrometry |
| GDP | Geranyl DiPhosphate |
| GGDP | Geranyl Geranyl DiPhosphate |

| | |
|---|---|
| HIV | Human Immunodeficiency Virus |
| HMBC | Heteronuclear Multiple Bond Correlation |
| HMQC | Heteronuclear Multiple-Quantum Correlation |
| HPLC | High Performance Liquid Chromatography |
| HTS | High Throughput Screening |
| iBu | isoButanoyl |
| IPP | IsoPentenyl diPhosphate |
| IR | InfraRed |
| *ispC* | 1-deoxy-D-xylulose-5-phosphate reductoisomerase |
| *ispD* | 4-diphosphocytidyl-2-C-methyl-Derythritol synthase |
| *ispE* | 4-diphosphocytidyl-2-C-methyl-D-erythritol kinase |
| *ispF* | 2-C-methyl-D-erythritol 2,4-cyclodiphosphate synthase |
| *ispG* | 4-hydroxy-3-methylbut-2-enyl diphosphate synthase |
| *ispH* | 4-hydroxy-3-methylbut-2-enyl diphosphate reductase |
| *J* | Coupling constant |
| $^{2}J_{C\text{-}H}$ | C-H coupling through two bonds (geminal coupling) |
| $^{3}J_{C\text{-}H}$ | C-H coupling through three bonds (vicinal coupling) |
| LC-MS | Liquid Chromatography-Mass Spectrometry |
| m | multiplet |
| m.p. | melting point |
| *m/z* | ratio of mass to charge |
| MDR | MultiDrug Resistance |
| Me | methyl |
| $MeOD_4$ | Deuterated methanol |
| MeOH | Methanol |
| MEP | MethylErythritol Phosphate Pathway |
| NMR | Nuclear Magnetic Resonance |
| NOE | Nuclear Overhauser Effect |
| NOESY | Nuclear Overhauser Enhancement Spectroscopy |
| NPP | Neryl DiPhosphate |
| P-gp | P-glycoprotein |
| Ppm | parts per million |
| Pr | Propyl |

| | |
|---|---|
| q | quadruplet |
| s | singlet |
| SAR | Structure Activity Relationship |
| t | Triplet |
| TLC | Thin Layer Chromatography |
| TMD | Transmembrane Domain |
| UV | UltraViolet |
| WHO | World Health Organization |
| δ | Chemical Shift |
| $\delta_C$ | Carbon chemical shift |
| $\delta_H$ | Proton chemical shift |
| $\nu_{max}$ | Maximum wave number |

# Chapter I

## Introduction

# 1. GENERAL CONSIDERATIONS

Since ancient times, plants have been at the core of human healthcare and are the main source for chemically active compounds for numerous purposes, including therapeutic agents [1]. Documents like the Ayurveda (Indian Traditional Medicine), which can be traced back to around 5000 BC, introduced some medicinal properties of plants and other natural products. Although the mechanisms by which the plants and other natural products were effective at treating the illnesses were unknown, nowadays, modern developments in areas such as chemistry, spectroscopic techniques, and High Throughput Screening (HTS) coupled with modern hyphenated techniques (e.g. GC-MS, LC-MS) made it easier to isolate and study the bioactivity of purified natural products [1-3].

Usually, the term natural product is used to refer to secondary metabolites produced by any living organism to enhance their survivability. These secondary metabolites are biosynthesized in a particular chiral form to exhibit biological activity in *in vitro* and *in vivo* test systems, helping major pharmaceutical companies by providing lead compound structures [2].

## 1.1. *Euphorbia* L. Genus – General considerations

The Euphorbiaceae family consists of around 300 genera and over 7000 species and is considered one of the largest families of flowering plants. Commonly known as "spurge" for the purgative properties of its latex [4], the *Euphorbia* genus is widely distributed worldwide, consisting approximately of 2160 species, subdivided into many subgenera and sections [5]. Plants from this genus are characterized by a wide range of annual or perennial herbs, woody shrubs, trees and succulent plants, all possessing a flower-like inflorescence and often containing a toxic milky latex [1, 6]. The name *Euphorbia* came to be in honour of Euphorbius, King Juba II of Mauretania's physician, who is supposed to have used the milky latex from *Euphorbia resinifera* as a remedy [7].

Widely used in traditional medicines, *Euphorbia* species are known to treat several diseases such as skin ulcers, tumours and intestinal parasites [8]. In the Chinese pharmacopoeias, five species of *Euphorbia*, namely *E. pekinensis*, *E. kansui*, *E. lathyris*, *E.*

*humifusa* and *E. maculata* are recommended for the treatment of oedema, gonorrhoea, migraines and warts, even though they are known to be extremely poisonous [5, 9].

Despite its traditional applications, the aforementioned toxic latex, causes extremely painful inflammations when in contact with mucous membranes and has hindered further uses of *Euphorbias* as medicines. This milky latex is rich in many diterpenes, triterpenes, sesquiterpenes and steroids, and its toxicity is attributed to the polycyclic diterpenoids with the ingenane, tigliane and daphnane scaffolds, also known as phorboids, compounds which are exclusive to the Euphorbiaceae and Thymelaeaceae families [8].

Nevertheless, *Euphorbia species* have been heavily studied and a high diversity of compounds have been isolated, many of them exhibiting important biological activities, such as anti-tumour, anti-malarial, cytotoxic, anti-microbial and anti-oxidant activities [9-12]. Particularly, they have afforded a large number of macrocyclic diterpenes possessing the structurally-unique lathyrane and jatrophane skeletons. These compounds share the existence of a very flexible macrocyclic ring and the presence of several acylating groups, which make them promising modulators for multidrug resistance in tumour cells [13, 14].

Apart from their medicinal purposes, several *Euphorbia* species have also shown great economic importance. Some of them are used as decorative pieces for their bright coloured leaves and flowers. Species like *E. pulcherrima* Willdt, commonly known as poinsettia, and *E. milli* or Christ's thorn, which are cultivated and used as decoration during Christmas time, and *E. resinifera* which is a popular house plant in European countries [7].

## 1.2. *Euphorbia boetica* and *Euphorbia pubescens*

*Euphorbia boetica* Boiss. and *Euphorbia pubescens* Vahl are the two species studied in this work. *Euphorbia boetica* is an herb endemic to Europe and widespread in the southern regions of Portugal [15]. It usually grows in pine woods or on acid soils at a very low altitude (0-100 meters) and flowering usually occurs in early spring. It is noteworthy that this species is considered endangered in some areas [16].

*Euphorbia pubescens* Vahl, also known as *Euphorbia hirsuta* L. (Figure 1) or by its common names hairy spurge or ésula-lanosa, is an herb endemic to the Mediterranean regions usually growing near river banks and streams and found at altitudes up to 1500 meters [17, 18].

The shrub grows between 30 to 60 cm high and its leaves are covered with small hairs on the upper side of the leaf or both sides. The flowering occurs between march and august [19].

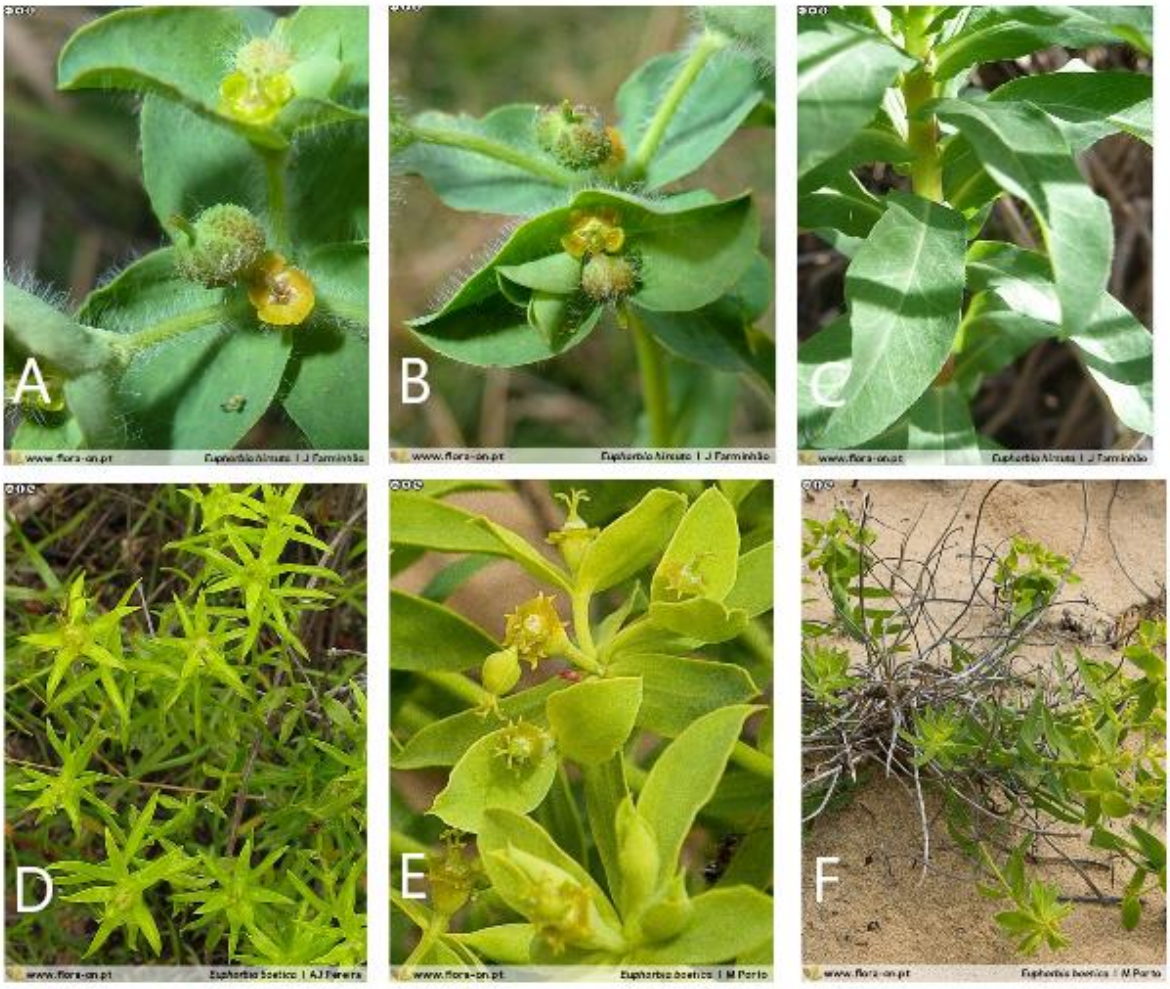


**Figure 1** Aerial parts from *E. pubescens* (A, B, C) and *E. boetica* (D, E, F). Adapted from http://flora-on.pt/index.php#/1euphorbia

## 1.3. Terpenoids: biogenetic considerations

Terpenoids are one of the most diverse family of natural compounds, widely distributed in nature and abundantly in higher plants, with a structural diversity associated with more than 40.000 compounds. Plant terpenoids could be classified as primary metabolites, necessary for cellular function like carotenoids and sterols (photoprotection and membrane permeability, respectively), and secondary metabolites, not involved in growth and development functions, but some of them often commercially attractive as flavour and colour enhancers, agricultural chemicals and medicine [20, 21]. Structurally, terpenoids derive from the branched $C_5$ carbon skeleton of isoprene which, depending on the number of isoprene motifs, cyclization reactions, rearrangement and further oxidation of the carbon skeleton, enables the enormous diversity of

structures. Therefore, terpenoids are classified as monoterpenes ($C_{10}$), sesquiterpenes ($C_{15}$), diterpenes ($C_{20}$), sesterterpenes ($C_{25}$) and triterpenes ($C_{30}$) [21-23].

The biosynthetic pathway for terpenoids can be divided into two main stages:

a) The first stage consists on the synthesis of isopentenyl diphosphate (IPP) and its isomer, dimethylallyl diphosphate (DMAPP) (Scheme 1);
b) In the second stage, IPP and DMAPP are used by prenyltransferases in head-to-tail condensation reactions to produce geranyl diphosphate (GDP), farnesyl diphosphate (FDP) and geranyl geranyl diphosphate (GGDP), the parent skeletons for each class (Scheme 2). Thus, GDP gives rise to monoterpenes, FDP to sesquiterpenes and GGDP to diterpenes [22, 24].

Higher order of terpenoids like triterpenes, derive from squalene ($C_{30}$). Squalene contains six isoprene units, as a result of tail-to-tail condensation of two FDP molecules. After the formation of GDP, FDP and GGDP, terpene synthases act to generate the different carbon skeletons, which in turn can suffer additional transformations such as oxidations, reductions, isomerizations and conjugations, producing countless different terpenoid metabolites [23].

As can be seen in Scheme 2, IPP and its allylic isomer DMAPP are the universal precursors and central intermediates for the biosynthesis of all terpenoids. IPP and DMAPP can be synthesized by two distinct pathways: the mevalonate (MVA) pathway and the methylerythritol phosphate (MEP) pathway (Scheme 1).

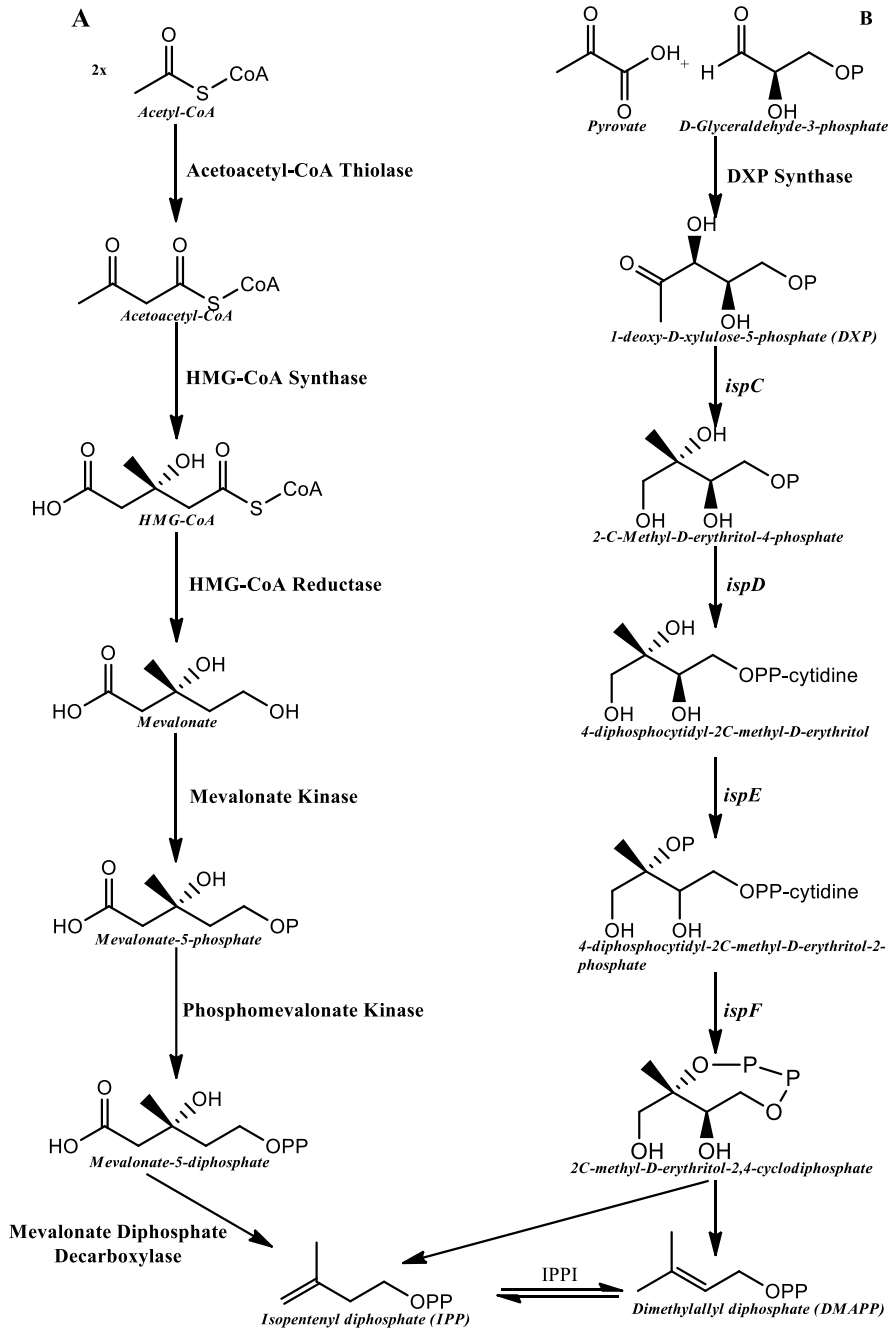


**Scheme 1** Biosynthesis of isopentenyl diphosphate (IPP) and dimethylallyl diphosphate (DMAPP) by the mevalonate (MVA) pathway (mammals and plants) (A) and MEP pathway (bacteria and protozoa) (B). Adapted from [25-28].

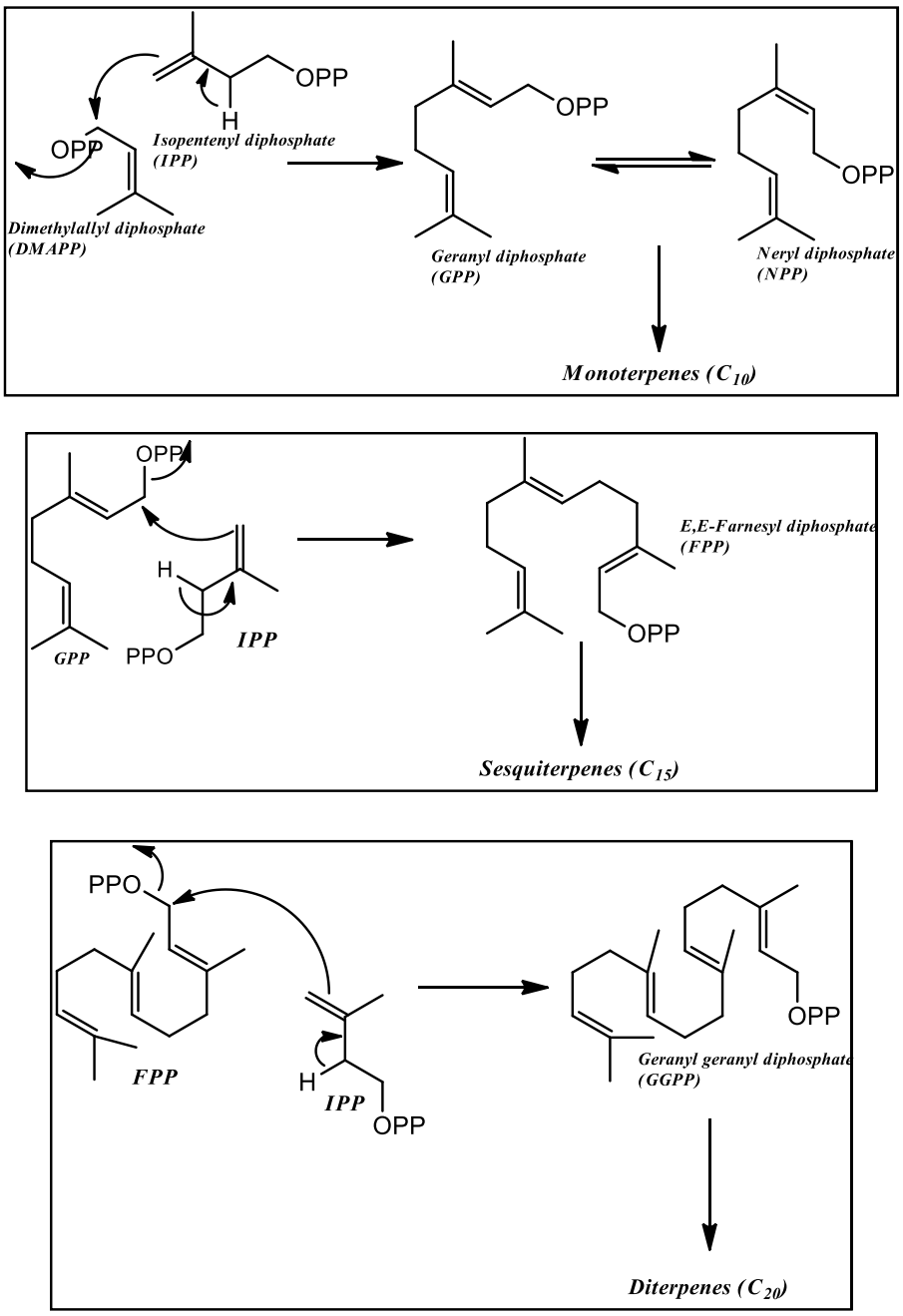


**Scheme 2** Suggested pathways for the biosynthesis of monoterpenes, sesquiterpenes and diterpenes. Adapted from [20].

### 1.3.1. The mevalonate pathway

Discovered in the 1950s in yeasts and animals, the mevalonate pathway was thought to be the sole source of IPP and DMAPP in all living organisms. Synthesized from two molecules of acetyl-CoA, mevalonic acid (branched chain $C_6$-skeleton) undergoes phosphorylation to mevalonate-5-phosphate, followed by further phosphorylation and decarboxylation to form the essential $C_5$-intermediates isopentenyl diphosphate (IPP) and its isomer dimethylallyl diphosphate (DMAPP). Later on, due to inconsistencies with this route, namely the absence from most bacteria, several experimental results showed that MVA pathway was much less prominent in secondary metabolism than the mevalonate-independent pathway *via* methylerythritol phosphate, also known as MEP pathway [27, 28].

### 1.3.2. The mevalonate-independent pathway *via* methylerythritol phosphate

Known by several terminologies, including mevalonate-independent pathway, non-mevalonate pathway, glyceraldehyde-3-phosphate/pyruvate pathway, deoxy xylulose phosphate pathway (DXP) or methylerythritol phosphate (MEP) pathway, this pathway was discovered in the 1990s, due to some experiments done in bacteria, protozoa, and plants [26, 27]. These experiments showed a considerably higher production of IPP and DMAPP in these organisms through the condensation of pyruvate and D-glyceraldehyde-3-phosphate by DXP synthase, mainly due to the lack of some of the enzymes necessary for the classic MVA pathway [28].

The first step in the MEP pathway is the formation of 1-deoxy-D-xylulose-3-phosphate (DXP) by the condensation of pyruvate and D-glyceraldehyde-3-phosphate, catalysed by DXP synthase (Scheme 1). Later on, DXP is converted to MEP through an α-ketol rearrangement and a reduction, catalysed by 1-deoxy-D-xylulose-5-phosphate reductoisomerase (*ispC*). MEP is then conjugated with CTP producing 4-diphosphocytidyl-2C-methyl-D-erythritol (CDP-ME), a reaction that is catalysed by the *ispD*. CDP-ME is then phosphorylated by *ispE*, affording 4-diphosphocytidyl-2C-methyl-D-erythritol-2-phosphate. This molecule is then converted into 2C-methyl-D-erythritol-2,4-cyclodiphosphate under release of CMP, catalysed by *ispF*. The conversion of 2C-methyl-D-erythritol-2,4-cyclodiphosphate into IPP and DMAPP is still uncertain, although it is known to be catalysed by two enzymes, *ispG* and *ispH* in *E. coli* and other microorganisms. These catalyse two reduction reactions into 1-hydroxy-2-

methyl-2(E)-butenyl-4-diphosphate (not shown) and finally IPP and DMAPP [26, 27]. In higher plants, both MVA and MEP pathways are present. In this way, the enzymes necessary for the mevalonate pathway are localized in the cytosol, providing cytosolic metabolites, particularly triterpenoids, steroids and some sesquiterpenoids. The MEP pathway, whose enzymes are located in the plastid organelles, supply plastid-related metabolites such as monoterpenes, diterpenes and tetraterpenoids (carotenoids), prenyl-side chains of chlorophylls and plastoquinones. These examples provide evidence of the cooperation between the cytosolic and plastidial pathways, especially in the biosynthesis of stress-related metabolites [20, 21, 26-28].

## 1.4. Literature Review

### 1.4.1. Diterpenoids

Diterpenoids constitute a vast class of isoprenoid natural products (over 12000 natural products) [29] derived from geranylgeranyl diphosphate (GGPP, Scheme 2). They can be found mainly in plants and fungi and, to a lesser extent, in marine organisms and insects. Depending on their skeletal type (cyclization patterns), diterpenoids can be divided into different classes, such as acyclic, bicyclic, tricyclic, tetracyclic or macrocyclic diterpenes [30].

#### *1.4.1.1. Diterpenoids isolated from Euphorbia sp.*

In this section, a literature review regarding new diterpenes isolated from *Euphorbia genus* is presented, covering works between 2013 and 2017. In Tables 1-3, new lathyrane and jatrophane skeletons and their polycyclic derivatives (tigliane, myrsinane and ingenane) are presented as well as their biological activities.

**Table 1** New diterpenes with lathyrane, jatrophane and myrsinane skeletons isolated from *Euphorbia* sp. (isolated between 2013 and 2017).

| Plant | Analysed part | Diterpene Skeleton | Biological activity | Structure number | Reference |
|---|---|---|---|---|---|
| ***E. aellenii*** | Aerial parts | Myrsinane | Immunomodulatory activity | **1,2** | [31] |
| ***E. microsciadia*** | Aerial parts | Myrsinane | Anti-angiogenic activity (**3**) | **3,4** | [32] |
| ***E. altotibetica*** | Whole plant | Lathyrane | Cytotoxic activity | **5** | [33] |
| ***E. lunulata*** | Whole plant | Jatrophane | Anti-proliferative activity against cancer cell lines | **6** | [34] |
| | | *Ent*-abietane diterpenic lactone | | **7** | |
| ***E. micractina*** | Roots | Minor diterpenoid | HIV-1 replication inhibitor | **8** | [35] |
| ***E. dracunculoides*** | Aerial parts | Lathyrane | - | **9** | [36] |
| ***E. connata*** | Flowering parts | Myrsinane | Cytotoxic (Inhibitory) activity in human breast cancer | **10** | [37] |
| | | Jatrophane | | **11** | |
| ***E. guyoniana*** | Aerial parts | Jatrophane | Atrial GIRK channels inhibitors | **12,13** | [38] |
| ***E. cyparissias*** | Whole plant | Jatrophane | P-gp inhibitors in ovarian cancer | **14,15** | [39] |
| ***E. stracheyi*** | Whole plant | *Ent*-kaurane | - | **16** | [40] |
| ***E. ebracteolata*** | Roots | Rosane | Cytotoxic activity in various cancer cell lines | **17,18** | [41] |
| | | Lathyrane | | **19** | |
| ***E. kansui*** | Roots | Euphorikanane (proposed named) | Cytotoxic activity in two human cancer cell lines | **20** | [42] |
| ***E. macrorrhiza*** | Whole plant | Jatropholane | Cytotoxic activity and some MDR (P-gp) reversal activity (**25-28**) | **21** | [43] |
| | | | | **22** | |
| | | Premyrsinane | | **23** | |
| | | Lathyrane | | **24** | |
| | | | | **25 (P-gp)** | |
| | | Lathyrane | | **26-27** | |
| | | Casbene | | **28-29** | |
| | | | | **30** | |
| ***E. fischeriana*** | Roots | *Ent*-atisane | Inhibitory activity in human breast cancer cell lines | **31,32** | [44] |

**Table 2** (continuation) New diterpenes with lathyrane, jatrophane and myrsinane skeletons isolated from *Euphorbia* sp. (isolated between 2013 and 2017).

| Plant | Analysed part | Diterpene Skeleton | Biological activity | Structure number | Reference |
|---|---|---|---|---|---|
| ***E. welwitschii*** | Roots | Jatrophane | - | **33,34** | [45] |
| | | Jatrophane | Antiproliferative selectivity in resistant gastric cell lines (**35** and **36**) and MDR-selective antiproliferative effect (**36**) | **35** | |
| | | | | **36** | |
| ***E. osyridea*** | Aerial parts | Jatrophane | Cytotoxicity in ovarian cancer cell lines | **37-39** | [46] |
| ***E. bupleuroides*** | Roots | Tigliane | - | **40** | [47] |
| ***E. squamosa*** | Aerial parts | Jatrophane | ABC-transporter *Ca*Cdr1p inhibitors (increased sensitivity to antifungals drugs) | **41-43** | [48] |
| ***E. piscatoria*** | Aerial parts | *Ent*-abietane | Antiproliferative activity | **44,45** | [49] |
| | | Lathyrane | | **46,47** | |
| ***E. nematocypha*** | Roots | Myrsinane | - | **48** | [50] |
| ***E. boetica*** | Aerial parts | Lathyrane | MDR reversal activity in lymphoma cells | **49,50** | [13] |
| ***E. stracheyi*** | Whole plant | Tigliane | - | **51** | [51] |
| | | Ingenane | | **52** | |
| | | *Ent*-abietane | | **53** | |
| ***E. amygdaloides ssp. semiperfoliata*** | Whole plant | Jatrophane | Viral replication inhibitors of CHIKV and HIV-1 and HIV-2 | **54-59** | [52] |
| ***E. helioscopia*** | Whole plant | Jatrophane | Inhibition of LPS-induced NO production in microglial cells | **60-63** | [53] |

**Table 3** (continuation) New diterpenes with lathyrane, jatrophane and myrsinane skeletons isolated from *Euphorbia* sp. (isolated between 2013 and 2017).

| Plant | Analysed part | Diterpene Skeleton | Biological activity | Structure number | Reference |
|---|---|---|---|---|---|
| ***E. erythradenia*** | Flowering parts | Ingenane | Cell proliferation inhibition through apoptosis | **64-67** | [54] |
| | | Myrsinane | - | **68** | |
| ***E. kansuensis*** | Roots | Lathyrane | Cytotoxicity against Hep-G2 and HeLa cells | **69,70** | [55] |
| ***E. prolifera*** | Roots | Myrsinane | - | **71-74** | [56] |
| ***E. sikkimensis*** | Aerial parts | Jatrophane | Anti-angiogenic activity | **75-78** | [57] |
| ***E. kopetdaghi Prokh*** | Aerial parts | Myrsinane | Immunomodulatory activities (**79**) | **79-81** | [58] |
| ***E. pseudocactus*** | Whole plant | Abietane | - | **82-84** | [59] |
| ***E. micractina*** | Roots | Lathyrane | - | **85-96** | [60] |
| ***E. antiquorum*** | Aerial parts | Ingol | Mouse 11β-HSD1 inhibitory activity (**97** and **110**) | **97-114** | [61] |

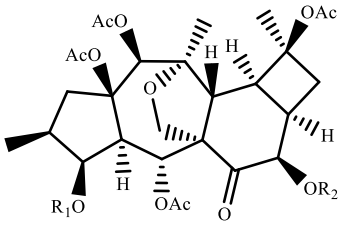

**1** $R_1$ = Nicotinyl, $R_2$ = 2',3'-dimethyl-butanoyl
**2** $R_1$ = Prop, $R_2$ = 2'-MeBu

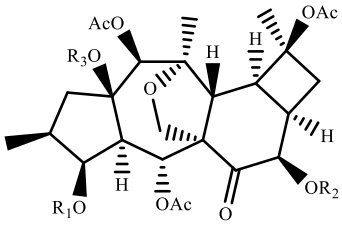

**3** $R_1$ = Prop, $R_2$ = 2'-MeBu, $R_3$ = H
**4** $R_1$ = Ac, $R_2$ = iBu, $R_3$ = Ac

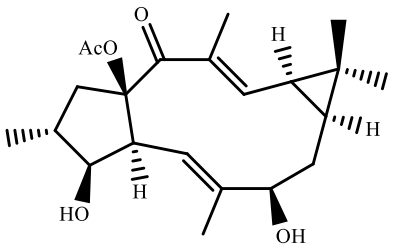

**5**

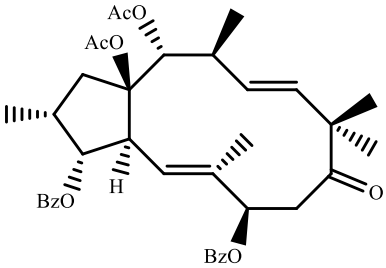

**6**

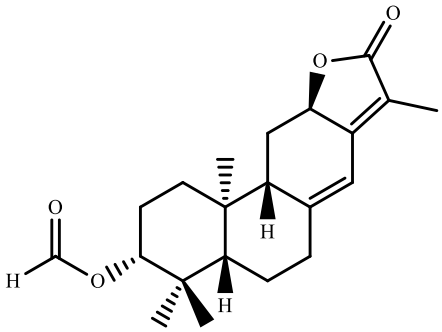

**7**

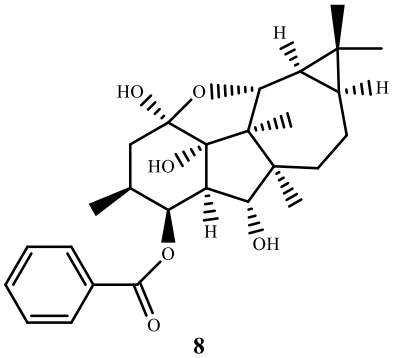

**8**

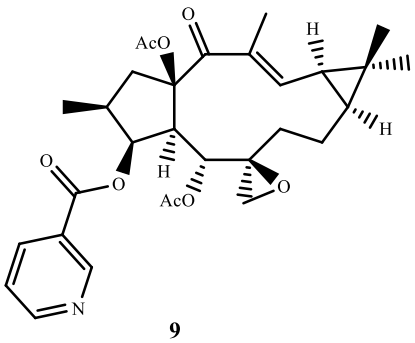

**9**

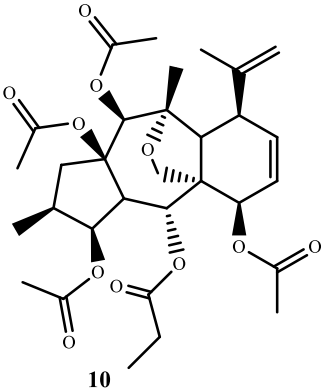

**10**

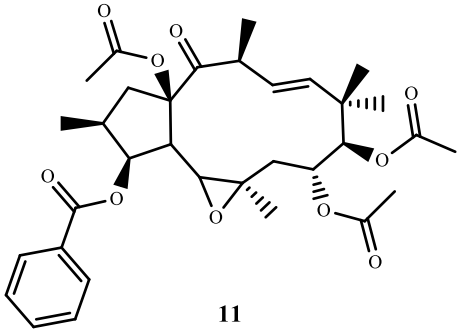

**11**

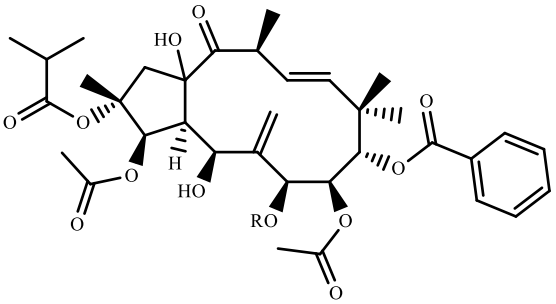

**12** R =

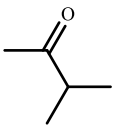

**13** R =

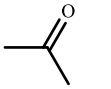

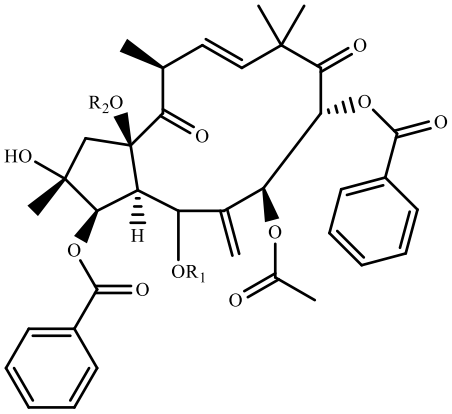

**14** $R_1$ = H, $R_2$ = Ac

**15** $R_1$ = Ac, $R_2$ = H

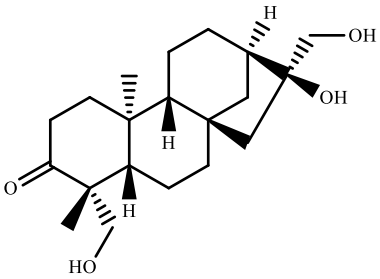

**16**

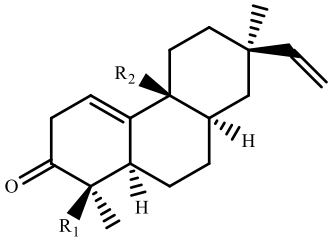

**17** $R_1 = CH_2OH$, $R_2$ = Me

**18** $R_1$ = Me, $R_2 = CH_2OH$

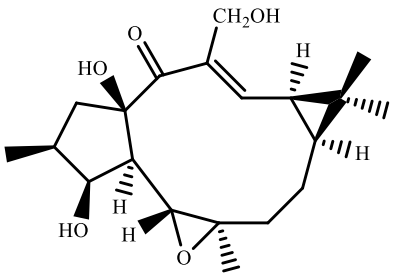

**19**

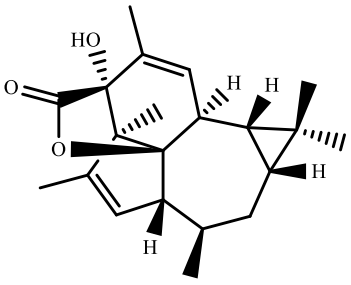

**20**

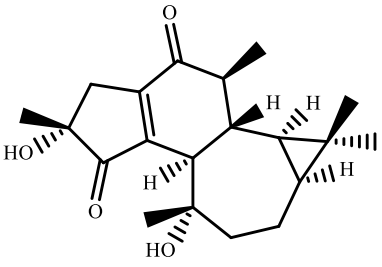

**21**

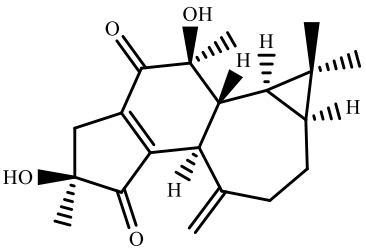

**22**

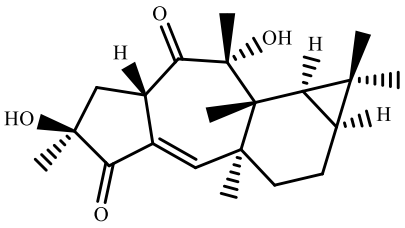

**23**

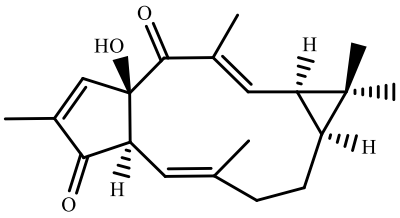

**24**

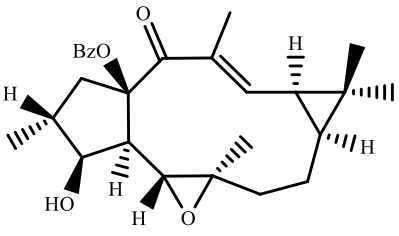

**25**

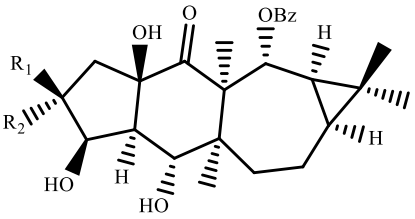

**26** $R_1$ = H, $R_2$ = Me

**27** $R_1$ = Me, $R_2$ = H

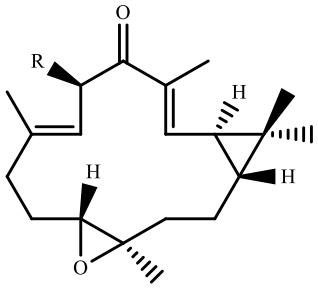

**28** R = H

**29** R = OH

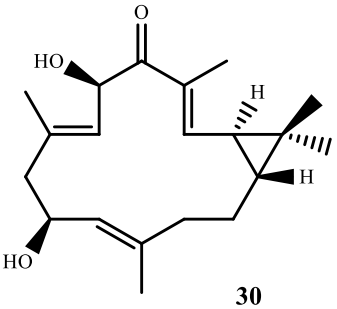

**30**

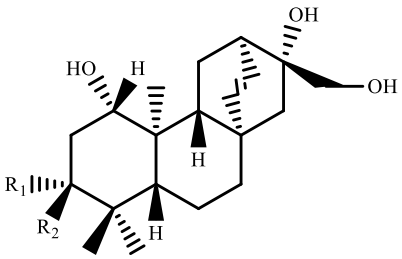

**31** $R_1$ = OH, $R_2$ = H

**32** $R_1$ = H, $R_2$ = OH

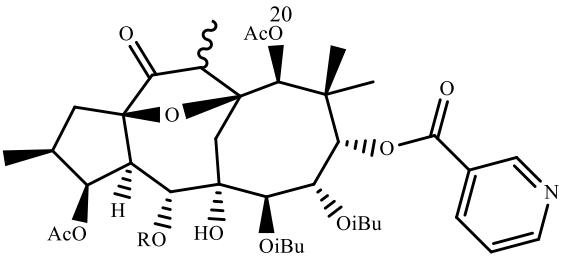

**33** R = Ac, 20a

**34** R = H, 20b

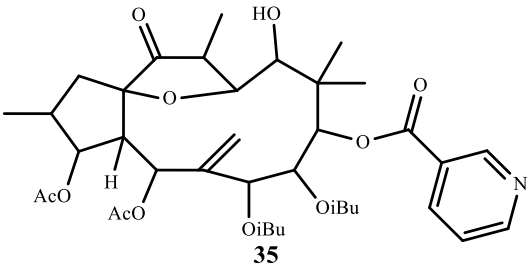

**35**

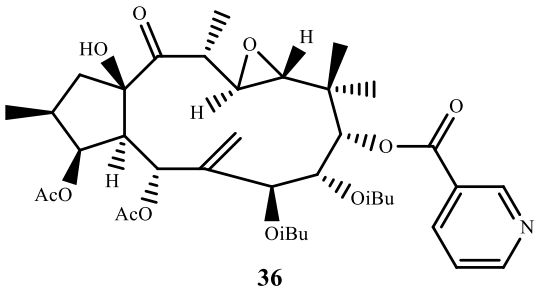

**36**

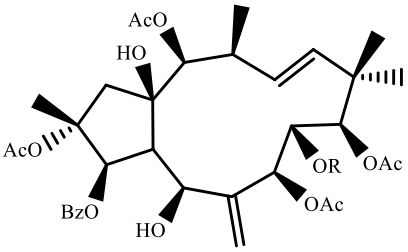


**37** R = But
**38** R = Prop
**39** R = Ac

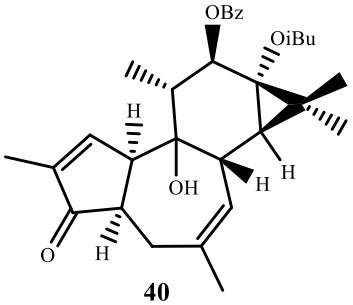


**40**

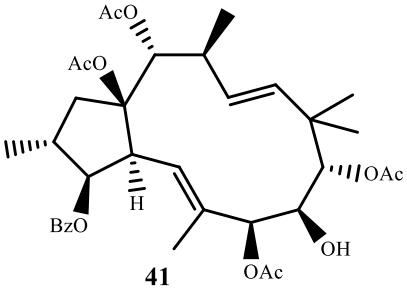


**41**

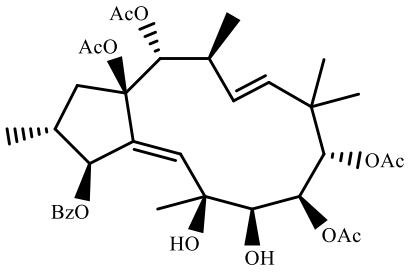


**42**

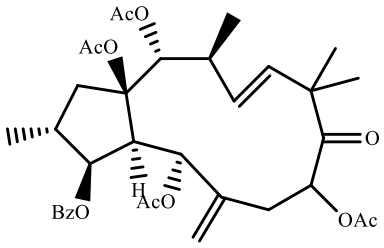


**43**

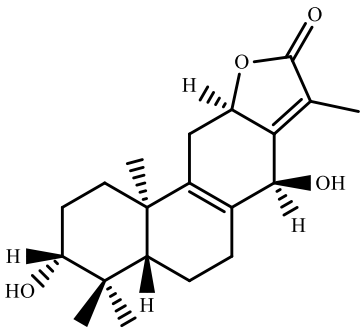


**44**

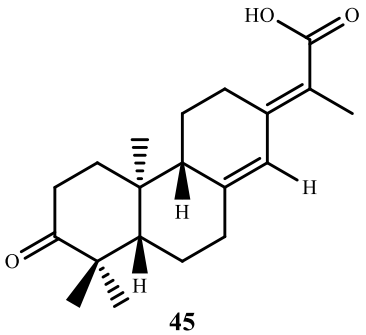


**45**

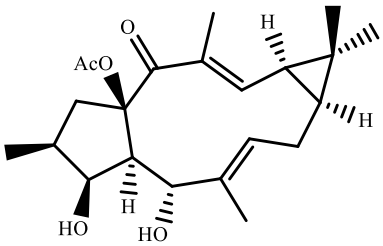


**46**

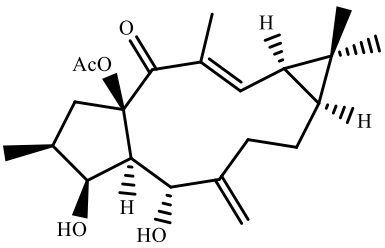


**47**

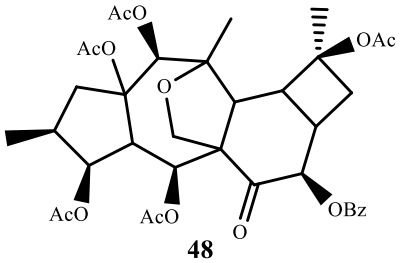


**48**

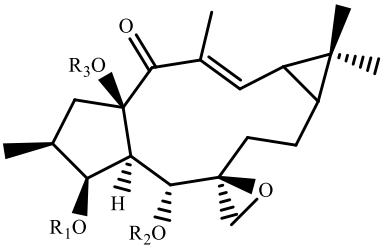


**49** $R_1 = R_2 = R_3 = Ac$
**50** $R_1$ = 3-MeBu, $R_2 = R_3 = Ac$

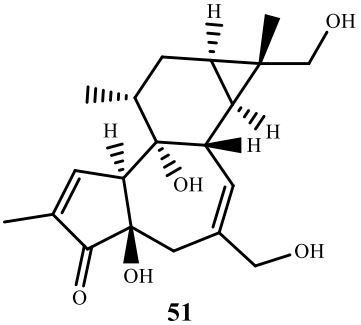


**51**

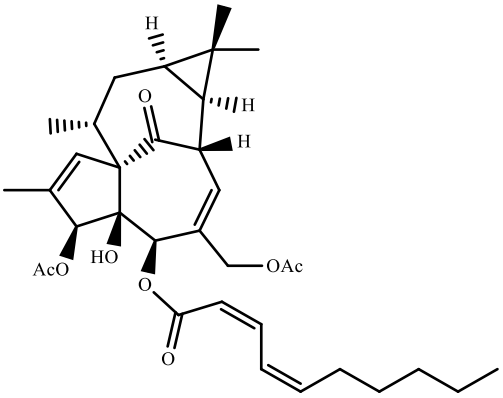

**52**

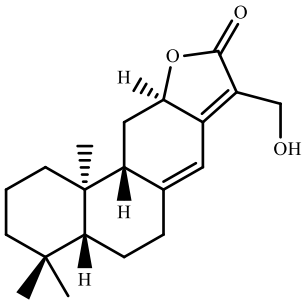

**53**

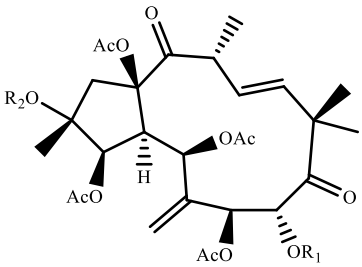

**54** $R_1$ = Ac, $R_2$ = H
**55** $R_1$ = iBu, $R_2$ = H
**56** $R_1$ = Tig, $R_2$ = H
**57** $R_1$ = Bz, $R_2$ = H

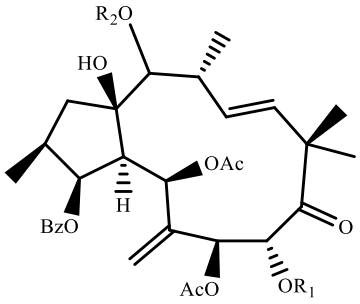

**58** $R_1$ = MeBu, $R_2$ = H
**59** $R_1$ = iBu, $R_2$ = H

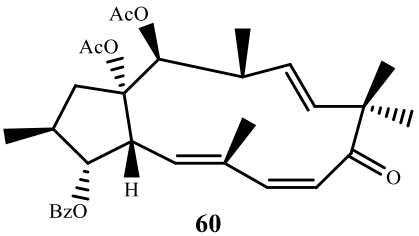

**60**

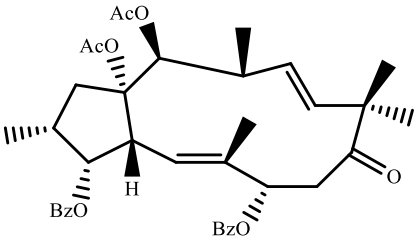

**61**

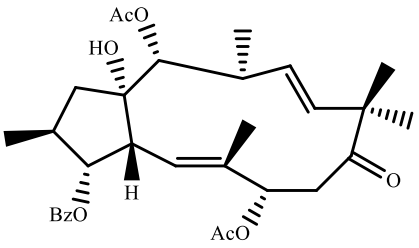

**62**

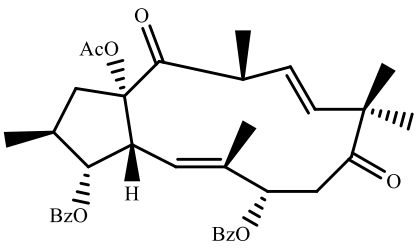

**63**

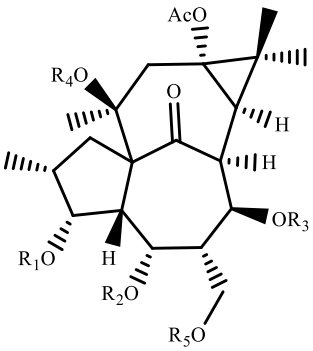

**64** $R_1$ = But, $R_2$ = Ang, $R_3$ = H, $R_4$ = H, $R_5$ = Nic
**65** $R_1$ = Pro, $R_2$ = Ang, $R_3$ = Ac, $R_4$ = H, $R_5$ = Nic
**66** $R_1$ = Pro, $R_2$ = Ac, $R_3$ = Bz, $R_4$ = H, $R_5$ = Nic
**67** $R_1$ = But, $R_2$ = Ang, $R_3$ = H, $R_4$ = Nic, $R_5$ = H

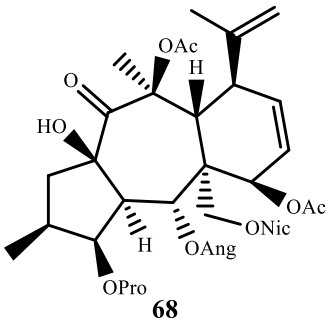

**68**

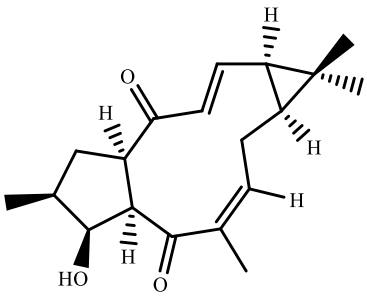

**69**

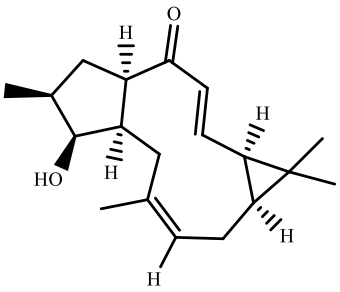

**70**

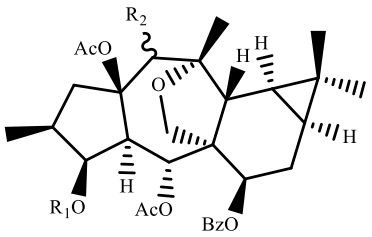

**71** $R_1$ = Ac, $R_2$ = β–OAc
**72** $R_1$ = Prop, $R_2$ = α–OBz
**73** $R_1$ = Ac, $R_2$ = β–ONic

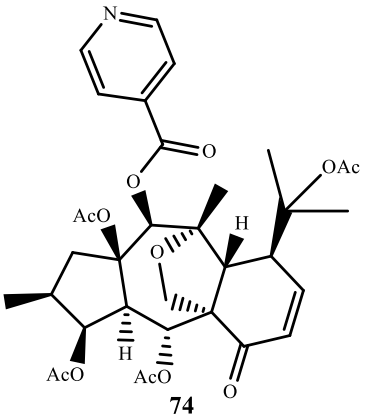

**74**

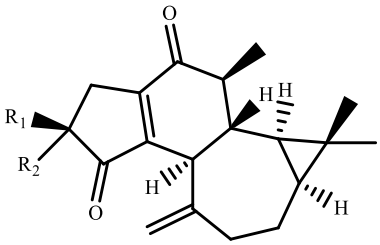

**75** $R_1$ = Me, $R_2$ = H
**76** $R_1$ = H, $R_2$ = Me
**77** $R_1$ = OH, $R_2$ = Me
**78** $R_1$ = Me, $R_2$ = OH

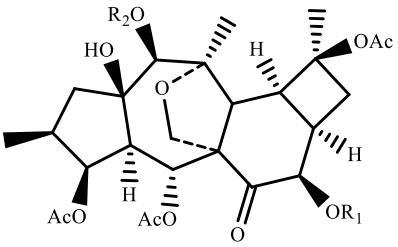

**79** $R_1$ = iBu, $R_2$ = Bz
**80** $R_1$ = 2'-MeBu, $R_2$ = Ac
**81** $R_1$ = iBu, $R_2$ = Ac

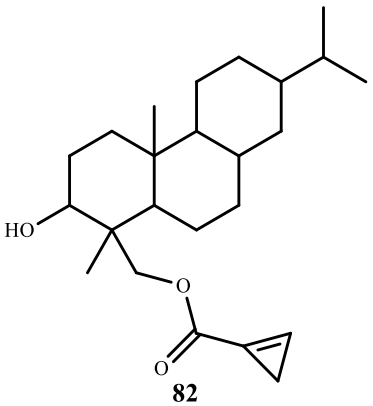

**82**

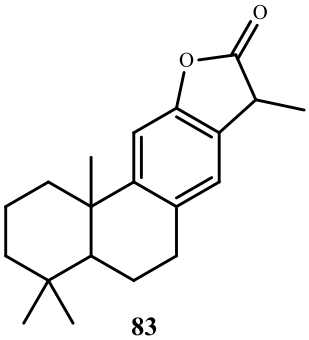

**83**

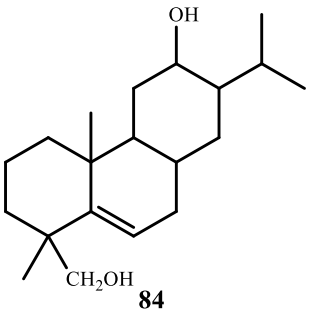

**84**

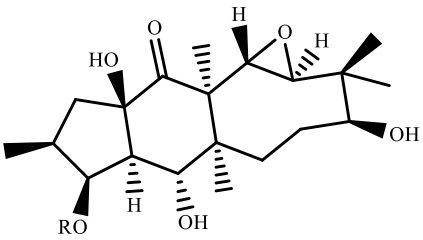

**85** R = Bz
**86** R = Cinnamoyl

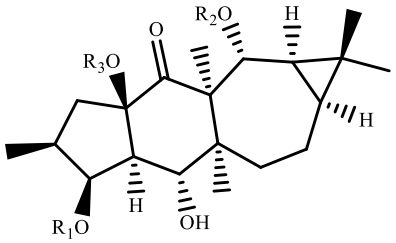

**87** $R_1$ = Bz, $R_2$ = $R_3$ = H
**88** $R_1$ = Cinnamoyl, $R_2$ = $R_3$ = H
**89** $R_1$ = H, $R_2$ = $CH_3$, $R_3$ = Bz
**90** $R_1$ = Bz, $R_2$ = Et, $R_3$ = H
**91** $R_1$ = Cinnamoyl, $R_2$ = Me, $R_3$ = H
**92** $R_1$ = Cinnamoyl, $R_2$ = Et, $R_3$ = H
**93** $R_1$ = Cinnamoyl, $R_2$ = $R_3$ = isopropylidene

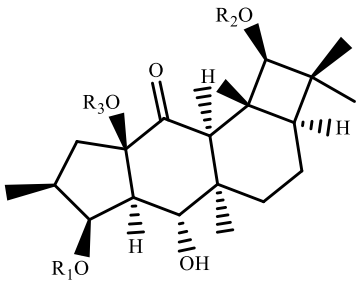

**94** $R_1$ = Bz, $R_2$ = $R_3$ = H
**95** $R_1$ = Cinnamoyl, $R_2$ = $R_3$ = H
**96** $R_1$ = H, $R_2$ = Me, $R_3$ = Cinnamoyl

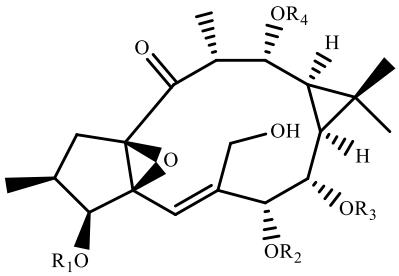

**97** $R_1$ = Ac, $R_2$ = Ang, $R_3$ = Me, $R_4$ = Ac
**98** $R_1$ = Ac, $R_2$ = Bz, $R_3$ = Me, $R_4$ = Ac

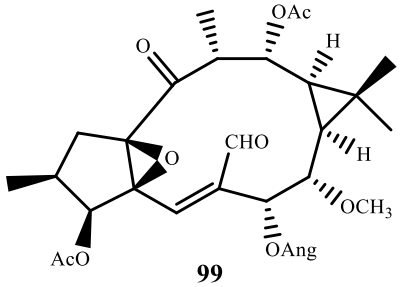

**99**

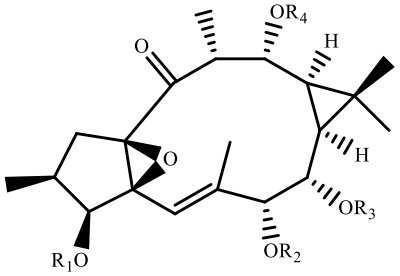

**100** $R_1$ = Ac, $R_2$ = A, $R_3$ = Me, $R_4$ = Ac
**101** $R_1$ = Ac, $R_2$ = B, $R_3$ = Me, $R_4$ = Ac
**102** $R_1$ = Ac, $R_2$ = Ac, $R_3$ = Me, $R_4$ = B
**103** $R_1$ = Ac, $R_2$ = C, $R_3$ = Me, $R_4$ = Ac
**104** $R_1$ = Ac, $R_2$ = Bz, $R_3$ = Me, $R_4$ = H
**105** $R_1$ = H, $R_2$ = Bz, $R_3$ = Me, $R_4$ = Ac
**106** $R_1$ = H, $R_2$ = Ang, $R_3$ = Me, $R_4$ = H
**107** $R_1$ = B, $R_2$ = $R_3$ = $R_4$ = Ac
**108** $R_1$ = $R_2$ = $R_4$ = Ac, $R_3$ = B
**109** $R_1$ = $R_4$ = Ac, $R_2$ = H, $R_3$ = MeBu
**110** $R_1$ = H, $R_2$ = $R_4$ = Ac, $R_3$ = MeBu
**111** $R_1$ = Ac, $R_2$ = $R_4$ = H, $R_3$ = Bz

A =

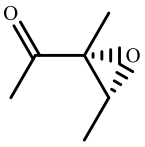

B =

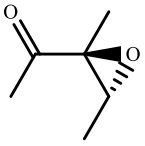

C =

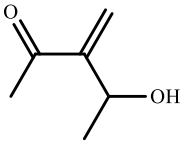

Ang =

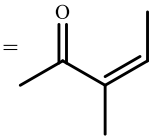

Tig =

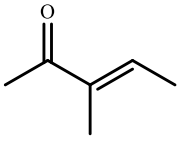

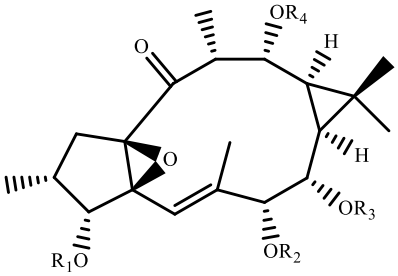

**112** $R_1$ = H, $R_2$ = Ang, $R_3$ = Me, $R_4$ = H
**113** $R_1$ = H, $R_2$ = Ang, $R_3$ = Me, $R_4$ = Ac
**114** $R_1$ = Ac, $R_2$ = H, $R_3$ = MeBu, $R_4$ = Ac

### 1.1.1. Triterpenes

Between 2013 and 2017, several triterpenes were also isolated from *Euphorbia* species. The triterpenes isolated in this period have the euphane (**115-123**), tirucallane (**119, 121, 122, 124**), cycloartane (**125-127**) and ergostane (**128**) skeletons (Table 4).

**Table 4** New triterpenes with euphane, tirucallane, cycloartane and ergostane skeletons isolated from *Euphorbia* sp. between 2013 and 2017.

| Plant | Analysed part | Skeleton | Biological activity | Compound | Reference |
|---|---|---|---|---|---|
| ***E. resinifera* Berg.** | Latex (Euphorbium) | Euphane | Cytotoxic effect (**115**, **117**, **118**) | **115**, **116**, **117**, **118**, **120**, **123** | [62] |
| | | Tirucallane | - | **119**, **121**, **122** | |
| ***E. polygonifolia*** | Latex | Tirucallane | - | **124** | [63] |
| ***E. fischeriana*** | Roots | Cycloartane | Human CYP3A4 promoter activity (**126**) | **125-126** | [64] |
| ***E. bupleuroides*** | Roots | Cycloartane | - | **127** | [47] |
| | | Ergostane | | **128** | |

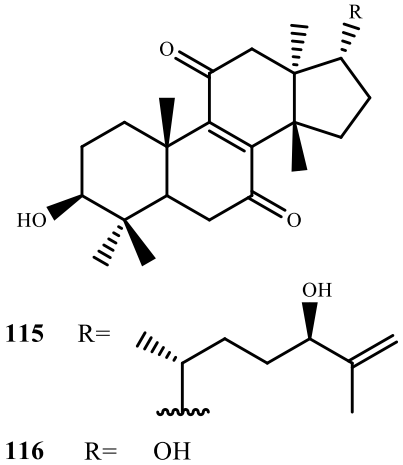


**115** R=

**116** R= OH

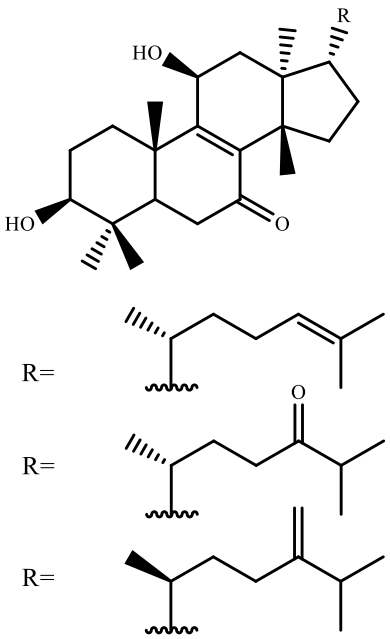


**117** R=

**118** R=

**119** R=

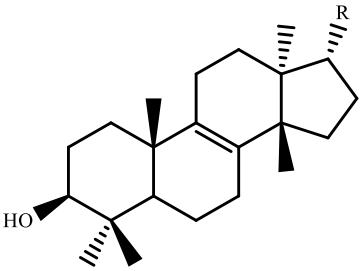


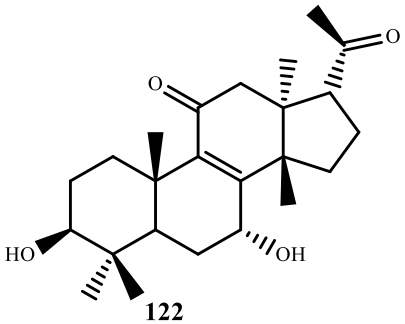


**122**

**120** R=

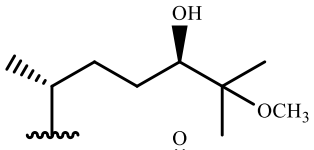


**121** R=

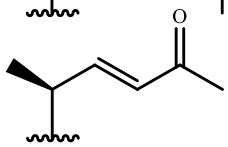


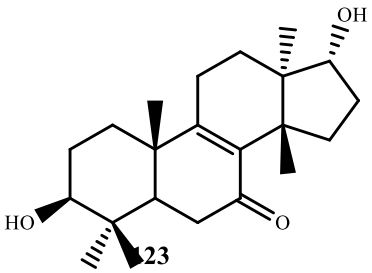


**123**

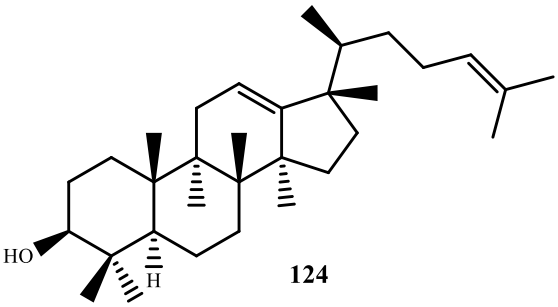


**124**

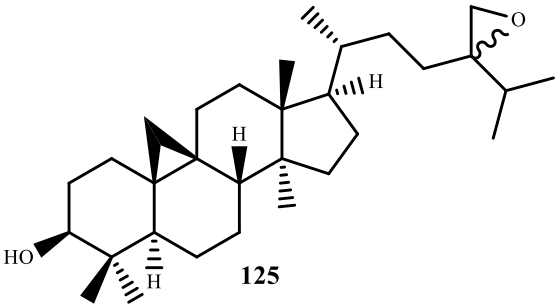


**125**

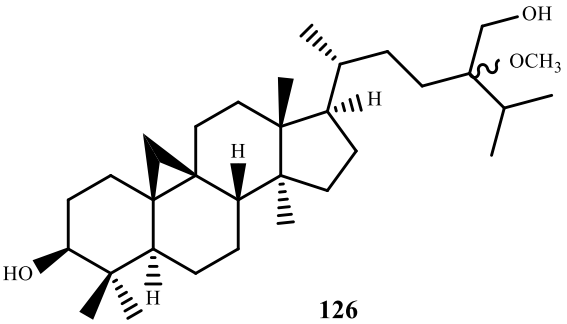


**126**

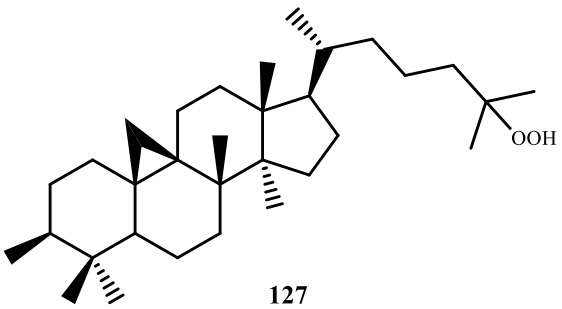


**127**

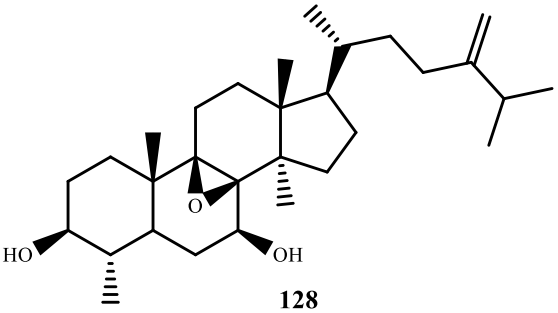


**128**

## 2. CANCER AND MULTIDRUG RESISTANCE

Cancer, malignant tumours, or neoplasms are generic terms for a group of diseases that can affect any part of the body. One defining feature of these diseases resides on the rapid and disorganized proliferation of abnormal cells, which can migrate outside their normal environment and invade adjoining parts of the body and/or spread to other organs, in a process called metastasis [65]. It is the second leading cause of death in developed countries [66] and, according to the World Health Organization (WHO), in 2015, 8.8 million people died from cancer worldwide and the number of new cases of cancer is expected to rise by 70% over the next 20 years [65]. Over the last few decades, a remarkable progress in prevention, detection and treatment of cancer has been achieved and the most common ways to treat these diseases lie on traditional approaches such as surgery, radiotherapy, chemotherapy and biologic therapy [66, 67].

Chemotherapy is considered the basis for cancer treatment, and sometimes the only feasible option. Chemotherapeutic agents are usually designed to impair cell division or to promote apoptosis in a non-specific way [68]. However, the resistance of cancer cells to many clinically used drugs is regarded as the major obstacle to therapeutic success [69]. This resistance can be divided in two categories: intrinsic or primary resistance, and acquired resistance. In the first case, drug resistance is related to the failure in response of many tumours to the initial chemotherapy. On the other hand, acquired resistance is related to the development of tumour cells capable of neutralizing the effects of chemotherapeutic agents, either by elimination (upregulated efflux mechanisms), decreased drug uptake, activation of DNA-repairing mechanisms or inhibition of apoptotic mechanisms [70].

Multidrug resistance (MDR) can be defined as the intrinsic or acquired simultaneous resistance of tumour cells to multiple classes of structurally and functionally divergent drugs [71]. Several mechanisms can be involved in MDR, such as increased drug metabolism, target modification and reduced drug accumulation within the cell. However, the overexpression of membrane proteins which mediate the active extrusion of drugs through the cellular membrane is one of the most studied and several ATP-Binding Cassette (ABC) transporters are known to be involved [70, 72].

## 2.1. ATP-binding Cassette (ABC) superfamily

The ABC transporter superfamily is one of the largest and most broadly expressed families of transporter protein currently known. These proteins can be found in every living organism, from prokaryotes to mammals, and are responsible for the active transport of a wide variety of compounds across biological membranes [73].

The vast majority of ABC transporters require energy derived from the hydrolysis of ATP to ADP to export a wide variety of substrates across the cell membrane against the concentration gradient, ranging from small molecules such as ions, to large biomolecules, such as oligopeptides [74]. The most critical problem in treatment failure occurs when ABC transporters are overexpressed, which leads to a decrease in intracellular drug concentration [73, 74]. ABC proteins are expressed not only in cancer cells but also in normal tissues such as liver, kidney, pancreas, intestine, heart and blood-brain barrier, indicating these proteins' physiological roles in protecting cells against exogenous and endogenous toxic compounds [75, 76].

In human cells, three main ABC transporter proteins are involved in MDR: P-glycoprotein (P-gp/MDR1/ABCB1), the multidrug resistant associated protein (MRP1/ABCC1) and the breast cancer resistant protein (BCRP/ABCG2) [77].

### 2.1.1. The ABCB Subfamily: P-glycoprotein (P-gp)

Discovered in 1976 in cancer cells expressing the MDR phenotype, P-gp was the first multidrug transporter reported to cause a reduced drug permeation in these cells. P-gp was recognized as an ATP-binding cassette transporter protein and proposed to function as an efflux pump, based on the presence of specific conserved sequences [78], and its overexpression is currently the best and most studied form of multidrug resistance [73, 77].

P-gp is coded in humans by the *mdr1* gene, located on chromosome 7, and consists of 170-kDa and 1280 amino acids arranged in two hydrophobic homologous halves, joined by a linker region, each containing six transmembrane domains and a nucleotide-binding domain (the ATP binding site) [79].

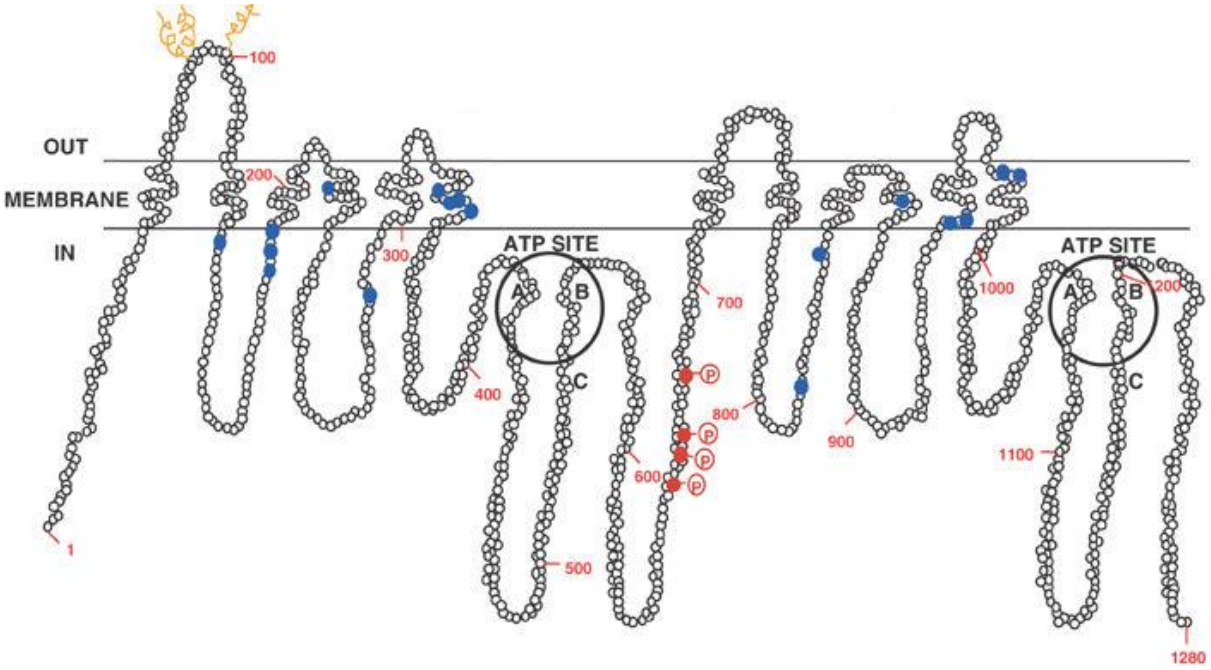


**Figure 2** Hypothetical bidimensional representation of human P-gp. Each circle represents one amino acid residue, with the blue circles representing showing the positions where mutations can alter the substrate specificity of P-gp. circled areas represent the ATP-binding sites. Phosphorylation sites are marked as red circles P and the glycosylation sites are marked as yellow curvy lines. Adapted from Ambudkar *et al.* (**2003**) [80].

P-gp acts as an efflux pump for a large variety of structurally diverse compounds. This protein is capable of transporting many structurally unrelated anti-cancer agents, such as vinka alkaloids (vincristine and vinblastine), anthracyclines (doxorubicin and daunorubicin), epipodophyllotoxins (etoposide) and taxanes (paclitaxel and docetaxel) (Figure 3), as well as other drugs, such as HIV protease inhibitors, antibiotics, antihypertensive and antihistamine drugs [79, 81].

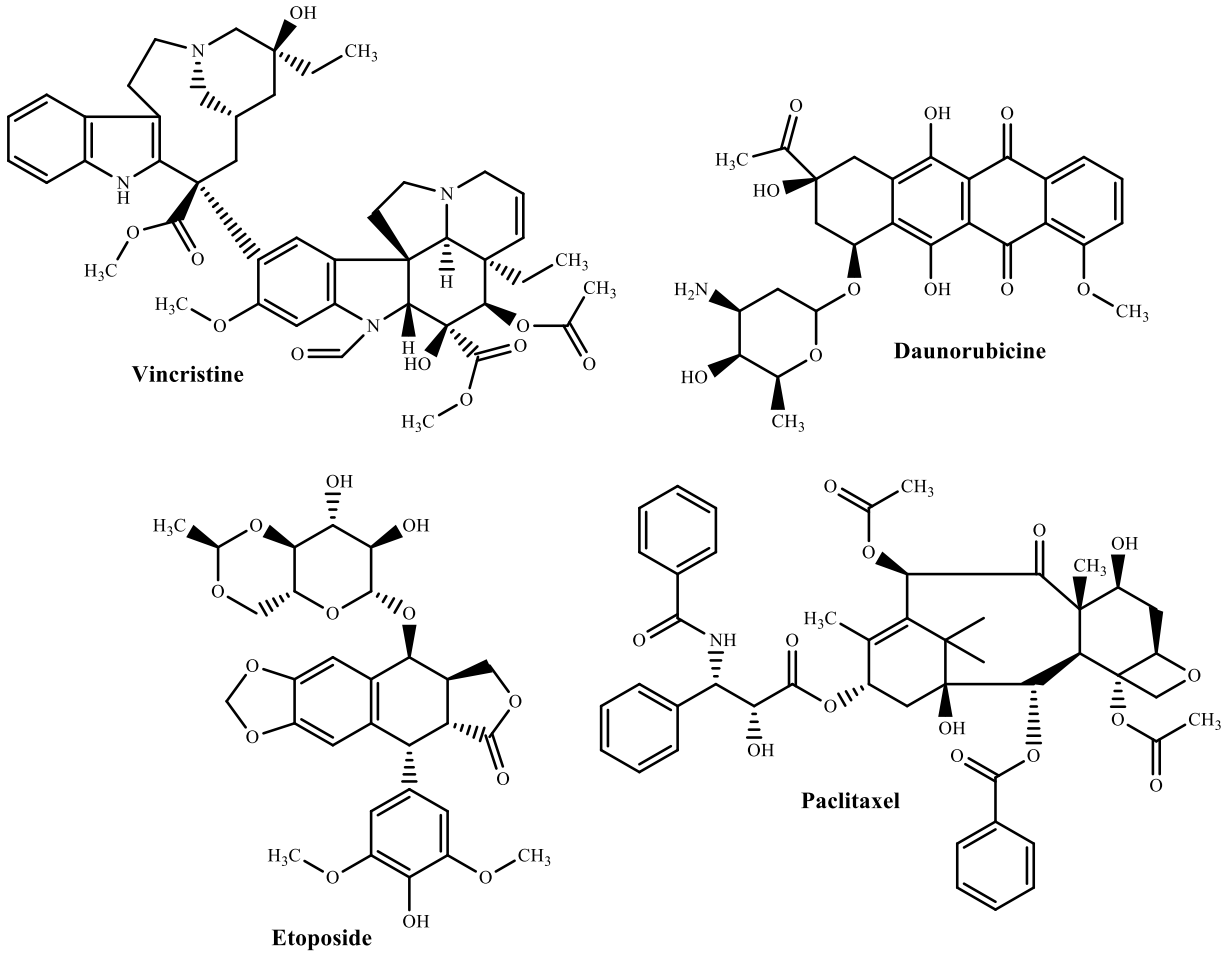


**Figure 3** Chemical structure of antitumor drugs vincristine, daunorubicin, etoposide and paclitaxel.

Over the years, several models have been proposed to explain the mechanism of action of P-gp efflux, based on kinetic and mutation experiments. Among them, the most accepted models are the "flippase" and "hydrophobic vacuum cleaner" models (Figure 4). In both models, ATP binding and hydrolysis is essential for the functioning of P-gp [82].

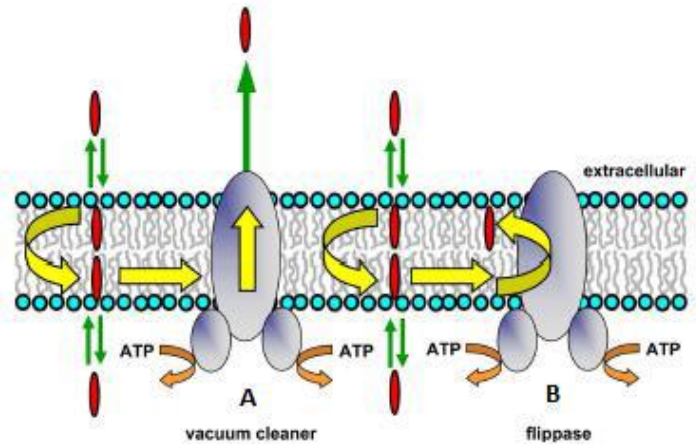


**Figure 4** Hydrophobic vacuum cleaner (A) and flippase (B) models for P-gp function. (Adapted from: SHarom *et al.*, 2014) [69].

With the "flippase" model, it is suggested that P-gp acts as a translocase or flippase. The amphoteric drug permeates into the lipid bilayer and, once there, interacts with the glycoprotein, which conducts the extrusion to the outer leaflet of the bilayer. Once in the outer leaflet, the substrates would then either passively diffuse into the extracellular aqueous phase or move back to the inner leaflet by spontaneous flip-flop [82].

In the "hydrophobic vacuum cleaner" model, it is suggested that P-gp recognizes the hydrophobic substrates that accumulate inside the lipid bilayer and translocate them through its central pore. The vacuum cleaner model is currently the most accepted [69].

## 2.2. Strategies for overcoming multidrug resistance

Over the last few decades, MDR has received considerable attention. Therefore, multiple strategies have been proposed to overcome this problem. One of the most promising strategies lies on the concomitant administration of anticancer drugs with other non-toxic compounds capable of modulating P-gp in order to restore and maintain the cytotoxic concentration of anticancer agents inside cancer cells [66] and great efforts have been made to discover effective P-gp modulators.

P-gp reversal can occur by several mechanisms, namely: (i) direct interaction with one or more binding sites of P-gp, thus blocking transport by acting as a competitive or non-competitive inhibitor; (ii) inhibition of ATP binding and hydrolysis, and; (iii) interaction with membrane phospholipids and consequent modification of the lipid environment of P-gp [76, 82, 83].

A variety of compounds, either synthetic or natural in origin, have been shown to act as MDR-modulators and some of them have undergone clinical trials. Since the 1980s, three generations of P-gp inhibitors have been considered. First-generation inhibitors are compounds developed with specific medicinal uses that have shown some P-gp-inhibition properties. Compounds like verapamil, cyclosporine A, quinidine and tamoxifen (Figure 5) have shown to inhibit P-gp, albeit high amounts of these compounds were needed to produce modulation effect due to their low specificity and affinity [76].

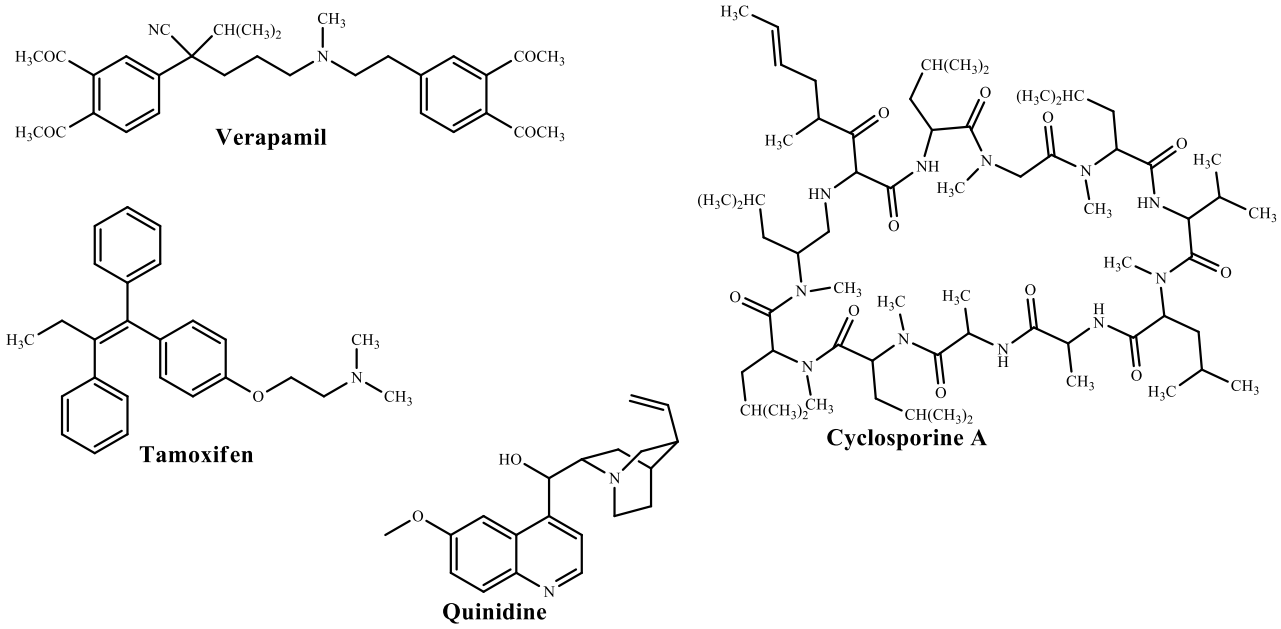


**Figure 5** Some examples of first-generation P-gp modulators [76].

Given the high doses of first-generation compounds needed to produce any modulatory effects on P-gp, which resulted in unacceptable high toxicity, these compounds were no longer investigated, giving rise to second- and third-generation of compounds.

Second-generation compounds were analogues of those from first generation. They were researched not only to reduce the toxicity of first generation drugs but also to increase their affinity to P-gp. Compounds like dexverapamil, valspodar and biricodar (Figure 6) were less toxic but still retained some of the characteristics that made them unusable for clinical practice, as their affinity to P-gp was still too low and high doses were still needed to produce any significant inhibition. Also, some pharmacokinetic interactions were reported affecting the metabolism and clearance mechanism as both modulators and anticancer agents were substrates for CYP 3A4, leading to enhanced adverse effects from the anticancer drugs [76].

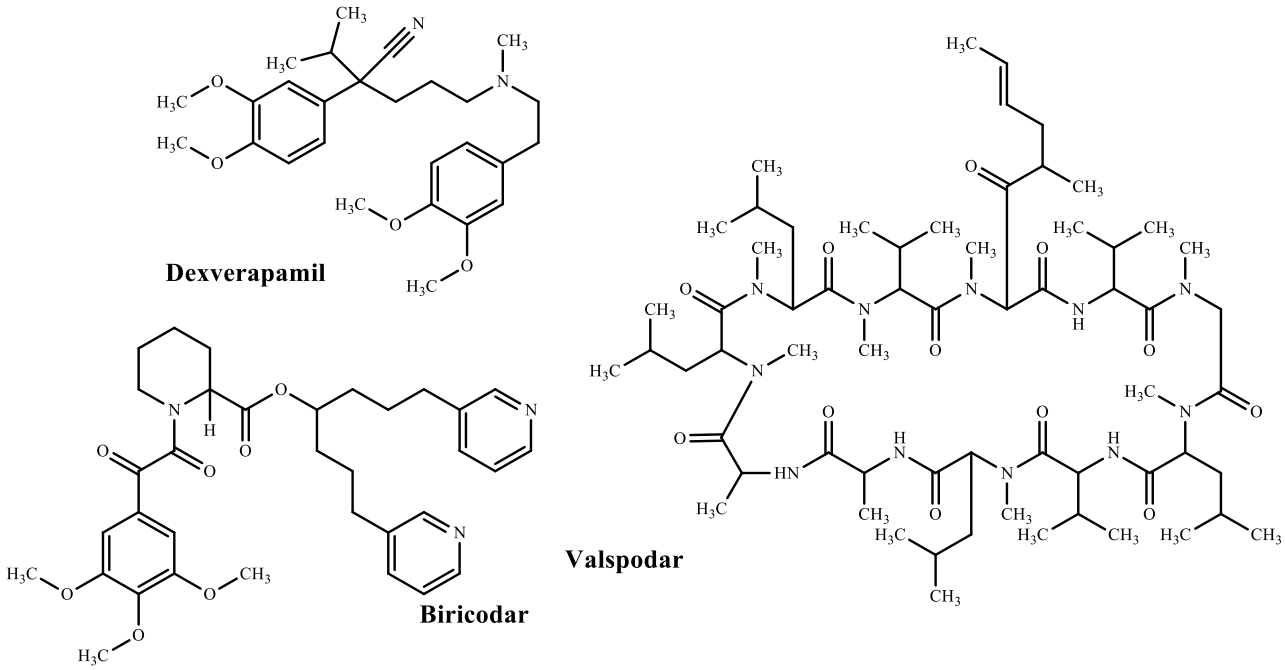


**Figure 6** Some example of second-generation P-gp modulators [76].

Given the problems with first- and second- generations of modulators, structure-activity relationship (SAR) coupled with HTS and combinatorial chemistry were necessary and resulted in the development of third-generation P-gp modulators. These novel modulators were designed and synthesized in order to reverse MDR and were capable to improve the treatment of MDR tumours by 10-fold by having high transport affinity and low pharmacokinetic interactions (not metabolised by CYP 3A4 and no alterations on plasma pharmacokinetics). Compounds like tariquidar and zosuquidar (Figure 7) are part of this generation on P-gp modulators [75, 76]. Some of these compounds have undergone several clinical trials, however, despite all the efforts, currently there is no reversal drug clinically available.

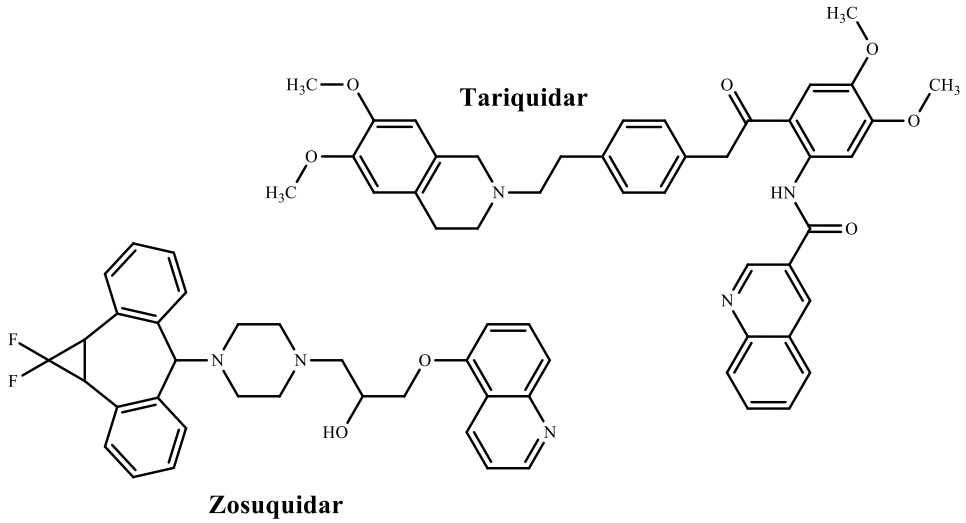


**Figure 7** Molecular structure of two third-generation P-gp modulators, zosuquidar and tariquidar.

Given the limitations of the synthetic third-generation P-gp inhibitors, researchers have turned to living organisms in order to find new potential agents. The therapeutic properties of plants and other living organisms were explored by Man since ancient times [1] and today, about 50% of modern drugs are related to natural products and most of them are derived from plants. Due to the wide structural variety of plant secondary metabolites, natural products have proven to be an undeniable source of information in drug design.

In the search for new MDR-reversing agents from plants, in last the few decades many diterpenes were isolated from *Euphorbia* species with interesting pharmacological activities, particularly jatrophane- and lathyrane-type diterpenes [2, 11, 12, 43, 84]. These diterpenes have shown promising inhibitory activity on P-gp and emerged as a new class of MDR modulators [46]. Moreover, since they present a structurally-homogenous skeleton differing only in their acylation pattern, they have been considered ideal targets for structure-activity relationship studies.

## 3. AIM OF THIS WORK

The main objective of this project was to search for bioactive compounds, mainly effective modulators of P-glycoprotein in resistant cancer cells through isolation and molecular derivatization of compounds found in high amounts.

Firstly, the work was focused on continuing the phytochemical study of *E. boetica* and *E. pubescens* methanolic extracts that had already been initiated. Then, the molecular manipulation of methyl gallate, a compound isolated in large amounts, was also performed, aiming to obtain a small set of galloyl derivatives. Due to time constraints, the obtained derivatives were not tested for their biological activity, allowing for future studies to be performed.

# Chapter II

## Results and Discussion

# 1. PHYTOCHEMICAL STUDY of *Euphorbia boetica* and *Euphorbia pubescens*

The phytochemical study of some fractions of *E. boetica* and *E. pubescens* aerial parts led to the isolation of several compounds.

From *E. boetica*, were isolated seven diterpenes, including one new polycyclic premyrsinane-type (**1**) diterpene, one known polycyclic premyrsinane-type diterpene (**2**), two new tigliane-type diterpenes (**3**, **4**) and three known macrocyclic lathyrane-type diterpenes (**5**, **6**, **7**). A large amount of a phenolic compound (**8**) and a cycloartane-type triterpene (**9**) were also isolated.

From *E. pubescens* one macrocyclic jatrophane diterpene polyester (**10**) and a diterpenic lactone (**11**) were isolated.

## 1.1. Isolated compounds – Structural Elucidation

### *1.1.1. Euphorbia boetica*

#### *1.1.1.1. Euphomyrsinane A*

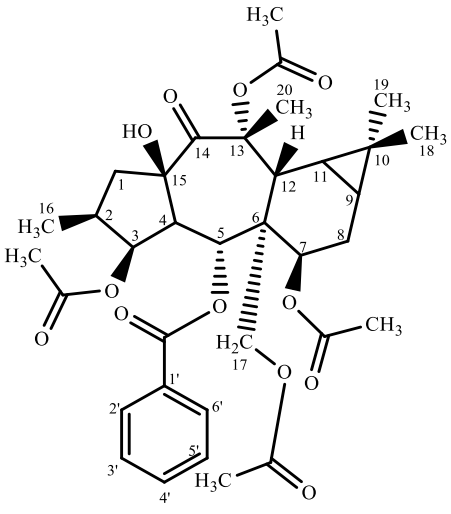

**1**

Compound **1,** named euphomyrsinane A**,** was obtained as a white amorphous powder. The IR spectrum displayed characteristic absorption bands for a hydroxyl group (3486 $cm^{-1}$) and several carbonyl groups (1700 - 1730 $cm^{-1}$). The ESI-MS spectrum showed a protonated ion at *m/z* 657 $[M + H]^+$ that, together with the NMR data (Tables 5 and 6), allowed the

establishment of the molecular formula $C_{35}H_{44}O_{12}$, corresponding to fourteen degrees of unsaturation.

In addition to the resonances of the ester moieties, the combined analysis of $^{13}$C-NMR and DEPT spectra showed the presence of twenty carbon signals corresponding to: four methyl groups ($\delta_C$ 14.0, 15.0, 25.1 and 29.6), three methylenes ($\delta_C$ 22.2, 42.9 and an oxygenated one at $\delta_C$ 62.9), eight methines (three oxygenated at $\delta_C$ 78.6, 70.7 and 69.9) and five quaternary carbons ($\delta_C$ 18.4, 47.9, two oxygenated at $\delta_C$ 84.2 and 85.8, and one carbonyl group at $\delta_C$ 204.4). The $^1$H-NMR spectrum provided information regarding the presence of a benzoate ($\delta_H$ 7.88, d, $J$ = 7.8 Hz; $\delta_H$ 7.51, t, $J$ = 7.35 Hz; $\delta_H$ 7.38, t, $J$ = 7.65 Hz) and several acetate substituents. The $^1$H-NMR spectrum also showed the presence of oxymethine protons at $\delta_H$ 4.80 (d, $J$ = 6.3 Hz), $\delta_H$ 5.35 (t, $J$ = 3.45 Hz), and $\delta_H$ 6.38 (d, $J$ = 11.4 Hz). These data suggested that this compound has a premyrsinane skeleton [5]. Through the analysis of COSY spectrum, it was possible to establish two sequences of correlated protons (Figure 8). The first sequence (fragment A) allowed the connection of carbons 1-5 and the second sequence (fragment B) the linkage of carbons 7-12 (Figure 8). In order to connect the two fragments, the heteronuclear connectivities displayed in the HMBC spectrum were utilized. In this way, the $^3J_{C\text{-}H}$ between the quaternary carbon C-14 ($\delta_C$ 204.4) and protons H-1β ($\delta_H$ 3.17, dd, $J$ = 13.5 and 7.5 Hz) and H-4 ($\delta_H$ 2.36, dd, $J$ = 11.4 and 3.9 Hz), and C-15 ($\delta_C$ 84.2) with H-3 ($\delta_H$ 5.35, t, $J$ = 3.4 Hz), allowed the establishment of the cyclopentane ring A. Moreover, $^3J_{C\text{-}H}$ correlations between carbon C-12 ($\delta_C$ 35.1), the oxymethine proton H-7 ($\delta_H$ 4.80) and the methylene proton H-17α ($\delta_H$ 4.33, d, $J$ = 11.7 Hz) were also observed and together with the $^2J_{C\text{-}H}$ correlation between the quaternary carbon C-6 ($\delta_C$ 47.9) and the methine proton H-12 ($\delta_H$ 3.51, d, $J$ = 6.3 Hz) confirmed the existence of the six-membered ring. The gem-dimethyl cyclopropane ring, was supported by the high field chemical shift of the quaternary carbon C-10 ($\delta_C$ 18.4) and the $^2J_{C\text{-}H}$ between this carbon and methyl groups at $\delta_H$ 0.94 and $\delta_H$ 1.06 (C-18 and C-19). On the other hand, the HMBC spectrum was also used to locate the acyl substituents. Therefore, the correlation of the carbonyl signal at $\delta_C$ 165.3 with the proton signal at $\delta_H$ 6.38 (H-5) indicated the presence of the benzoyl group at C-5. Similarly, the three acetyl esters could be assigned to C-3, C-7 and C-17 due to the long-range correlations between the carbonyl carbons ($\delta_C$ 170.9, 170.6 and 170.4) with H-3, H-7 and H-17, respectively.

The third acetyl group could be located either at the quaternary carbons C-13 or C-15. The location at C-13 was made on the basis of the observed differences between the C-13 chemical shift ($\delta_C$ 82.8) of a similar diterpene already published in the literature, which has an

hydroxyl group at this position [15]. In fact, a downfield chemical shift of about 3.0 ppm was observed for compound **1**, suggesting that the acetyl group could be located at this carbon.

The relative stereochemistry of compound **1** was deduced from comparison of its coupling constants values to those of similar compounds and confirmed by the analysis of the NOESY spectrum [15]. In this way, assuming the α-orientation for H-4 based on biogenetic reasons [85], the strong NOE cross-peaks between H-4/H-3, H-4/H-2, H-4/H-17α, H-4/H-20 and H-20/H-11 indicated that these protons were on the same side of the molecule. The strong NOE cross-peaks observed between H-5/H-12 results in the β-orientation for H-5 and H-12.

All the above data are in agreement with structure **1**, corresponding to a new polycyclic diterpene.

**Table 5** NMR data of compound **1** ($CDCl_3$, $^1H$ 300 MHz, $^{13}C$ 75.45 MHz, δ in ppm, J in Hz).

| Position | $^1H$ (*J* in Hz) | | $^{13}C$ | DEPT | HMBC |
|---|---|---|---|---|---|
| **1α** | 3.14 | dd (13.5; 7.5) | 42.9 | $CH_2$ | 3, 16 |
| **1β** | 1.65 | s | | | |
| **2** | 1.84 | m | 37.3 | CH | 16 |
| **3** | 5.35 | t (3.45) | 78.6 | CH | 1β, 16 |
| **4** | 2.39 | dd (11.6; 3.9) | 50.3 | CH | 1β, 5 |
| **5** | 6.38 | d (11.4) | 69.9 | CH | 4, 17α |
| **6** | - | - | 47.9 | C | 7, 8α, 12, 17α, 17β |
| **7** | 4.80 | d (6.3) | 70.7 | CH | 5, 8α, 17β |
| **8α** | 2.13 | m | 22.2 | $CH_2$ | - |
| **8β** | 1.80 | m | | | |
| **9** | 0.74 | d (1.8) | 19.0 | CH | - |
| **10** | - | - | 18.4 | C | 8β, 9, 12, 18, 19 |
| **11** | 0.72 | d (3.3) | 24.0 | CH | 11, 18, 19 |
| **12** | 3.51 | d (6.3) | 35.1 | CH | 7, 20 |
| **13** | - | - | 85.8 | C | 12, 20 |
| **14** | - | - | 204.4 | C | 1α, 1β, 4, 20 |
| **15** | - | - | 84.2 | C | 3, 20 |
| **16** | 0.87 | d (6.6) | 14.0 | $CH_3$ | 1α, 1β, 4, 20 |
| **17α** | 4.71 | d (11.7) | 62.9 | $CH_2$ | 5 |
| **17β** | 4.33 | d (11.7) | | | |
| **18** | 0.94 | s | 15.0 | $CH_3$ | 9, 11, 19 |
| **19** | 1.05 | s | 29.6 | $CH_3$ | 9, 11, 18 |
| **20** | 1.71 | s | 25.1 | $CH_3$ | - |
| **3-OAc** | - | - | 170.9 | C | 3 |
| | 2.12 | s | 21.4 | $CH_3$ | - |

**Table 6** (continuation) NMR data of compound **1** ($CDCl_3$, $^1H$ 300 MHz, $^{13}C$ 75.45 MHz, δ in ppm, J in Hz).

| Position | $^1H$ (*J* in Hz) | | $^{13}C$ | DEPT | HMBC |
|---|---|---|---|---|---|
| **5-OBz** | - | - | 165.3 | C | 5 |
| | - | - | 129.7 | C | 3', 5' |
| | 7.88 | d (7.8) | 129.9 | CH | 3', 4', 5' |
| | 7.38 | t (7.65) | 128.4 | CH | 2', 6' |
| | 7.51 | t (7.35) | 133.2 | CH | 2', 6' |
| **7-OAc** | - | - | 170.6 | C | 7, 8β |
| | 1.95 | s | 21.1 | $CH_3$ | - |
| **13-OAc** | - | - | 170.9 | C | 20 |
| | 1.46 | s | 20.6 | $CH_3$ | - |
| **17-OAc** | - | - | 170.4 | C | 17β |
| | 2.16 | s | 21.5 | $CH_3$ | - |

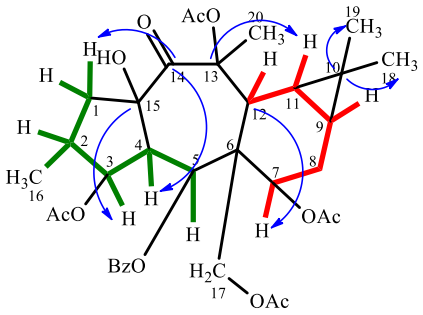


**Figure 8** $^1H$-spin systems of compound **1** assigned by HMQC and $^1H$-$^1H$ COSY (fragments A and B, in green and red, respectively) and their connection by the main $^2J_{C\text{-}H}$ and $^3J_{C\text{-}H}$ correlations displayed in the HMBC spectrum (➔)

### *1.1.1.2. Premyrsinol-3-propanoate-5-benzoate-7,13,17-triacetate*

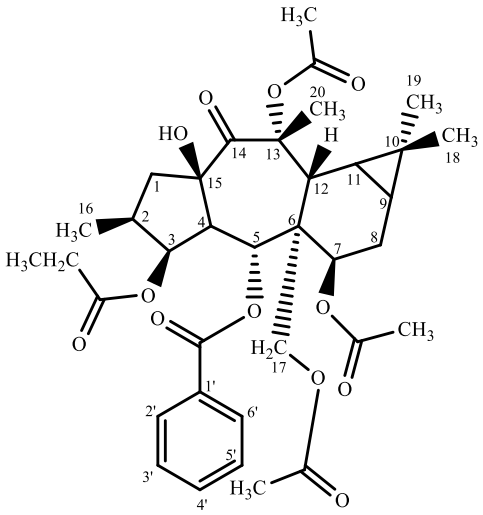

**2**

Compound **2** was isolated as a white powder. Its IR spectrum displayed absorption bands for carbonyl groups (1700 - 1739 $cm^{-1}$) and for a hydroxyl group (3487 $cm^{-1}$). The ESI-MS spectrum exhibited a protonated molecule at *m/z* 671 $[M + H]^+$ that, together with the NMR data, allowed the establishment of the molecular formula $C_{36}H_{46}O_{12}$, from which fourteen degrees of unsaturation were deduced. The spectroscopic data of compound **2** were very similar to compound **1** pointing also to the existence of a premysinane skeleton.

The $^1$H-NMR spectrum (Table 7) showed signals for three tertiary methyls (displayed as singlets at $\delta_H$ 0.93, 1.04 and 1.70), one secondary methyl group at $\delta_H$ 0.84 (d, $J$ = 6.3 Hz), one diastereotopic oxymethylene group at $\delta_H$ 4.29 (d, $J$ = 11.4 Hz; 4.68 d, $J$ = 11.7 Hz) and three oxymethine protons ($\delta_H$ 4.78 d, $J$ = 6.6 Hz; $\delta_H$ 5.36 t, $J$ = 3.3 Hz; 6.36 d, $J$ = 11.4 Hz). In addition, several signals corresponding to acyl groups were also observed, namely, one benzoate ($\delta_H$ 7.86, d, $J$ = 7.8 Hz; $\delta_H$ 7.49, t, $J$ = 7.35 Hz; $\delta_H$ 7.35, t, $J$ = 7.65 Hz), one propanoate ($\delta_H$ 2.26, q, $J$ = 7.5 Hz; $\delta_H$ 0.94, t, $J$ = 7.5 Hz) and three acetyl groups suggested by the presence of three methyl singlets at $\delta_H$ 1.46, 2.10 and 2.14.

Besides the signals due to the ester functions, the $^{13}$C-NMR spectrum (Table 7) exhibited twenty-carbon resonances, that were discriminated by a DEPT experiment as four methyl groups, three methylenes (one oxygenated at $\delta_C$ 62.9), eight methines (three oxygenated at $\delta_C$ 78.2, 70.7 and 69.9), four quaternary carbons (two oxygenated at $\delta_C$ 85.8 and 84.2) and a carbonyl group at $\delta_C$ 204.4). The unambiguous assignment of all proton and carbon resonances was possible through the combined analysis of 2D-NMR spectra, namely COSY, HMQC and

HMBC. In particular, $^{1}$H-$^{1}$H-COSY and HMQC spectra defined two structural fragments with correlated protons (fragments A and B, Figure 9). The linkage of these fragments was possible through the $^{2}J_{C\text{-}H}$ and $^{3}J_{C\text{-}H}$ correlations displayed in the HMBC spectrum, namely, those between the quaternary carbon C-14 and H-1α, H-1β, H-4, H-12 and H-20 in addition to those found between C-13 and H-11, H-12 and H-20. These correlations locate the carbonyl group at C-14 and build up the cyclopentane ring. Moreover, the heteronuclear $^{2}J_{C\text{-}H}$ and $^{3}J_{C\text{-}H}$ correlations allowed the assignment of the cyclohexane ring, which was established due to the observed correlations between C-6 and H-7, H-17 and H-12, along with those found between C-7 and H-12 and H-17, and C-12 and H-17 (Figure 9).

Analysis of HMBC spectrum also allowed the location of the ester groups. Accordingly, the correlations of the carbonyl signals at $\delta_C$ 165.2 and 173.6 with the oxymethine protons H-5 ($\delta_H$ 6.36) and H-3 ($\delta_H$ 5.36), respectively, indicated the presence of the benzoyl and propanoyl groups at these carbons. Similarly, two acetyl esters could be undoubtedly assigned to carbons C-7 and C-17 due to the observed long-range correlations between the carbonyl carbons and the proton signals at $\delta_H$ 4.78, $\delta_H$ 4.29 and $\delta_H$ 4.68. The position of the remaining acetyl group could not be established based on the HMBC correlations, since it should be located at C-13 or C-15 that are quaternary carbons. Thus, the position of this acetyl group was assigned to C-13, regarding the chemical shift differences between compound **2** ($\delta_C$ 85.8) and that of a similar diterpene already published in the literature ($\delta_C$ 82.8), which has a hydroxyl group at this position [15]. In fact, a downfield chemical shift of about 3.0 ppm was observed for compound **2**, suggesting that the acetyl group could be located at C-13.

The relative configuration of compound **2** was deduced through the analysis of a NOESY spectrum and by comparison of the coupling constant values with those reported in the literature [85]. In this way, assuming the α-orientation for H-4 based on biogenetic reasons, the strong NOE cross-peaks between H-4/H-3, H-4/H-2, H-4/H-17α, H-4/H-20 and H-20/H-11 indicated that these protons were on the same side of the molecule. The strong NOE cross-peaks observed between H-5/H-12 results in the β-orientation for H-5 and H-12.

All the above data are in agreement with those reported in the literature [86] allowing for the identification of compound **2** as an already known premyrsinane-type diterpene, premyrsinol-3-propanoate-5-benzoate-7,13,17-triacetate that differs from compound **1** by the presence of a propanoyl instead of an acetyl group at C-3.

**Table 7** NMR data of compound **2** ($CDCl_3$, $^1H$ 300 MHz, $^{13}C$ 75.45 MHz, δ in ppm, *J* in Hz)

| Position | $^1H$ (*J* in Hz) | | $^{13}C$ | DEPT | HMBC |
|---|---|---|---|---|---|
| **1α** | 3.14 | dd (13.5; 7.5) | 42.9 | $CH_2$ | 3, 16 |
| **1β** | 1.63 | m | | | |
| **2** | 1.85 | m | 37.3 | CH | 1, 16 |
| **3** | 5.36 | t (3.3) | 78.2 | CH | 1, 16 |
| **4** | 2.39 | dd (9.8; 3.9) | 50.3 | CH | 1, 5 |
| **5** | 6.36 | d (11.4) | 69.9 | CH | 4, 17 |
| **6** | - | - | 47.8 | C | 7, 8, 12, 17 |
| **7** | 4.78 | d (6.6) | 70.7 | CH | 5, 8, 9, 17 |
| **8α** | 2.14 | m | 22.1 | $CH_2$ | - |
| **8β** | 1.86 | m | | | |
| **9** | 0.73 | br s | 18.9 | CH | 7, 11 |
| **10** | - | - | 18.4 | C | 11, 18, 19 |
| **11** | 0.71 | d (3.2) | 23.9 | CH | 1, 3, 12 |
| **12** | 3.50 | d (6.6) | 35.1 | CH | 17, 20 |
| **13** | - | - | 85.8 | C | 11, 12, 20 |
| **14** | - | - | 204.4 | C | 1, 4, 20 |
| **15** | - | - | 84.2 | C | 1, 3, 5 |
| **16** | 0.84 | d (6.3) | 13.9 | $CH_3$ | - |
| **17α** | 4.68 | d (11.4) | 62.9 | $CH_2$ | 5 |
| **17β** | 4.29 | d (11.4) | | | |
| **18** | 0.93 | s | 14.9 | $CH_3$ | 11, 19 |
| **19** | 1.04 | s | 29.5 | $CH_3$ | 9, 18 |
| **20** | 1.70 | s | 25.0 | $CH_3$ | - |
| **3-OPr** | - | - | 173.6 | C | 3 |
| | 2.26 | q (7.5) | 27.6 | $CH_2$ | - |
| | 0.94 | t (7.5) | 8.8 | $CH_3$ | - |
| **5-OBz** | - | - | 165.2 | C | 5 |
| | - | - | 129.9 | C | - |
| | 7.86 | d (7.8) | 129.7 | CH | - |
| | 7.35 | t (7.65) | 128.3 | CH | - |
| | 7.49 | t (7.35) | 133.1 | CH | - |
| **7-OAc** | - | - | 170.8 | $CH_2$ | - |
| | 1.45 | s | 20.6 | $CH_3$ | - |
| **13-OAc** | - | - | 170.8 | C | - |
| | 2.1 | s | 21.5 | $CH_3$ | - |
| **17-OAc** | - | - | 170.3 | C | 17 |
| | 2.14 | s | 21.4 | $CH_3$ | - |

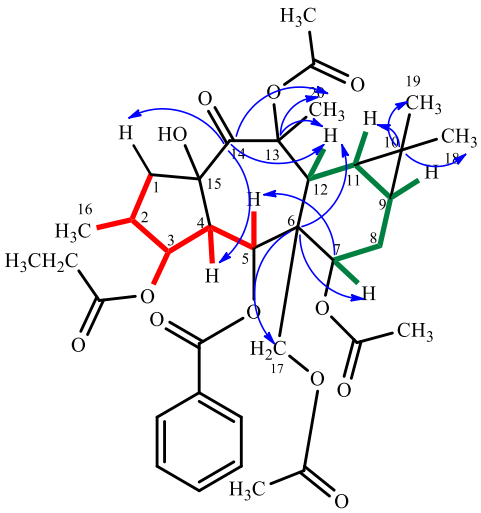

**Figure 9** $^{1}$H-spin systems of compound **2** assigned by HMQC and $^{1}$H-$^{1}$H COSY (fragments A and B, in green and red, respectively) and their connection by the main $^{2}J_{C\text{-}H}$ and $^{3}J_{C\text{-}H}$ correlations displayed in the HMBC spectrum (➔).

### *1.1.1.3. Phorboboetirane A*

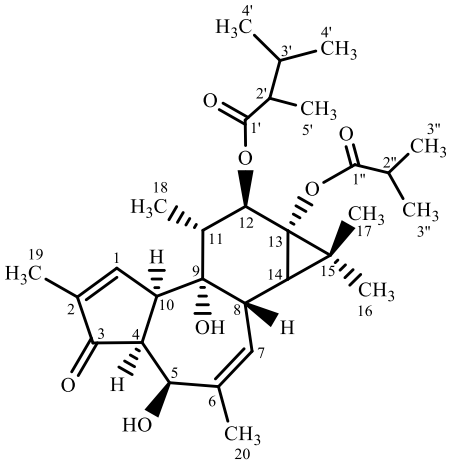

**3**

Compound **3**, named phorboboetirane A, was isolated as white crystals (m.p. 190 ºC). Its IR spectrum displayed absorption bands for hydroxyl group (3303 $cm^{-1}$) and carbonyl groups (1699 - 1757 $cm^{-1}$). The ESI-MS spectrum exhibited a protonated molecule at *m/z* 517 $[M + H]^{+}$ that, together with the NMR data, allowed the establishment of the molecular formula $C_{30}H_{44}O_7$, from which nine degrees of unsaturation were deduced.

The $^{1}$H-NMR spectrum (Tables 8 and 9) showed signals for two tertiary methyls (displayed as singlets at $\delta_H$ 1.18 and 1.20), one secondary methyl group at $\delta_H$ 1.09 (*d*, *J* = 6.3 Hz), and two vinylic methyl groups at $\delta_H$ 1.80 (s) and 1.89 (t, *J* = 1.5 Hz). Signals corresponding to two oxymethine protons ($\delta_H$ 4.44 d, *J* = 4.5 Hz; 5.47 *m*) and two olefinic

protons at $\delta_H$ 4.85 (br s) and 7.04 (s), were also observed. From this spectrum two ester residues were identified, namely an isobutyryl ($\delta_H$ 2.55 m, δH 1.15 d, $J$ = 4.5 Hz, $\delta_H$ 1.17 d, $J$ = 6.8 Hz) and a 2,3-dimethylbutyryl group ($\delta_H$ 2.22 m; $\delta_H$ 1.89 m; $\delta_H$ 1.14 d, $J$ = 4.5 Hz, $\delta_H$ 0.98 d, $J$ = 6.9 Hz and $\delta_H$ 0.96 d, $J$ = 6.9 Hz).

Additionally, to the signals due to the ester functions, the $^{13}$C-NMR spectrum (Tables 8 and 9) exhibited twenty carbon resonances, that were discriminated by a DEPT experiment as five methyl groups, nine methines (two olefinic at $\delta_C$ 125.6 and 154.8 and two oxygenated at $\delta_C$ 71.0 and 74.1), and six quaternary carbons (two oxygenated at $\delta_C$ 64.9 and 78.5, two $sp^2$ carbons at $\delta_C$ 137.7 and 144.1 and a carbonyl group at $\delta_C$ 207.7). The high-field carbonyl signal at $\delta_C$ 207.7, together with the olefinic proton at $\delta_H$ 7.04 ($\delta_C$ 154.8), confirmed the presence of an α,β-unsaturated ketone. On the other hand, the high field quaternary carbon at $\delta_C$ 25.4, pointed out the existence of a gem-dimethyl-cyclopropane ring. Based on all these data, a tigliane-type diterpene skeleton was proposed for compound **3**. The unambiguous assignment of the all proton and carbon resonances was possible through the combined analysis of 2D-NMR spectra, namely COSY, HMQC and HMBC (Figure 10).

In particular, $^1$H-$^1$H-COSY and HMQC spectra defined four structural fragments with correlated protons (Figure 10), which were separated by quaternary carbons (fragments A – D). The linkage of these fragments was possible through the $^2J_{C\text{-}H}$ and $^3J_{C\text{-}H}$ correlations displayed in the HMBC spectrum, namely, those between C-3 and H-1, H-4 and H-19 which located the carbonyl group and build up the cyclopentene ring. The connection of fragments A and B was possible due to the observed cross-peaks between C-6 and H-4, and C-5 and H-7 and H-20. On the other hand, the correlation between C-7 and H-14 established the linkage between the fragments B and C. The correlations between C-13 and H-12, H-14 and H-17 together with those found between C-15 and H-12, H-14, H-15 and H-16 allowed the establishment of the cyclopropane ring and the linkage between fragments D and C. Heteronuclear $^2J_{C\text{-}H}$ and $^3J_{C\text{-}H}$ correlations between C-9 with H-4, H- 11 and H-18 established the linkage of fragments A and D. Finally, the correlation between C-9 and H-7 confirmed the linkage between C-8 and C-9, proving the existence of a four-ring skeleton (Figure 10).

The ester substituents were also allocated by the combined analysis of 2D-NMR spectra. Thus, the assignment of the 2,3-dimethylbutanoate ester at C-12 was deduced by the existence of a HMBC cross-peak between the carbonyl signal at $\delta_C$ 175.8 and the oxymethine proton at $\delta_H$ 5.47 (H-12). The assignment of the isobutyrate group at C-13 could not be done through the HMBC spectrum since it is a quaternary carbon. Thus, the location of this ester group was established regarding the information obtain in the literature for similar compounds

[87, 88]. The relative configuration of compound **3** was deduced through the analysis of a NOESY spectrum and by comparison of the coupling constant values with those reported in the literature [89]. Accordingly, the majority of 4-deoxyphorbol diterpenes isolated to date have β- and α- configurations for H-4 and H-10, possessing, therefore an A/B *trans*-ring junction [87, 88, 90]. However, some differences were observed on the chemical shifts, multiplicity and coupling constants of compound **3**, when compared to those diterpenes. The main differences were the signal resonance for H-1 that was shifted upfield in compound **3** ($\delta_H$ 7.04) instead of c.a 7.57 [87, 88], and the multiplicity and coupling constants of H-4 that appeared at $\delta_H$ 3.12 (dd, $J$ = 6.6 and 4.5 Hz), differing from those observed for H-4β tigliane diterpenes (dd, $J$ = 10.9 and 4.5 Hz) [91]. The $^{13}$C NMR also showed some significant chemical shift differences, namely in carbons C-1, C-2 and C-3 that were shifted upfield, and C-4 that was shifted downfield. Moreover, NOE cross-peaks between H-4/H-10, H-4/H-5 and $CH_3$-18/H-12 indicated that these protons had the same orientation (α). On the other hand, the correlations between H-11/H-8 and H-8/$CH_3$-17 suggested that these protons were β-orientation. The absence of correlation between H-4 and H-8 confirmed the α arrangement for H-4 and β arrangement for H-8.

**Table 8** NMR data of compound **3** ($CDCl_3$, $^1$H 300 MHz, $^{13}$C 75.45 MHz, δ in ppm, $J$ in Hz).

| Position | $^1$H ($J$ in Hz) | | $^{13}$C | DEPT | HMBC |
|---|---|---|---|---|---|
| **1** | 7.04 | s | 154.8 | CH | 10, 19 |
| **2** | - | - | 144.1 | C | 19 |
| **3** | - | - | 207.7 | C | 1, 4, 19 |
| **4** | 3.12 | dd (6.6; 4.5) | 56.2 | CH | - |
| **5** | 4.44 | d (4.5) | 71.0 | CH | 4, 7, 20 |
| **6** | - | - | 137.7 | C | 4, 20 |
| **7** | 4.85 | br s | 125.6 | CH | 14, 20 |
| **8** | 1.99 | m | 40.2 | CH | - |
| **9** | - | - | 78.5 | C | 4, 7, 11, 18 |
| **10** | 3.62 | m | 47.9 | CH | 4 |
| **11** | 1.70 | m | 43.1 | CH | 12, 18 |
| **12** | 5.47 | m | 74.1 | CH | 14, 18 |
| **13** | - | - | 64.9 | C | 12, 14, 16, 17 |
| **14** | 0.76 | d (4.8) | 38.1 | CH | 7, 16, 17 |
| **15** | - | - | 25.5 | C | 12, 14, 16, 17 |
| **16** | 1.20 | s | 16.6 | $CH_3$ | 17 |
| **17** | 1.18 | s | 24.9 | $CH_3$ | 16 |
| **18** | 1.09 | d (6.3) | 11.8 | $CH_3$ | 12 |
| **19** | 1.80 | s | 10.6 | $CH_3$ | - |

**Table 9** (continuation) NMR data of compound **3** ($CDCl_3$, $^1H$ 300 MHz, $^{13}C$ 75.45 MHz, δ in ppm, *J* in Hz).

| Position | $^1H$ (*J* in Hz) | | $^{13}C$ | DEPT | HMBC |
|---|---|---|---|---|---|
| **20** | 1.89 | t (1.5) | 27.3 | $CH_3$ | 7 |
| **12-O(2,3-dMB)** | - | - | 175.8 | C | 12 |
| | 2.22 | m | 47.4 | CH | - |
| | 1.89 | m | 31.3 | CH | - |
| | 0.98 | d (6.9) | 20.9 | $CH_3$ | - |
| | 0.96 | d (6.9) | 19.5 | $CH_3$ | - |
| | 1.14 | d (4.5) | 18.6 | $CH_3$ | - |
| **13-OiBu** | - | - | 179.4 | C | - |
| | 2.55 | m | 34.4 | CH | - |
| | 1.15 | d (4.5) | 18.6 | $CH_3$ | - |
| | 1.17 | d (6.8) | 14.7 | $CH_3$ | - |

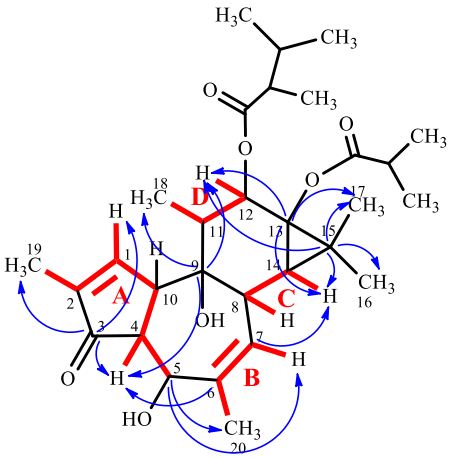


**Figure 10** $^1H$-spin systems of compound 3 assigned by HMQC and $^1H$-$^1H$ COSY (-) and their connection by the main $^2J_{C\text{-}H}$ and $^3J_{C\text{-}H}$ correlations displayed in the HMBC spectrum (→).

### *1.1.1.4. Phorboboetirane B*

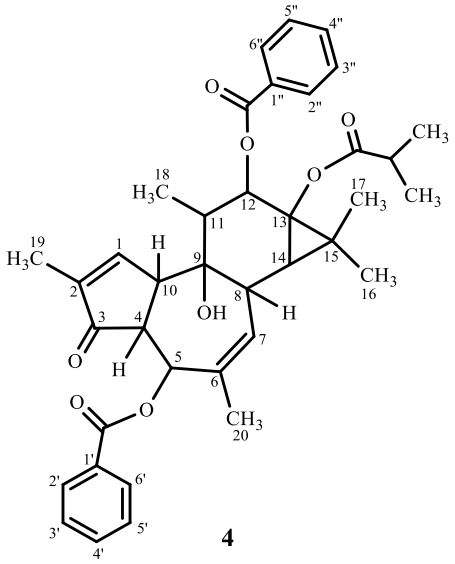

**4**

Compound **4**, named phorboboetirane B, was isolated as an oil. The $^{1}$H-NMR spectrum (Tables 10 and 11) showed signals for two tertiary methyls at $\delta_H$ 1.23 and 1.33 (both displayed as singlets), one secondary methyl group at $\delta_H$ 1.00 (d, $J$ = 6.4 Hz), and two vinylic methyl groups at $\delta_H$ 1.62 (dd, $J$ = 2.5, 1.3 Hz) and 1.75 (s). Signals corresponding to two oxymethine protons at $\delta_H$ 6.48 (d, $J$ = 3.7) and 5.66 (d, $J$ = 9.6) and two olefinic protons at $\delta_H$ 5.48 (d, $J$ = 4.9) and $\delta_H$ 7.72 (br s) were also observed. From this spectrum, three esters residues were identified, namely, one isobutyryl ($\delta_H$ 2.63 p, $J$ = 7.0; $\delta_H$ 1.21 d, $J$ = 3.4; $\delta_H$ 1.18, s) and two benzoyl (one at $\delta_H$ 7.58, m; $\delta_H$ 7.48, m; $\delta_H$ 8.01, m; and another one $\delta_H$ 7.84, d, $J$ = 1.5 Hz; $\delta_H$ 7.38, t, $J$ = 7.6; and $\delta_H$ 7.52, t, $J$ = 2.0).

Additionally to the signals due to the esters functions, the $^{13}$C-NMR spectrum (Tables 10 and 11) exhibited twenty-carbon resonances, discriminated by DEPT as five methyl groups, nine methines (two olefinic at $\delta_C$ 130.0 and 161.0 and two oxygenated at $\delta_C$ 73.8 and 77.7) and six quaternary carbons (two oxygenated at $\delta_C$ 65.2 and 78.9; two sp$^2$ carbons at $\delta_C$ 138.0 and 138.4; and a carbonyl group at $\delta_C$ 205.5). The high-field carbonyl group signal at $\delta_C$ 205.5 coupled with the olefinic proton at $\delta_H$ 7.72 ($\delta_C$ 161.0), confirmed the presence of an α,β-unsaturated ketone. On the other hand, the high-field quaternary carbon at $\delta_C$ 26.5 suggested the existence of a gem-dimethyl-cyclopropane ring. Based on all this data, a tigliane-type diterpene skeleton was proposed for compound **4**, similar to that of compound **3**. The unambiguous assignment of all the proton and carbon resonances was possible through the combined analysis of 2D-NMR spectra, such as COSY, HMQC and HMBC (Figure 11).

In particular, $^{1}$H-$^{1}$H COSY and HMQC spectra defined four structural fragments with correlated protons (fragments A-D, Figure 11). The linkage of these fragments was possible through the $^{2}J_{C\text{-}H}$ and $^{3}J_{C\text{-}H}$ correlations displayed in the HMBC spectrum, namely, those between C-3 and H-1 and H-4 which located the carbonyl group and build up the cyclopentene ring. Additionally, the connection of fragments A and B was possible due to the observed cross-peaks between C-5 and H-7 and H- 20. On the other hand, the correlation between C-7 and H-14 established the linkage between the fragments B and C. The correlations between C-13 and H-12, H-14, H-16, H-17 and H-18 together with those found between C-15 and H-12, H-14, H-16 and H-17 allowed the establishment of the cyclopropane ring and the linkage between fragments D and C. Heteronuclear $^{2}J_{C\text{-}H}$ and $^{3}J_{C\text{-}H}$ correlations between C-9 with H-4 and H-18 established the linkage of fragments A and D.

The combined analysis of 2D-NMR spectra also located the position of the ester substituents. The assignment of one of the benzoyl groups was deduced by the existence of a HMBC cross-peak between the carbonyl group at $\delta_C$ 166.1 and the oxymethine proton at $\delta_H$ 5.66 (H-12) [92]. The second benzoyl group was assigned to C-5 due to the HMBC cross-peak between the carbonyl group at $\delta_C$ 165.40 and the oxymethine proton at $\delta_H$ 6.48 (H-5). Similar to the previous compound, the assignment of the isobutyrate group at C-13 could not be accomplished through the HMBC spectrum since it is a quaternary carbon. Thus, the location of this ester group was established regarding the information obtained in the literature for similar compounds [87, 88].

**Table 10** NMR data of compound **4** ($CDCl_3$, $^{1}$H 300 MHz, $^{13}$C 75.45 MHz, δ in ppm, *J* in Hz).

| Position | $^{1}$H (*J* in Hz) | | $^{13}$C | DEPT | HMBC |
|---|---|---|---|---|---|
| **1** | 7.72 | br s | 161.0 | CH | - |
| **2** | - | - | 138.0 | C | 1 |
| **3** | - | - | 205.5 | C | 1, 4 |
| **4** | 2.81 | t (4.4) | 49.3 | CH | 1 |
| **5** | 6.48 | d (3.7) | 73.8 | CH | 7, 20 |
| **6** | - | - | 138.4 | C | 5, 11, 20 |
| **7** | 5.48 | d (4.9) | 130.0 | CH | 14, 20 |
| **8** | 2.46 | br s | 42.6 | CH | 7, 12, 18 |
| **9** | - | - | 78.9 | C | 4, 18 |
| **10** | 3.81 | m | 52.6 | CH | 1, 4, 5 |
| **11** | 1.70 | d (3.1) | 43.2 | CH | 12, 18 |
| **12** | 5.66 | d (9.6) | 77.7 | CH | 4, 11, 18 |
| **13** | - | - | 65.2 | C | 12, 14, 16, 17, 18 |

**Table 11** (continuation) NMR data of compound **4** ($CDCl_3$, $^1H$ 300 MHz, $^{13}C$ 75.45 MHz, δ in ppm, *J* in Hz).

| Position | $^1H$ (*J* in Hz) | | $^{13}C$ | DEPT | HMBC |
|---|---|---|---|---|---|
| **14** | 1.10 | d (1.6) | 36.8 | CH | 7, 16, 17 |
| **15** | - | - | 26.5 | C | 12, 14, 16, 17 |
| **16** | 1.23 | s | 23.8 | $CH_3$ | 14, 17 |
| **17** | 1.33 | s | 17.2 | $CH_3$ | 14, 16 |
| **18** | 1.00 | d (6.4) | 15.5 | $CH_3$ | 12 |
| **19** | 1.62 | dd (2.5; 1.3) | 10.2 | $CH_3$ | - |
| **20** | 1.75 | s | 21.7 | $CH_3$ | 7 |
| **5-OBz** | - | - | 165.4 | C | 5 |
| | - | - | 130.1 | C | - |
| | 7.84 | d (1.5) | 129.8 | CH | - |
| | 7.38 | t (7.6) | 128.4 | CH | - |
| | 7.52 | t (2.0) | 133.4 | CH | - |
| **12-OBz** | - | - | 166.1 | C | 12 |
| | - | - | 130.1 | C | - |
| | 8.01 | m | 129.8 | CH | - |
| | 7.48 | m | 128.7 | CH | - |
| | 7.58 | m | 133.1 | CH | - |
| **13-OiBu** | - | - | 179.6 | C | - |
| | 2.63 | m | 34.4 | CH | - |
| | 1.21 | d (3.4) | 18.7 | $CH_3$ | - |
| | 1.18 | s | 18.8 | $CH_3$ | - |

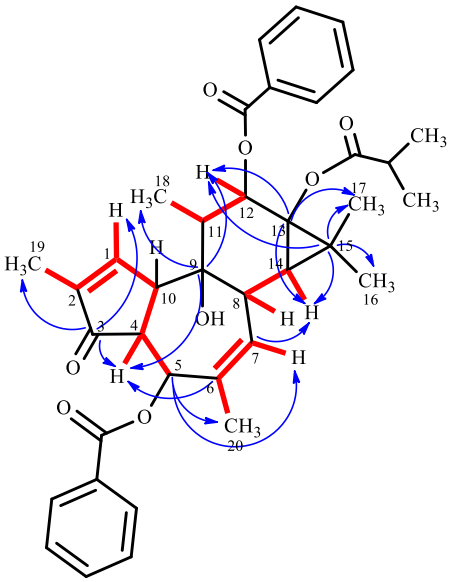

**Figure 11** $^1H$-spin systems of compound **4** assigned by HMQC and $^1H$-$^1H$ COSY (-) and their connection by the main $^2J_{C\text{-}H}$ and $^3J_{C\text{-}H}$ correlations displayed in the HMBC spectrum (→)

### *1.1.1.5. Euphoboetirane A*

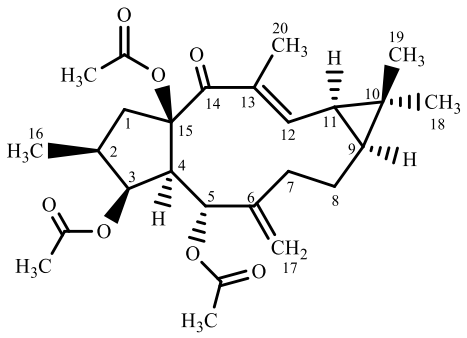

**5**

Compound **5** was obtained as a white powder. The IR spectrum displayed characteristic absorption bands for an α,β-unsaturated ketone (1644 $cm^{-1}$) and ester carbonyl groups (1736 $cm^{-1}$). The ESI-MS spectrum showed a protonated ion at *m/z* 461 $[M + H]^+$. The data obtained from the $^1$H-NMR and $^{13}$C-NMR spectra (Table 12) showed that this compound has a lathyrane scaffold. The $^{13}$C-NMR and DEPT spectra confirmed the existence of five quaternary carbons (two olefinic at $\delta_C$ 144.5 and 134.3, one oxygenated at $\delta_C$ 92.4 and one carbonylic at $\delta_C$ 197.0), seven methines (one olefinic at $\delta_C$ 146.9 and two oxygenated at $\delta_C$ 80.3 and 65.9), four methylenes ($\delta_C$ 21.7, 35.1, 48.4 and one exocyclic methylene at $\delta_C$ 115.7) and four methyl groups. Furthermore, three acetate groups were also observed (Table 12).

The combined analysis of HMQC and $^1$H-$^1$H-COSY spectra provided the data that allowed the establishment of two fragments of correlated protons (Figure 12) that were connected by the analysis of the long-range correlations ($^2J_{C\text{-}H}$ and $^3J_{C\text{-}H}$) provided by HMBC spectrum. Accordingly, the cross-peaks observed between the quaternary carbon C-15 ($\delta_C$ 92.4) and protons H-1α and H-4 allowed the establishment of the cyclopentane ring. The observed long-range correlations between the quaternary carbon C-6 ($\delta_C$ 144.5) and the protons H-5, H-8α and H-17α allowed the connection of the two fragments with the exocyclic double bond. The complete linkage of the fragments followed from the observed $^3J_{C\text{-}H}$ correlations of the carbonyl group at C-14 ($\delta_C$ 197.0) with H-1β and $CH_3$-20 (Figure 5). Finally, the long-range interaction between the carbons C-9 ($\delta_C$ 35.5) and C-11 ($\delta_C$ 28.5) and the protons H-18 ($\delta_H$ 1.12, s) and H-19 ($\delta_H$ 1.14, s) confirmed the existence of the cyclopropane ring. The relative configuration of compound **5** was deduced from the analysis of coupling constant values and a NOESY spectrum, assuming α orientation for H-4 and was found to be identical to other $\Delta^{6,17}$-lathyrane diterpenes isolated to date [93]. All data described above was in agreement with those reported in the literature allowing the identification of compound **5** as euphoboetirane A [93].

**Table 12** NMR data of compound **5** ($CDCl_3$, $^1H$ 300 MHz, $^{13}C$ 75.45 MHz, δ in ppm, *J* in Hz).

| Position | $^1H$ (*J* in Hz) | | $^{13}C$ | DEPT | HMBC |
|---|---|---|---|---|---|
| **1α** | 1.56 | dd (15.75; 8.7) | 48.4 | $CH_2$ | 3, 16 |
| **1β** | 3.42 | dd (12.3; 7.8) | | | |
| **2** | 2.24 | m | 37.3 | CH | 1α, 1β, 16 |
| **3** | 5.53 | t (3.75) | 80.3 | CH | 1β, 16 |
| **4** | 2.72 | dd (7.65; 2.55) | 52.3 | CH | 5 |
| **5** | 6.04 | d (7.8) | 65.9 | CH | 4, 17α, 17β |
| **6** | - | - | 144.5 | C | 5, 8α, 17α |
| **7α** | 1.11 | m | 35.1 | $CH_2$ | 5, 17α, 17β |
| **7β** | 2.20 | m | | | |
| **8α** | 1.69 | d (5.1) | 21.7 | $CH_2$ | 7β |
| **8β** | 2.07 | s | | | |
| **9** | 1.14 | m | 35.5 | CH | 18, 19 |
| **10** | - | - | 25.4 | C | 18, 19 |
| **11** | 1.38 | dd (8.7; 6.3) | 28.5 | CH | 18, 19 |
| **12** | 6.49 | dd (11.4; 1.2) | 146.9 | CH | - |
| **13** | - | - | 134.3 | C | 11, 20 |
| **14** | - | - | 197.0 | C | 1β, 4, 12, 20 |
| **15** | - | - | 92.4 | C | 1α, 3, 5 |
| **16** | 0.88 | d (5.1) | 14.2 | $CH_3$ | 1α |
| **17α** | 4.70 | s | 115.7 | $CH_2$ | 5 |
| **17β** | 4.97 | s | | | |
| **18** | 1.12 | s | 16.9 | $CH_3$ | 9, 11, 19 |
| **19** | 1.14 | s | 29.1 | $CH_3$ | 9, 18 |
| **20** | 1.66 | m | 12.6 | $CH_3$ | 12 |
| **3-OAc** | - | - | 170.9 | C | 3 |
| | 2.02 | s | 21.4 | $CH_3$ | - |
| **5-OAc** | - | - | 170.7 | C | 5 |
| | 1.96 | s | 21.0 | $CH_3$ | - |
| **15-OAc** | - | - | 170.0 | C | - |
| | 2.09 | s | 22.1 | $CH_3$ | - |

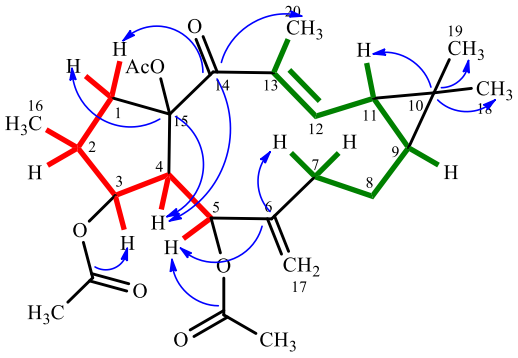


**Figure 12** $^1H$-spin systems of compound **5** assigned by HMQC and $^1H$-$^1H$ COSY (-) and their connection by the main $^2J_{C\text{-}H}$ and $^3J_{C\text{-}H}$ correlations displayed in the HMBC spectrum (➔)

### *1.1.1.6. Epoxyboetirane A*

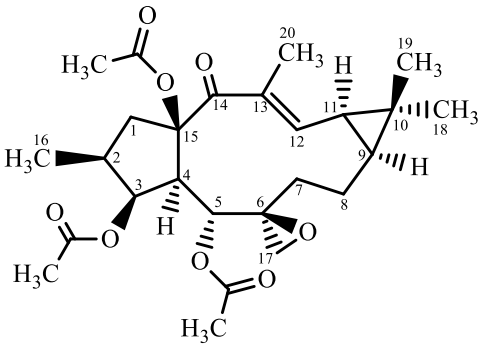

**6**

Compound **6** was isolated and identified as epoxyboetirane A. The IR spectrum displayed absorption bands for ester functions (1736 and 1256 $cm^{-1}$) and for an α,β-unsaturated ketone (1671 $cm^{-1}$). The ESI-MS spectrum exhibited a protonated molecule at *m/z* 477 $[M + H]^+$ that, together with the NMR data, allowed the establishment of the molecular formula $C_{26}H_{36}O_8$, from which nine degrees of unsaturation were deduced.

The $^1$H-NMR spectrum (Table 13) showed signals for two tertiary methyls (both displayed as singlets at $\delta_H$ 1.18), one secondary methyl group at $\delta_H$ 0.85 (d, $J$ = 6.7 Hz), one vinylic methyl group at $\delta_H$ 1.83 (s) and three downfield singlets ($\delta_H$ 2.00, 2.06 and 2.08) that suggested the presence of three acetyl groups. Signals corresponding to two oxymethine protons ($\delta_H$ 5.44 t, $J$ = 3.1 Hz; 6.19 d, $J$ = 9.3 Hz), one diastereotopic oxymethylene group ($\delta_H$ 2.29 br s; 2.46 d, $J$ = 3.4 Hz) and one olefinic proton at $\delta_H$ 6.57 (d, $J$ = 11.4 Hz), were also observed.

Besides the signals due to the ester functions, the $^{13}$C-NMR spectrum (Table 13) exhibited twenty carbon resonances, that were discriminated by a DEPT experiment as four methyl groups, four methylenes (one oxygenated at $\delta_C$ 55.4), seven methines (one olefinic at $\delta_C$ 143.9 and two oxygenated at $\delta_C$ 80.4 and 65.3), and five quaternary carbons (two oxygenated at $\delta_C$ 59.0 and 91.9, one $sp^2$ carbon at $\delta_C$ 136.1 and a carbonyl group at $\delta_C$ 197.0). The high-field carbonyl signal at $\delta_C$ 197.0 together with the olefinic proton at $\delta_H$ 6.57 ($\delta_C$ 143.9) confirmed the presence of an α,β-unsaturated ketone. On the other hand, the high field quaternary carbon at $\delta_C$ 25.7, pointed out to the existence of a gem-dimethyl-cyclopropane ring. Based on all these data, a lathyrane-type diterpene skeleton was proposed for compound **6**. The unambiguous assignment of the all proton and carbon resonances was possible through the combined analysis of 2D-NMR spectra, namely COSY, HMQC and HMBC.

In particular, $^{1}$H-$^{1}$H-COSY and HMQC spectra defined two structural fragments with correlated protons (Figure 6), which are separated by quaternary carbons. The linkage of these fragments was possible through the $^{2}J_{C\text{-}H}$ and $^{3}J_{C\text{-}H}$ correlations displayed in the HMBC spectrum, namely those between C-14 and H-1α, H-1β, H- 4 and H-20, which locate the carbonyl group at C-14 and build up the cyclopentane ring. Moreover, the heteronuclear $^{2}J_{C\text{-}H}$ and $^{3}J_{C\text{-}H}$ correlations allowed the assignment of an epoxy ring at C-6/C- 17, which was connected to the two fragments due to the observed correlations between C-5 ($\delta_C$ 65.3) and C-7 ($\delta_C$ 33.6) with $CH_2$-17. Analysis of HMBC spectrum also allowed the location of the acetyl groups at C-3 and C-5. The lack of $^{3}J_{C\text{-}H}$ correlations between the carbonyl carbon at $\delta_C$ 170.7 and oxymethine protons allowed the assignment of the third acetyl group at C-15. The location of this third acetyl group was also corroborated by the downfield chemical shift of C-15 [13].

The relative configuration of compound **6** was deduced through the analysis of a NOESY spectrum and by comparison of the coupling constant values with those reported in the literature for epoxyboetirane A [13].

**Table 13** NMR data of compound **6** ($CDCl_3$, $^1H$ 300 MHz, $^{13}C$ 75.45 MHz, δ in ppm, *J* in Hz).

| Position | $^1H$ (*J* in Hz) | | $^{13}C$ | DEPT | HMBC |
|---|---|---|---|---|---|
| **1α** | 3.38 | dd (14.4; 8.4) | 48.0 | $CH_2$ | 3, 16 |
| **1β** | 1.48 | m | | | |
| **2** | 2.10 | m | 37.6 | CH | 1, 16 |
| **3** | 5.44 | t (3.4) | 80.4 | CH | 1, 16 |
| **4** | 1.86 | dd (9.2; 3.6) | 50.1 | CH | 1α, 5 |
| **5** | 6.19 | t (9.3) | 65.3 | CH | 4, 7, 17 |
| **6** | - | - | 59.0 | C | 4, 5, 7, 17 |
| **7α** | 0.90 | m | 33.6 | $CH_2$ | 5, 17 |
| **7β** | 2.11 | m | | | |
| **8** | 1.70 | m | 20.1 | $CH_2$ | - |
| **9** | 1.07 | m | 34.3 | CH | 11, 18, 19 |
| **10** | - | - | 25.7 | C | 11, 18, 19 |
| **11** | 1.46 | m | 29.1 | CH | 9, 18, 19 |
| **12** | 6.57 | d (11.6) | 143.9 | CH | 20 |
| **13** | - | - | 136.1 | C | 11, 20 |
| **14** | - | - | 197.0 | C | 1, 4, 12 |
| **15** | - | - | 91.9 | C | 1, 3, 5 |
| **16** | 0.85 | d (6.4) | 14.1 | $CH_3$ | - |
| **17α** | 2.29 | br s | 55.4 | $CH_2$ | - |
| **17β** | 2.46 | d (3.4) | | | |
| **18** | 1.18 | s | 29.0 | $CH_3$ | 11, 19 |
| **19** | 1.18 | s | 16.8 | $CH_3$ | 18 |
| **20** | 1.83 | s | 12.5 | $CH_3$ | - |
| **3-OAc** | - | - | 170.4 | C | 3 |
| | 2.00 | s | 20.9 | $CH_3$ | - |
| **5-OAc** | - | - | 170.7 | C | 5 |
| | 2.06 | s | 21.1 | $CH_3$ | - |
| **15-OAc** | - | - | 165.9 | C | - |
| | 2.08 | s | 22.0 | $CH_3$ | - |

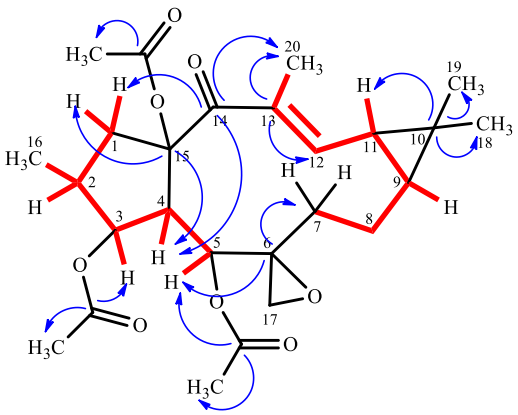

**Figure 13** $^1H$- spin systems of compound **6** assigned by HMQC and $^1H$-$^1H$ COSY (-) and their connection by the main $^2J_{C\text{-}H}$ and $^3J_{C\text{-}H}$ correlations displayed in the HMBC spectrum (➔)

### *1.1.1.7. Epoxyboetirane K*

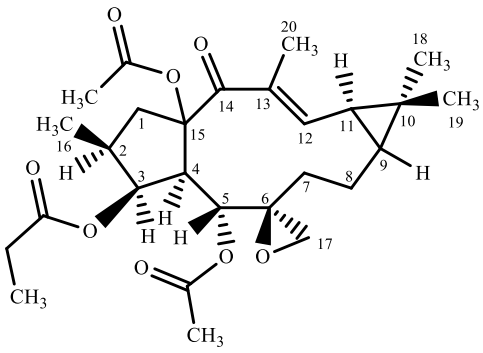

**7**

Compound **7** was obtained as white crystals (m.p. 205 ºC). The IR spectrum displayed absorption bands for ester carbonyl groups (1738 $cm^{-1}$) and α,β-unsaturated ketone (1652 $cm^{-1}$). The data obtained from the $^{1}$H-NMR and $^{13}$C-NMR spectra (Table 14) suggested that the compound is a macrocyclic diterpene with the lathyrane scaffold similar to compound **6** [13]. The $^{13}$C-NMR and DEPT spectra confirmed the existence of four methylenes ($\delta_C$ 20.1, 337.0 and 48.1 and one oxygenated at $\delta_C$ 55.6) and five quaternary carbons (of which two oxygenated at $\delta_C$ 59.0 and 91.9, one olefinic at $\delta_C$ 136.1 and one carbonyl group at $\delta_C$ 197.0). The $^{1}$H-NMR spectrum established the existence of two oxymethine protons $\delta_H$ 5.48 (t, $J$ = 3.2 Hz) and $\delta_H$ 6.17 (d, $J$ = 9.2 Hz) and one olefinic proton $\delta_H$ 6.56 (d, $J$ = 11.6 Hz).

The analysis of spectroscopic data led to the conclusion that compounds **6** and **7** were rather similar. The major difference resided on the presence of signals corresponding to a propanoyl group at C-3 in compound **7** ($\delta_H$ 2.29 d, $J$ = 2.7 Hz; 1.1 t, $J$ = 7.6 Hz and $\delta_C$ 173.6, 27.8, 9.1) instead of the acetyl group in compound **6**. The structure of **7** was confirmed by $^{1}$H-$^{1}$H COSY, HMQC and HMBC experiments that allowed the unequivocal assignment of all $^{1}$H and $^{13}$C signals. The relative stereochemistry of all tetrahedral centres was found to be identical to those of compound **6**. From the above data, it was concluded that compound **7** was an already isolated diterpene named epoxyboetirane K [13, 94].

**Table 14** NMR data of compound **7** ($CDCl_3$, $^1H$ 300 MHz, $^{13}C$ 75.45 MHz, δ in ppm, *J* in Hz).

| Position | $^1H$ (*J* in Hz) | | $^{13}C$ | DEPT | HMBC |
|---|---|---|---|---|---|
| **1α** | 1.50 | dd (9.2; 3.6) | 48.1 | $CH_2$ | 3, 16 |
| **1β** | 3.39 | dd (11.4; 8.4) | | | |
| **2** | 2.11 | m | 37.7 | CH | 1α, 1β, 16 |
| **3** | 5.48 | t (3.2) | 80.2 | CH | 1β, 4, 16 |
| **4** | 1.87 | dd (11.0; 3.2) | 50.1 | CH | 1β, 2, 5 |
| **5** | 6.17 | d (9.2) | 65.3 | CH | 4, 7α, 9, 17β |
| **6** | - | - | 59.0 | C | 4, 5, 7α, 8α, 8β, 17α, 17β |
| **7α** | 0.89 | t (12.8) | 33.7 | $CH_2$ | 5, 9, 17β |
| **7β** | 2.11 | m | | | |
| **8α** | 1.69 | t (6.8) | 20.1 | $CH_2$ | 7α, 11 |
| **8β** | 2.02 | m | | | |
| **9** | 1.06 | m | 34.9 | CH | 7α, 8α, 8β, 11, 12, 18, 19 |
| **10** | - | - | 25.7 | C | 9, 18, 19 |
| **11** | 1.46 | m | 29.1 | CH | 8β, 18, 19 |
| **12** | 6.56 | d (11.6) | 143.9 | CH | 9, 20 |
| **13** | - | - | 136.1 | C | 12, 20 |
| **14** | - | - | 197.0 | C | 1α, 4, 12, 20 |
| **15** | - | - | 91.9 | C | 1α, 1β, 2, 3, 4, 5 |
| **16** | 0.83 | d (6.8) | 14.1 | $CH_3$ | 1α, 1β |
| **17α** | 2.29 | m | 55.6 | $CH_2$ | 7α |
| **17β** | 2.46 | d (3.6) | | | |
| **18** | 1.18 | s | 29.0 | $CH_3$ | 9, 11, 19 |
| **19** | 1.18 | s | 16.8 | $CH_3$ | 11, 18 |
| **20** | 1.82 | s | 12.5 | $CH_3$ | 12 |
| **3-OPr** | - | - | 173.6 | C | 2', 3' |
| | 2.29 | d (2.7) | 27.8 | $CH_2$ | 3' |
| | 1.10 | t (7.6) | 9.1 | $CH_3$ | 2' |
| **5-OAc** | - | - | 170.7 | C | 5 |
| | 2.04 | s | 21.1 | $CH_3$ | - |
| **15-OAc** | - | - | 169.8 | C | - |
| | 2.07 | s | 21.9 | $CH_3$ | - |

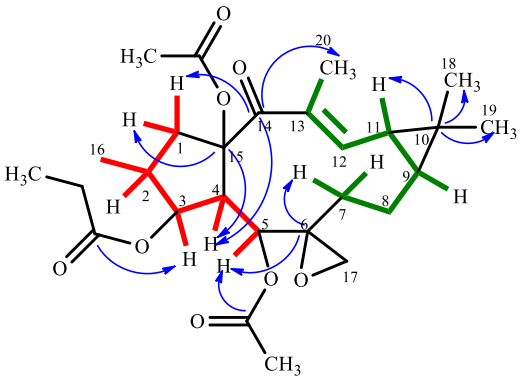

**Figure 14** $^{1}$H-spin system of compound **7** assigned by HMQC and $^{1}$H-$^{1}$H COSY (-) and their connection by the main $^{2}J_{C\text{-}H}$ and $^{3}J_{C\text{-}H}$ correlations displayed in the HMBC spectrum (→)

#### *1.1.1.8. Methyl gallate*

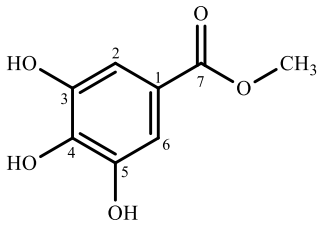

**8**

Compound **8** was isolated as white crystals (m.p. 204 ºC) and identified as methyl gallate based on its spectroscopic data.

The $^{1}$H-NMR spectrum exhibited two singlet signals at $\delta_H$ 7.03 and 3.80, which hinted at a very simple structure (Table 15). On the other hand, the $^{13}$C-NMR spectrum exhibited six carbon signals: five quaternary (one carbonyl at $\delta_C$ 167.6), two methines and one oxygenated at $\delta_C$ 50.9. These NMR data were consistent with those published in the literature for the methyl ester of 3,4,5-trihydroxybenzoic acid or methyl gallate [95, 96].

**Table 15** NMR data of compound **8** ($MeOD_4$, $^{1}$H 300 MHz, $^{13}$C 75.45 MHz, δ in ppm, *J* in Hz).

| Position | $^{1}$H (*J* in Hz) | | $^{13}$C | DEPT |
|---|---|---|---|---|
| **1** | - | - | 126.3 | C |
| **2** | 7.03 | s | 106.8 | CH |
| **3** | - | - | 153.0 | C |
| **4** | - | - | 142.2 | C |
| **5** | - | - | 153.0 | C |
| **6** | 7.03 | s | 106.8 | C |
| **7** | - | - | 166.9 | C |
| **7-$OCH_3$** | 3.8 | s | 52.4 | $CH_3$ |

### *1.1.1.9. 24-Methylenecycloartanol*

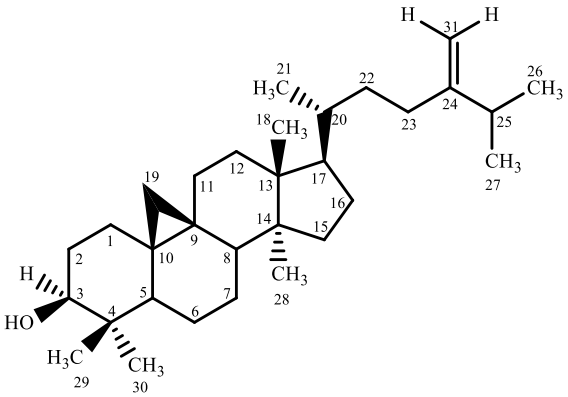

**9**

Compound **9**, named 24-methylenecycloartanol, was obtained as white crystals (m.p. 120 ºC). The IR spectrum displayed absorption bands for a hydroxyl group (3371 $cm^{-1}$). The data obtained from the $^{1}$H-NMR and $^{13}$C-NMR spectra (Tables 16 and 17) suggested that this compound was a cycloartane-type triterpene.

The $^{1}$H-NMR spectrum exhibited two highly shielded doublets at $\delta_H$ 0.33 (d, *J* = 4.1 Hz) and $\delta_H$ 0.55 (d, *J* = 4.0 Hz). The $^{1}$H-NMR spectrum also showed the presence of seven methyl groups, four of which were singlets and three were displayed as doublets at $\delta_H$ 0.88 (d, *J* = 1.3 Hz), $\delta_H$ 1.01 (d, *J* = 1.7 Hz) and $\delta_H$ 1.03 (d, *J* = 1.7 Hz). Moreover, an axial hydroxymethine at $\delta_H$ 3.28 (m), and two exomethylene protons displayed as broad singlets at $\delta_H$ 4.66 and $\delta_H$ 4.71 could also be observed.

The $^{13}$C-NMR spectrum displayed thirty-one carbon signals that were discriminated by a DEPT experiment as seven methyls, eleven methylenes (one $sp^2$ at $\delta_C$ 106.1), six methines (one oxygen-bearing carbon at $\delta_C$ 79.0) and five quaternary carbons (one olefinic at $\delta_C$ 157.1).

All data described above was in agreement with those reported in the literature allowing the identification of compound **9** as 24-methylenecycloartanol [97].

**Table 16** $^{1}$H NMR data for compound **9** ($CDCl_3$, $^{1}$H 300 MHz, δ in ppm, *J* in Hz)

| Position | $^{1}$H (*J* in Hz) | |
|---|---|---|
| **3** | 3.28 | dd (11.0; 4.4) |
| **18** | 0.96 | s |
| **19α** | 0.55 | d (4.23) |
| **19β** | 0.33 | d (4.21) |
| **21** | 0.88 | d (1.7) |
| **23** | 5.29 | s |
| **26** | 1.30 | s |
| **27** | 1.03 | d (1.7) |
| **28** | 0.89 | s |
| **29** | 1.01 | d (1.7) |
| **30** | 0.80 | s |
| **31α** | 4.66 | d (1.5) |
| **31β** | 4.71 | d (1.8) |

**Table 17** $^{13}$C NMR data for compound **9** ($CDCl_3$, $^{13}$C 75.45 MHz, δ in ppm)

| Position | $^{13}$C | DEPT |
|---|---|---|
| **1** | 32.1 | $CH_2$ |
| **2** | 30.5 | $CH_2$ |
| **3** | 79.0 | CH |
| **4** | 40.6 | C |
| **5** | 47.2 | CH |
| **6** | 21.3 | $CH_2$ |
| **7** | 28.3 | $CH_2$ |
| **8** | 48.1 | CH |
| **9** | 20.1 | C |
| **10** | 26.2 | C |
| **11** | 26.2 | $CH_2$ |
| **12** | 35.7 | $CH_2$ |
| **13** | 45.4 | C |
| **14** | 48.9 | C |
| **15** | 32.9 | $CH_2$ |
| **16** | 26.6 | $CH_2$ |
| **17** | 52.4 | CH |
| **18** | 18.2 | $CH_3$ |
| **19** | 29.9 | $CH_2$ |
| **20** | 36.3 | $CH_3$ |
| **21** | 18.4 | CH |
| **22** | 31.5 | $CH_2$ |
| **23** | 29.5 | $CH_2$ |
| **24** | 157.1 | C |
| **25** | 33.9 | CH |
| **26** | 22.0 | $CH_3$ |
| **27** | 22.1 | $CH_3$ |
| **28** | 19.5 | $CH_3$ |
| **29** | 25.6 | $CH_3$ |
| **30** | 14.2 | $CH_3$ |
| **31** | 106.1 | $CH_2$ |

### *1.1.2. Euphorbia pubescens*

#### *1.1.2.1. Euphopubescenol*

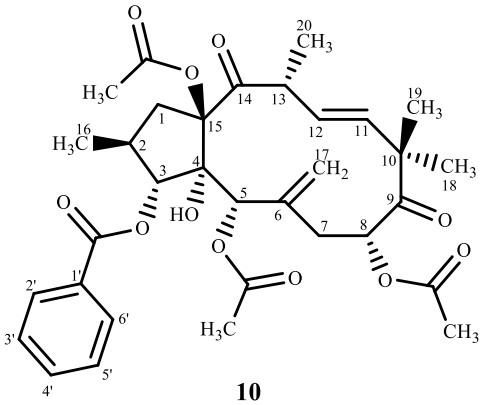

**10**

Compound **10** was obtained as a white amorphous powder.

The $^{1}$H-NMR spectrum showed signals for two tertiary methyl groups at $\delta_H$ 1.22 (s) and $\delta_H$ 1.46 (s), two secondary methyl groups at $\delta_H$ 1.24 (d, $J$ = 6.8 Hz) and 1.38 (m), and three protons geminal to the ester functions at $\delta_H$ 4.86 (s), 5.61 (d, $J$ = 18.1, 9.8 Hz), and 5.67 (d, $J$ = 9.1 Hz). Two double bonds were also observed, one endocyclic at $\delta_H$ 5.90 (m) and $\delta_H$ 5.93 (s) and an exocyclic one at $\delta_H$ 5.12 (br s) and 4.86 (br s). A proton signal at $\delta_H$ 3.47 without correlation in the HMQC spectrum suggested the existence of a hydroxyl group in the molecule.

Besides the signals due to the ester functions, the $^{13}$C-NMR spectrum (Table 18) exhibited thirty-carbon resonances, that were discriminated by a DEPT experiment as four methyl groups ($\delta_C$ 17.8, 24.6 and 20.0), three methylenes (one $sp^2$ at $\delta_C$ 116.9), seven methines (two $sp^2$ at $\delta_C$ 136.9 and 132.8 and three oxymethines at $\delta_C$ 77.9, 73.3 and 72.4), six quaternary carbons (two carbonyl groups at $\delta_C$ 208.2 and 204.6, one oxygenated carbon at $\delta_C$ 82.9 and an olefinic carbon at $\delta_C$ 140.2). The combined analysis of 2D-NMR spectra allowed the unambiguous assignment of all $^{1}$H and $^{13}$C resonances (Figure 15).

The compound was identified as euphopubescenol and all of the spectroscopic data was in agreement with the literature [98].

**Table 18** NMR data of compound **10** ($CDCl_3$, $^1H$ 300 MHz, $^{13}C$ 75.45 MHz, δ in ppm, *J* in Hz).

| Position | $^1H$ (*J* in Hz) | | $^{13}C$ | DEPT | HMBC |
|---|---|---|---|---|---|
| **1α** | 2.41 | dd (10.4; 1.6) | 38.9 | $CH_2$ | 16 |
| **1β** | 2.41 | dd (10.4; 1.6) | | | |
| **2** | 2.91 | m | 36.9 | CH | 1α, 1β, 16, |
| **3** | 5.61 | d (10.5) | 77.9 | CH | 1α, 1β, 16 |
| **4** | - | - | 82.9 | C | - |
| **5** | 4.86 | s | 73.3 | CH | 17α, 17β |
| **6** | - | - | 140.2 | C | 7α, 7β,8, 17α, 17β |
| **7α** | 1.71 | dd (14.9; 9.2) | 36.0 | $CH_2$ | 5, 8, 17α, 17β, |
| **7β** | 2.00 | s | | | |
| **8** | 5.67 | d (9.1) | 72.4 | CH | 7α |
| **9** | - | - | 208.2 | C | 18, 19 |
| **10** | - | - | 50.7 | C | 11, 12, 18, 19 |
| **11** | 5.91 | m | 136.9 | CH | 13, 18, 19 |
| **12** | 5.84 | s | 132.8 | CH | 20 |
| **13** | 3.84 | m | 46.9 | CH | 11, 12, 20 |
| **14** | - | - | 204.6 | C | 1α, 1β, 20 |
| **15** | - | - | 94.6 | C | 1α, 1β, 5 |
| **16** | 1.24 | d (6.8) | 17.8 | $CH_3$ | 1α, 1β, 3, 12, 18, 19 |
| **17α** | 4.85 | s | 116.9 | $CH_2$ | 5, 7α, 7β |
| **17β** | 5.12 | br s | | | |
| **18** | 1.22 | s | 24.6 | $CH_3$ | 11, 19 |
| **19** | 1.46 | s | 24.6 | $CH_3$ | 11, 18 |
| **20** | 1.38 | d (6.5) | 20.2 | $CH_3$ | - |
| **3-OBz** | - | - | 166.6 | C | 3, 2', 6' |
| | - | - | 129.1 | C | - |
| | 7.97 | m | 130.2 | CH | - |
| | 7.43 | m | 128.5 | CH | - |
| | 7.57 | m | 133.7 | CH | - |
| **5-OAc** | - | - | 168.4 | C | 5 |
| | 2.08 | s | 20.7 | $CH_3$ | - |
| **8-OAc** | - | - | 169.9 | C | - |
| | 1.91 | s | 20.4 | $CH_3$ | - |
| **15-OAc** | - | - | 168.9 | C | - |
| | 2.16 | s | 21.1 | $CH_3$ | - |

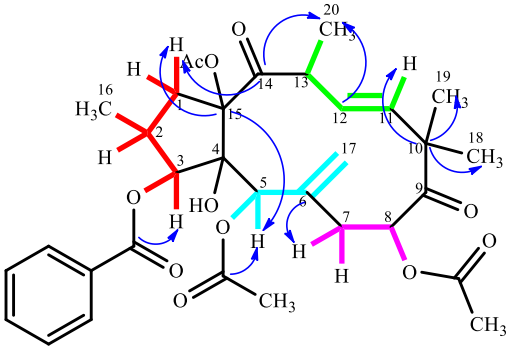

**Figure 15** $^{1}$H-spin systems of compound **10** assigned by HMQC and $^{1}$H-$^{1}$H COSY (-) and their connection by the main $^{2}J_{C\text{-}H}$ and $^{3}J_{C\text{-}H}$ correlations displayed in the HMBC spectrum (➔).

### *1.1.2.2. Helioscopinolide A*

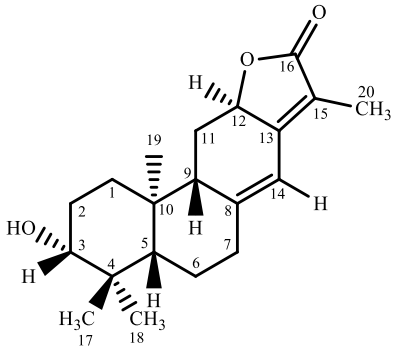

**11**

Compound **11** was isolated as white crystals (m.p. 205 ºC). This compound was identified as helioscopinolide A on the basis of the comparison of its spectroscopic data to those found in the literature [99].

The $^{1}$H-NMR spectrum showed signals for three tertiary methyl groups displayed as singlets at $\delta_H$ 0.81, 0.92 and 1.02 and one vinylic methyl at $\delta_H$ 1.82 (d, $J$ = 1.6 Hz). Moreover, this spectrum also showed signals for an olefinic proton at $\delta_H$ 6.27 (s) and two protons on oxygen-bearing carbons at $\delta_H$ 3.27 (dd, $J$ = 11.6 and 4.4 Hz) and 4.85 (ddd, $J$ = 13.5, 6.2 and 1.8 Hz).

The $^{13}$C-NMR spectrum revealed the presence of twenty signals, discriminated by a DEPT experiment as four methyl groups (one vinylic at $\delta_C$ 8.4), five methylenes, five methines (two of which oxygenated at $\delta_C$ 76.0 and 78.7 and one olefinic at $\delta_C$ 114.3), and six quaternary carbons (one carbonyl at $\delta_C$ 175.4, and three olefinic at $\delta_C$ 116.6, 151.6 and 156.2).

All the spectroscopic data was compared to those described in the literature [99] and confirmed that this compound was an *ent*-abietane diterpenic lactone, identified as helioscopinolide A.

**Table 19** NMR data of compound **11** ($CDCl_3$, $^1H$ 300 MHz, $^{13}C$ 75.45 MHz, δ in ppm, *J* in Hz).

| Position | $^1H$ (*J* in Hz) | | $^{13}C$ | DEPT | HMBC |
|---|---|---|---|---|---|
| **1** | 1.95 | dt (13.1; 3.6) | 37.5 | $CH_2$ | 19, 3, 10, 5 |
| **2** | 1.62 | m | 27.7 | $CH_2$ | 20 |
| **3** | 3.27 | dd (11.6; 4.4) | 78.7 | CH | 18, 17, 4 |
| **4** | - | - | 39.2 | C | 18 |
| **5** | 1.14 | dd (12.5; 2.5) | 54.5 | CH | 19, 6, 17, 9, 3 |
| **6** | 1.87 | dt (5.2; 2.5) | 23.6 | $CH_2$ | 16, 13, 8, 15, |
| **7** | 2.49 | m | 37.1 | $CH_2$ | 14, 9, 5, 8 |
| **8** | - | - | 151.6 | C | - |
| **9** | 2.16 | d (8.9) | 51.7 | CH | 19, 2, 1, 10, 5, 12, 14, 8, 13, |
| **10** | - | - | 41.3 | C | - |
| **11** | 2.53 | m | 27.7 | $CH_2$ | 6, 10, 9, 12, 14, 8, 13, 5 |
| **12** | 4.85 | ddd (13.5; 6.2; 1.8) | 76.0 | CH | 11, 13 |
| **13** | - | - | 156.2 | C | - |
| **14** | 6.27 | s | 114.3 | CH | 7, 9, 12, 15, 13 |
| **15** | - | - | 116.6 | C | - |
| **16** | - | - | 175.4 | C | - |
| **17** | 1.02 | s | 28.8 | $CH_3$ | 18, 4, 5, 3 |
| **18** | 0.81 | s | 15.7 | $CH_3$ | 2, 3, 4, 5 |
| **19** | 0.92 | s | 16.8 | $CH_3$ | 12, 5, 9, 10, 1 |
| **20** | 1.82 | d (1.6) | 8.4 | $CH_3$ | 16, 13, 15, 12 |

## 2. MOLECULAR DERIVATIZATION of methyl gallate

Considering the several biological activities of gallic acid derivatives described in the literature [100-103], and that methyl gallate (**8**) was isolated from *E. boetica* in large amount, some chemical transformations were carried out taking advantage of its simple structure and chemical reactivity (Figure 16).

Three main reactions were considered: i) methylation of the hydroxyl groups on the aromatic ring by reaction with dimethylsulfate, obtaining methyl 3,4,5-trimethoxybenzoate (**8.1**); ii) reaction of methyl 3,4,5-trimethoxybenzoate with hydrazine yielding 3,4,5-trimethoxybenzohydrazide (**8.2**); iii) condensation of the 3,4,5-trimethoxybenzohydrazide (**8.2**) with aromatic aldehydes to yield imines **8.3**-**8.5**. The chemical structures of all the compounds were deduced from their NMR data.

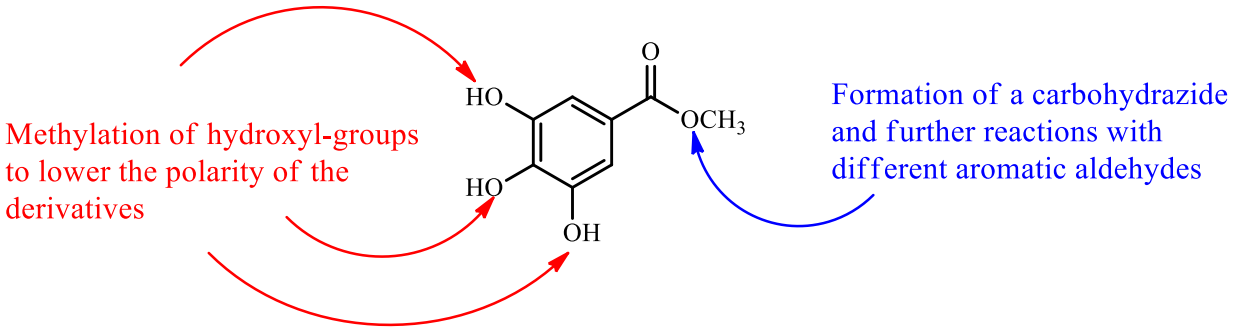


**Figure 16** Chemical functions of methyl gallate (**8**) used to perform the derivatization reactions.

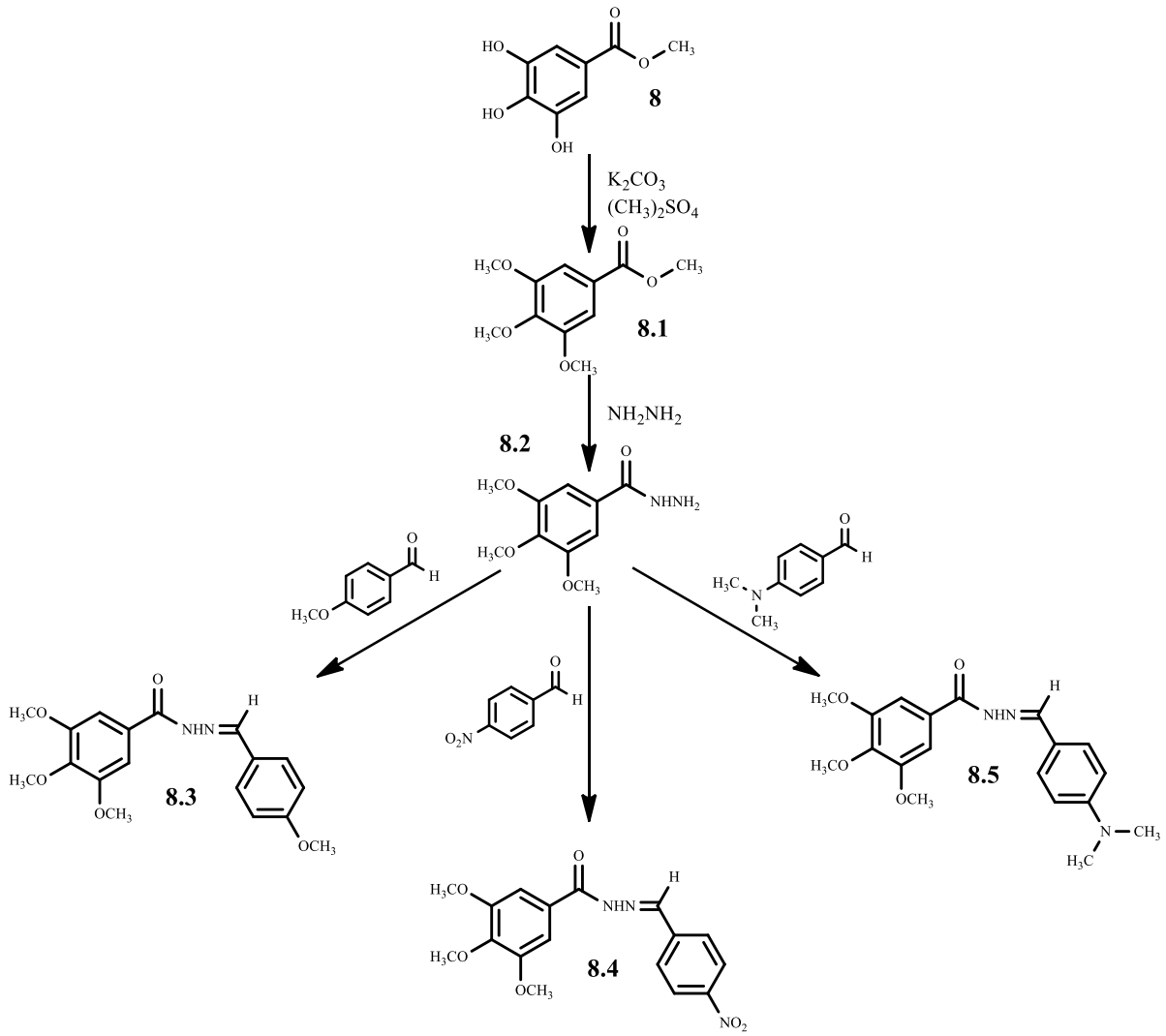


**Scheme 3** General representation of methyl gallate (**8**) derivatives (**8.1-8.5**).

## 2.1. Methylation of methyl gallate and formation of the carbohydrazide

The first chemical transformation carried out was the methylation of the hydroxyl groups linked to the benzene ring of methyl gallate (**8**). Methyl gallate (**8**) was suspended in acetone and combined with an excess of dimethylsulphate and $K_2CO_3$ yielding methyl 3,4,5-trimethoxybenzoate (**8.1**). After purification, **8.1** was suspended in ethanol, treated with $NH_2NH_2.H_2O$ 64% and refluxed for 24h. The solid obtained was filtered and recrystallized from hot methanol yielding 3,4,5-trimethoxybenzohydrazide (**8.2**) (78.5%) [103] (Scheme 4).

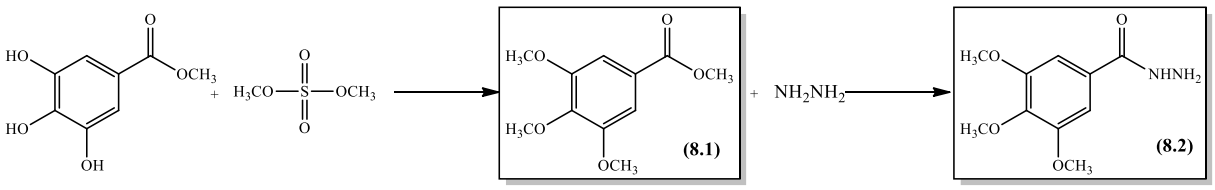


**Scheme 4** Transformation of **8** into **8.1** using dimethylsulfate and, subsequently, into **8.2** with hydrazine hydrate.

3,4,5-trimethoxybenzohydrazide (**8.2**) then underwent a condensation reaction with the aromatic aldehydes (Table 20) to yield the corresponding imines (**8.3-8-5**) (Scheme 5).

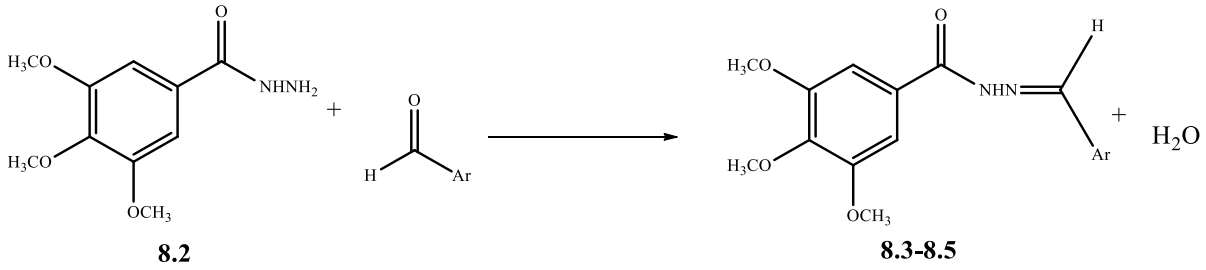


**Scheme 5** General reaction mechanism of 3,4,5-trimethoxybenzohydrazide (**8.2**) with aromatic aldehydes to yield compounds **8.3-8.5**.

**Table 20** Aromatic aldehydes used in the synthesis of imines **8.3-8-5**

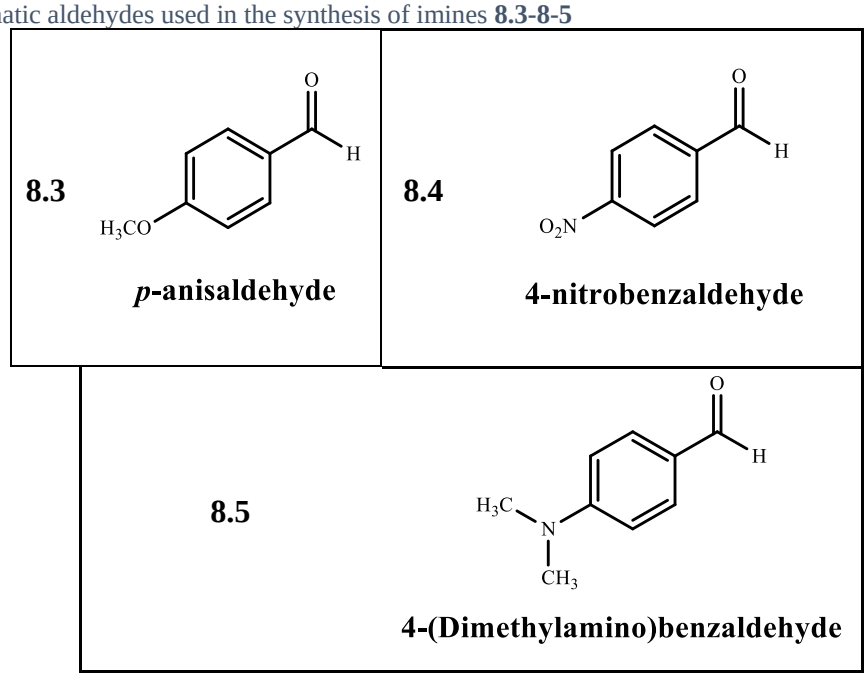


The structural elucidation of the derivatives **8.2-8.5** was achieved by comparison of their spectroscopic data with those of methyl gallate (**8**). It should be noted, however, that, due to poor spectral resolution of some of the derivatives when dissolved in $CDCl_3$, other solvents had to be used to overcome this problem, such as $MeOD_4$ and DMSO-$d_6$.

With the exception of the signals due to the three new methyl groups on positions 3, 4 and 5 and the new imine moiety (**8.1-8.5**), the analysis of $^{1}$H-NMR and $^{13}$C-NMR showed very similar data to that of methyl gallate (Tables 21 and 22).

**Table 21** $^{1}$H-NMR spectra for compounds **8-8.5** [$MeOD_4$ and $CDCl_3$, 300 MHz, δ (ppm), *J* (Hz)]

| Position | 8 ($MeOD_4$) | 8.1 ($CDCl_3$) | 8.2 ($MeOD_4$) | 8.3 ($CDCl_3$) | 8.4 ($CDCl_3$) | 8.5 ($CDCl_3$) |
|---|---|---|---|---|---|---|
| **2** | 7.03, s | 7.30, s | 7.15, s | 7.22, s | 7.25, s | 7.23, s |
| **6** | 7.03, s | 7.30, s | 7.15, s | 7.22, s | 7.25, s | 7.23, s |
| **3-OCH$_3$** | - | 3.90, s | 3.89, s | 3.86, s | 3.86, s | 3.75, s |
| **4-OCH$_3$** | - | 3.90, s | 3.81, s | 3.77, br s | 3.77, s | 3.78, s |
| **5-OCH$_3$** | - | 3.90, s | 3.89, s | 3.86, s | 3.86, s | 3.75, s |
| **7-OCH$_3$** | 3.8, s | 3.92, s | - | - | - | - |
| **2'** | - | - | - | 7.72, d (8.3) | 8.01, d (8.8) | 7.38, d (8.5) |
| **3'** | - | - | - | 6.92, d (8.3) | 8.23, d (8.8) | 6.42, d (8.47) |
| **4'-OCH$_3$** | - | - | - | 3.77, br s | - | - |
| **5'** | - | - | - | 6.92, d (8.3) | 8.23, d (8.8) | 6.42, d (8.47) |
| **6'** | - | - | - | 7.72, d (8.3) | 8.01, d (8.8) | 7.38, d (8.5) |
| **7'** | - | - | - | 8.25, s | 8.40, s | 8.28 |
| **N-(CH$_3$)$_2$** | - | - | - | - | - | 2.83, s |
| **CH=N** | - | - | - | - | - | 8.28, s |

**Table 22** $^{13}$C-NMR spectra for compounds **8-8.5** [$MeOD_4$ and $CDCl_3$, 300 MHz, δ (ppm), *J* (Hz)]

| Position | 8 ($MeOD_4$) | 8.1 ($CDCl_3$) | 8.2 ($MeOD_4$) | 8.3 ($MeOD_4$) | 8.4 ($MeOD_4$) | 8.5 ($CDCl_3$) |
|---|---|---|---|---|---|---|
| **1** | 126.3 | 129.5 | 129.5 | 130.6 | 129.5 | 129.3 |
| **2** | 106.8 | 105.8 | 105.8 | 106.3 | 106.5 | 104.9 |
| **3** | 153.0 | 154.5 | 154.5 | 154.5 | 154.6 | 151.9 |
| **4** | 142.2 | 142.1 | 142.1 | 141.8 | 141.6 | 140.9 |
| **5** | 106.8 | 105.8 | 105.8 | 154.5 | 154.6 | 104.9 |
| **6** | 153.0 | 154.5 | 154.5 | 106.3 | 106.5 | 151.9 |
| **7** | 166.9 | 169.1 | 169.1 | 163.2 | 164.1 | 164.1 |
| **3-$OCH_3$** | 56.4 | 56.7 | 56.7 | 56.8 | 56.9 | 56.3 |
| **4-$OCH_3$** | 61.1 | 61.1 | 61.1 | 61.2 | 61.3 | 61.0 |
| **5-$OCH_3$** | 56.4 | 56.7 | 56.7 | 56.8 | 56.9 | 56.3 |
| **7-$OCH_3$** | 52.4 | - | - | - | - | - |
| **1'** | - | - | - | 126.6 | 122.7 | 121.3 |
| **2'** | - | - | - | 128.0 | 125.0 | 128.9 |
| **3'** | - | - | - | 114.1 | 125.0 | 111.7 |
| **4'** | - | - | - | 163.1 | 149.8 | 153.2 |
| **5'** | - | - | - | 114.1 | 125.0 | 111.7 |
| **6'** | - | - | - | 128.0 | 125.0 | 128.9 |
| **7'** | - | - | - | 150.8 | 149.8 | 150.1 |
| **4'-$OCH_3$** | - | - | - | 55.9 | - | - |
| **4'-$N(\underline{CH_3})_2$** | - | - | - | - | - | 40.2 |

# Chapter III

## Experimental Section

# 1. GENERAL EXPERIMENTAL PROCEDURES

Analytical thin layer chromatography (TLC) was performed on precoated silica-gel $F_{254}$ plates (Merck 5554) and visualized under UV light (254 and 366 nm) and by spraying with $H_2SO_4$/MeOH (1:1) followed by heating. Preparative TLC chromatography was carried out on 20 x 20 cm silica plates (Merck 5774). Column chromatography (CC) was performed over $SiO_2$ (Merck 9385) or using CombiFlash® Rf 200 (Teledyne Isco) with $SiO_2$ or reverse-phase $C_{18}$ prepacked columns. Column chromatography on reverse-phase $C_{18}$ silica (YMC-GEL ODS-A 12nm S-50µm AA12S50) was also performed.

High-performance liquid chromatography (HPLC) was performed on a Merck-Hitachi instrument, with UV detection and a Merck-Hitachi integrator. Analytical studies and semi preparative HPLC were performed with Merck LiChrospher columns: 100 RP-18 (5 µm, 125 x 4 mm) and 100 RP-18 (10 µm, 250 x 10 mm), respectively. The HPLC study was carried out with several different mixtures of MeOH/$H_2O$ as mobile phase.

Infrared (IR) spectra were collected on an Affinity-1 (Shimadzu) FTIR spectrophotometer in KBr pellets and only the most significant absorption bands are reported.

NMR spectra were recorded on a Bruker Fourier 300 spectrometer ($^1$H 300 MHz; $^{13}$C 75 MHz) using $CDCl_3$, $CD_3OD$, DMSO-$d_6$ or $CD_3COCD_3$ as solvents. $^1$H and $^{13}$C chemical shifts are expressed in δ (ppm) and the proton coupling constants (*J*) in hertz (Hz).

Low resolution mass spectrometry (ESI-MS) was performed on a triple quadrupole (QT) mass spectrometer (Micromass Quattro Micro API, Waters) with ionization by electrospray (ESI), operating in positive mode.

# 2. PHYTOCHEMICAL STUDY OF *Euphorbia boetica*

## 2.1. Extraction and isolation

*Euphorbia boetica* Boiss. (Euphorbiaceae) was collected at Alcochete, Portugal (2014), and identified by Dr. Teresa Vasconcelos of Instituto Superior de Agronomia (ISA), University of Lisbon. A voucher has been deposited at the herbarium of ISA.

The air-dried powdered plant (17.2 kg) was extracted exhaustively with methanol at room temperature. Evaporation of the solvent (under vacuum, 40 °C) from the crude extract yielded a residue of 4.1 kg. This residue was resuspended in MeOH/$H_2O$ solution (1:2) and extracted with EtOAc. The ethyl acetate-soluble fraction was dried ($Na_2SO_4$) and evaporated under vacuum, yielding a residue (2.2 kg), which was chromatographed over $SiO_2$, using mixtures of *n*-hexane/EtOAc (1:0 to 0:1) and EtOAc/MeOH (9:1 to 3:7), in increasing gradients of 5%. According to differences in composition as indicated by TLC, seven crude fractions were obtained (fractions A−G) (Table 23). The process of extraction and fractionation were both conducted by other members of our Natural Products group.

**Table 23** Column chromatography of EtOAc extract (*E. boetica*).

| Fraction | Weight (g) |
|---|---|
| **A** | 110.7 |
| **B** | 8.965 |
| **C** | 68.43 |
| **D** | 62.88 |
| **E** | 181 |
| **F** | 259.49 |
| **G** | 23.9 |

### 2.1.1. Study of Fraction B

Fraction B (8.965 g, eluted with *n*-hexane/EtOAc 3:1), was chromatographed over $SiO_2$ (200 g) and eluted with mixtures of *n*-hexane/EtOAc with increasing polarity. According to differences in composition as indicated by TLC, ten fractions were obtained (Scheme 6).

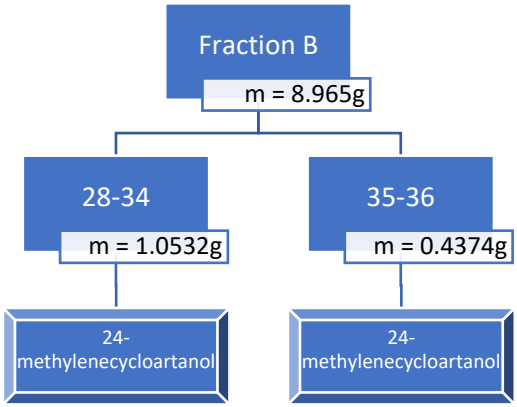


**Scheme 6** Overall workup of Fraction B.

#### *2.1.1.1. Study of fractions 28-34 and 35-36*

Fractions 28-34 (1.05 g) and 35-36 (0.42 g) were precipitated with *n*-hexane/EtOAc, yielding 0.8845 g of compound **9** as white crystals.

**24-Methylenecycloartanol (9)**

**White crystals**

**m.p.** 120 ºC (lit. 120-121 ºC) [104]

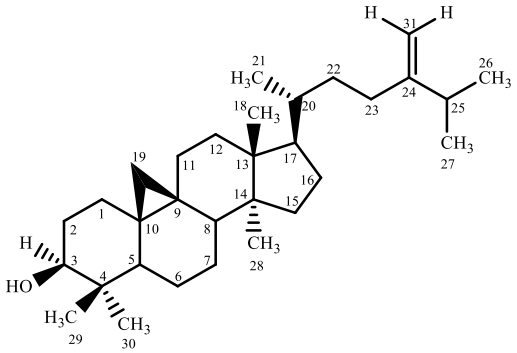

**9**

**$^1$H NMR (300 MHz, $CDCl_3$):** δ 0.33 (1H, d, *J* = 4.21 Hz, H-19β), 0.55 (1H, d, *J* = 4.23 Hz, H-19α), 0.80 (3H, s, $CH_3$-30), 0.88 (1H, d, *J* = 1.7 Hz, H-21), 0.89 (3H, s, $CH_3$-28), 0.96 (3H, s, $CH_3$-18), 1.01 (3H, d, *J* = 1.7 Hz, $CH_3$-29), 1.03 (3H, d, *J* = 1.7 Hz, $CH_3$-27), 1.3 (3H, s, $CH_3$-26), 3.28 (1H, dd, *J* = 11.0 and 4.4 Hz, H-3), 4.66 (1H, d, *J* = 1.5 Hz, H-31α), 4.71 (1H, d, *J* = 1.8 Hz, H-31β), 5.29 (2H, s, $CH_2$-23).

**$^{13}$C NMR (75.45 MHz, $CDCl_3$):** δ 32.1 (C-1), 30.5 (C-2), 79.0 (C-3), 40.6 (C-4), 47.2 (C-5), 21.3 (C-6), 28.3 (C-7), 48.1 (C-8), 20.1 (C-9), 26.2 (C-10), 26.2 (C-11), 35.7 (C-12), 45.4 (C-13), 48.9 (C-14), 32.9 (C-15), 26.6 (C-16), 52.4 (C-17), 18.2 (C-18), 29.9 (C-19), 36.3 (C-20), 18.4 (C-21), 31.5 (C-22), 29.5 (C-23), 157.1 (C-24), 33.9 (C-25), 22.0 (C-26), 22.1 (C-27), 19.5 (C-28), 25.6 (C-29), 14.2 (C-30), 106.1 (C-31).

### 2.1.2. Study of Fraction D

Fraction D (62.88 g, eluted with *n*-hexane/EtOAc 13:7 to 6:4) was subjected to chromatographic fractionation ($SiO_2$, 1 Kg) using mixtures of *n*-hexane/EtOAc (1:0 to 0:1) to yield fractions $D_1$ to $D_9$ (Scheme 7).

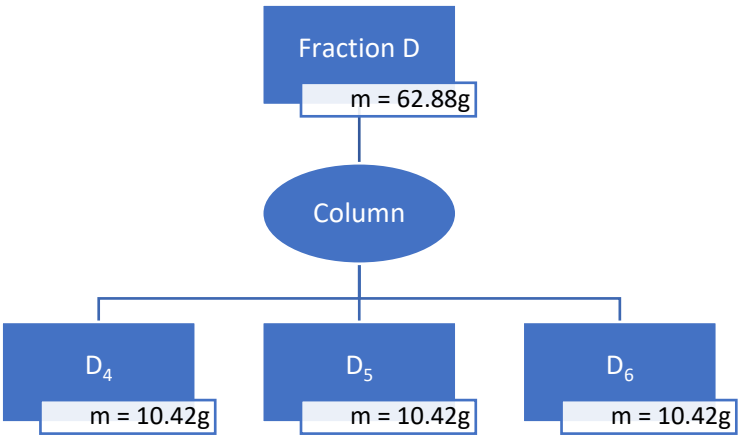


**Scheme 7** Overall workup of fraction D and studied subfractions.

#### *2.1.2.1. Study of fraction $D_4$*

Fraction $D_4$ (10.42 g) was chromatographed using a reverse-phase $C_{18}$ column (400 g; MeOH/$H_2O$, 1:1 to 1:0, 10% gradient) (Scheme 8).

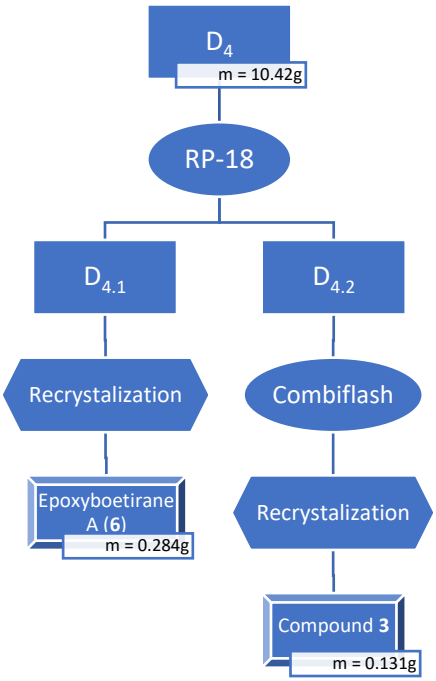


**Scheme 8** General workup of Fraction $D_4$ and isolated compounds.

Fraction $D_{4.1}$ (eluted with MeOH/$H_2O$ (7:3)) was evaporated and recrystallized, from *n*-hexane/EtOAc, to afford 0.284 g of compound **6** (Epoxyboetirane A).

**Epoxyboetirane A (6)**

**White amorphous powder**

**IR, $\nu_{max}$ cm$^{-1}$ (KBr):** 1736, 1671, 1256 (lit. 1734, 1671) [13]

**ESI-MS, *m/z*:** 477 $[M + H]^+$

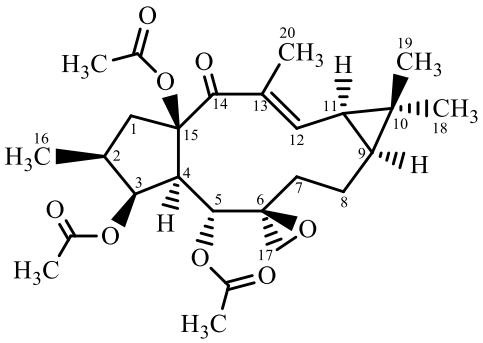

**6**

**$^1$H NMR (300 MHz, $CDCl_3$):** δ 0.85 (3H, d, *J* = 6.4 Hz, $CH_3$-16), 0.90 (1H, m, H-7α), 1.07 (1H, m, H-9), 1.18 (3H, s, $CH_3$-18), 1.18 (3H, s, $CH_3$-19), 1.46 (1H, m, H-11), 1.48 (1H, m, H-1β), 1.70 (2H, m, H-8), 1.83 (3H, s, $CH_3$-20), 1.86 (1H, dd, *J* = 9.2 and 3.6 Hz, H-4), 2.00 (3H, s, 3-OCO$\underline{CH_3}$), 2.06 (3H, s, 5-OCO$\underline{CH_3}$), 2.08 (3H, s, 15-OCO$\underline{CH_3}$), 2.1 (1H, m, H-2), 2.11 (1H, m, H-7β), 2.29 (1H, br s, H-17α), 2.46 (1H, d, *J* = 3.4 Hz, H-17β), 3.38 (1H, dd, *J* = 14.4 and 8.4 Hz, H-1α), 5.44 (1H, t, *J* = 3.4 Hz, H-3), 6.19 (1H, t, *J* = 9.3 Hz, H-5), 6.57 (1H, d, *J* = 11.6 Hz, H-12).

**$^{13}$C NMR (75.45 MHz, $CDCl_3$):** δ 48.0 (C-1), 37.6 (C-2), 80.4 (C-3), 50.1 (C-4), 65.3 (C-5), 59.0 (C-6), 33.6 (C-7), 20.1 (C-8), 34.3 (C-9), 25.7 (C-10), 29.1 (C-11), 143.9 (C-12), 136.1 (C-13), 197.0 (C-14), 91.9 (C-15), 14.1 (C-16), 55.4 (C-17), 29.0 (C-18), 16.8 (C-19), 12.5 (C-20), 170.4 (3-O<u>C</u>OCH$_3$), 20.9 (3-OCO<u>CH$_3$</u>), 170.7 (5-O<u>C</u>OCH$_3$), 21.1 (OCO<u>CH$_3$</u>), 165.9 (15-O<u>C</u>OCH$_3$), 22.0 (OCO<u>CH$_3$</u>).

Fraction D$_{4.2}$, eluted with MeOH/$H_2O$ (9:1), was evaporated, and the residue (1.2 g) was separated on a Combiflash system (120 g, RediSepRf) with *n*-hexane/EtOAc (1:0 to 0:1, 5% gradients; 7 ml/min). To obtain compound **3**, a sub fraction was recrystallized with *n*-hexane yielding 0.131 g of pure compound.

**Phorboboetirane A (3)**

**White crystals**

**IR, $\nu_{max}$cm$^{-1}$ (KBr):** 3303, 1757, 1699

**ESI-MS, *m/z*:** 517 $[M + H]^+$

**m.p.:** 190 $^oC$

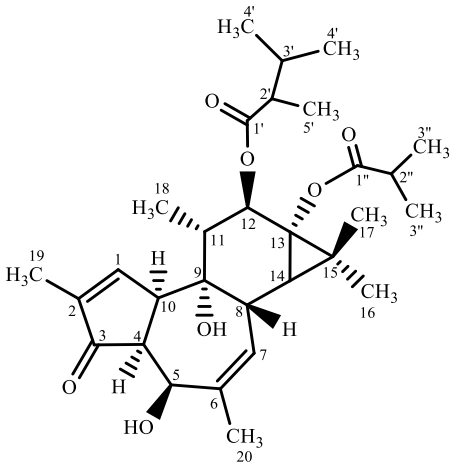

**3**

**$^1$H NMR (300 MHz, $CDCl_3$):** δ 0.76 (1H, d, *J* = 4.8 Hz, H-14), 0.96 (3H, d, *J* = 6.9 Hz, CH$_3$-4'), 0.98 (3H, d, *J* = 6.9 Hz, CH$_3$-4'), 1.09 (3H, d, *J* = 6.3 Hz, CH$_3$-18), 1.14 (3H, d, *J* = 4.5 Hz, CH$_3$-5'), 1.15 (3H, d, *J* = 4.5 Hz, CH$_3$-3''), 1.17 (3H, d, *J* = 6.8 Hz, CH$_3$-3''), 1.18 (3H, s, CH$_3$-17), 1.20 (3H, s, CH$_3$-16), 1.7 (1H, m, H-11), 1.80 (3H, s, CH$_3$-19), 1.89 (3H, t, *J* = 1.5 Hz, CH$_3$-20), 1.89 (1H, m, H-3'), 1.99 (1H, m, H-8), 2.22 (1H, m, H-2'), 2.55 (1H, m, H-2''), 3.12 (1H, dd, *J* = 6.6 and 4.5 Hz, H-4), 3.62 (1H, m, H-10), 4.44 (1H, d, *J* = 4.5 Hz, H-5), 4.85 (1H, br s, H-7), 5.47 (1H, m, H-12), 7.04 (1H, s, H-1).

**$^{13}$C NMR (75.45 MHz, $CDCl_3$):** δ 154.8 (C-1), 144.1 (C-2), 207.7 (C-3), 56.2 (C-4), 71.0 (C-5), 137.7 (C-6), 125.6 (C-7), 40.2 (C-8), 78.5 (C-9), 47.9 (C-10), 43.1 (C-11), 74.1 (C-12), 64.9 (C-13), 38.1 (C-14), 25.5 (C-15), 16.6 (C-16), 24.9 (C-17), 11.8 (C-18), 10.6 (C-19),

27.3 (C-20), 175.8 (C-1'), 47.4 (C-2'), 31.3 (C-3'), 20.9 (C-4'), 19.5 (C-4'), 18.6 (C-5'), 179.4 (C-1''), 34.4 (C-2''), 18.6 (C-3''), 14.7 (C-3'').

#### *2.1.2.2. Study of fraction $D_5$*

Fraction $D_5$ (10.42 g) was chromatographed through a reverse-phase $C_{18}$ column (400 g; MeOH/$H_2O$, 1:1-1:0) using increasing gradients of 10%) (Scheme 9).

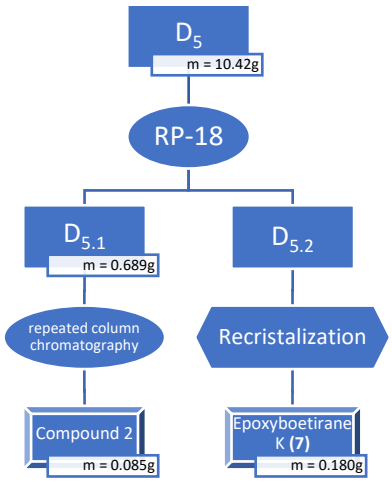


**Scheme 9** General workup of Fraction $D_5$ and isolated compounds.

Fraction $D_{5.1}$ (0.689 g, eluted with MeOH/$H_2O$ (7:3), was chromatographed over $SiO_2$ (40 g with *n*-hexane/$CH_2Cl_2$ (1:9 and 0:1) and $CH_2Cl_2$/acetone (1:0 to 9:1), used in increasing gradients of 1%. Some fractions were associated per their similarity as indicated by TLC (0.190 g) and further purified through chromatography over $SiO_2$ (30 g) with $CH_2Cl_2$/acetone (1:0 to 9:1, 0.5% gradient) yielding 0.085 g of compound **2**.

**Premyrsinol-3-propanoate-5-benzoate-7,13,17-triacetate (2)**

**White powder**

**IR, $\nu_{max}$cm$^{-1}$ (KBr):** 3487, 1739, 1700 (lit. 3450, 1745, 1660, 1370, 1297, 1241, 1136, 1031 cm$^{-1}$) [86]

**ESI-MS, *m/z*:** 671 $[M + H]^+$ (lit. 670.2989 $[M]^+$) [86]

**m.p.:** 190 °C (lit. N/A)

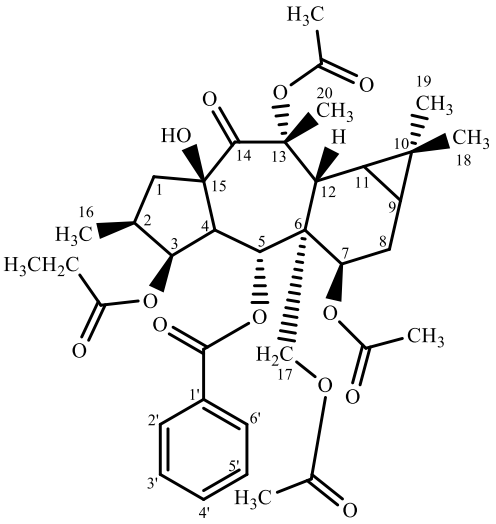

**2**

**$^1$H NMR (300 MHz, $CDCl_3$):** δ 0.71 (1H, d, *J* = 3.2 Hz, H-11), 0.73 (1H, br s, H-9), 0.84 (3H, d, *J* = 6.3 Hz, $CH_3$-16), 0.93 (3H, s, $CH_3$-18), 0.94 (3H, t, *J* = 7.5 Hz, OCOCH$_2$<u>CH$_3$</u>), 1.04 (3H, s, $CH_3$-19), 1.45 (3H, s, 7-OCO<u>CH$_3$</u>), 1.63 (1H, m, H-1β), 1.70 (3H, s, $CH_3$-20), 1.85 (1H, m, H-2), 1.86 (1H, m, H-8β), 2.1 (3H, s, 13-OCO<u>CH$_3$</u>), 2.14 (1H, m, H-8α), 2.14 (3H, s, 17-OCO<u>CH$_3$</u>), 2.26 (2H, q, *J* = 7.5 Hz, 3-OCO<u>CH$_2$</u>CH$_3$), 2.39 (1H, dd, *J* = 9.8 and 3.9 Hz, H-4), 3.14 (1H, dd, *J* = 13.5 and 7.5 Hz, H-1α), 3.5 (1H, d, *J* = 6.6 Hz, H-12), 4.29 (1H, d, *J* = 11.4 Hz, H-17β), 4.68 (1H, d, *J* = 11.4 Hz, H-17α), 4.78 (1H, d, *J* = 6.6 Hz, H-7), 5.36 (1H, t, *J* = 3.3 Hz, H-3), 6.36 (1H, d, *J* = 11.4 Hz, H-5), 7.35 (2H, t, *J* = 7.65 Hz, H-3' and H-5'), 7.49 (1H, t, *J* = 7.35 Hz, H-4') 7.86 (2H, d, *J* = 7.8 Hz, H-2' and H-6').

**$^{13}$C NMR (75.45 MHz, $CDCl_3$):** δ 42.9 (C-1), 37.3 (C-2), 78.2 (C-3), 50.3 (C-4), 69.9 (C-5), 47.8 (C-6), 70.7 (C-7), 22.1 (C-8), 18.9 (C-9), 18.4 (C-10), 23.9 (C-11), 35.1 (C-12), 85.8 (C-13), 204.4 (C-14), 84.2 (C-15), 13.9 (C-16), 62.9 (C-17), 14.9 (C-18), 29.5 (C-19), 25.0 (C-20), 173.6 (3-O<u>C</u>OCH$_2$CH$_3$), 27.6 (3-OCO<u>CH$_2$</u>CH$_3$), 8.8 (3-OCOCH$_2$<u>CH$_3$</u>), 165.2 (5-O<u>C</u>OBz), 129.9 (C-1'), 129.7 (C-2' and 6'), 128.3 (C-3' and 5'), 133.1 (C-4'), 170.8 (7-O<u>C</u>OCH$_3$), 20.6 (7-OCO<u>CH$_3$</u>), 170.8 (13-O<u>C</u>OCH$_3$), 21.5 (13-OCO<u>CH$_3$</u>), 170.3 (17-O<u>C</u>OCH$_3$), 21.4 (17-OCO<u>CH$_3$</u>).

Fraction $D_{5.2}$ was recrystallized with EtOAc/*n*-hexane yielding 180 mg of compound **7** (epoxyboetirane K).

**Epoxyboetirane K (7)** [13]

**White crystals**

**IR, $\nu_{max}$cm$^{-1}$ (KBr):** 1738, 1652

**m.p.:** 205 $^{o}$C (lit. 216-217 $^{o}$C)

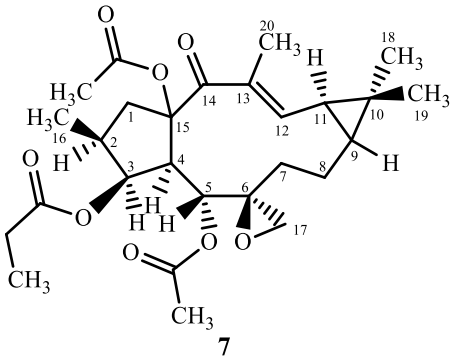

7

**$^{1}$H NMR (300 MHz, $CDCl_3$):** δ 0.83 (3H, d, *J* = 6.8 Hz, $CH_3$-16), 0.89 (1H, t, *J* = 12.8 Hz, H-7α), 1.06 (1H, m, H-9), 1.1 (3H, t, *J* = 7.6 Hz, 3-OCOCH$_2$CH$_3$), 1.18 (3H, s, $CH_3$-18), 1.18 (3H, s, $CH_3$-19), 1.46 (1H, m, H-11), 1.50 (1H, dd, *J* = 9.2 and 3.6 Hz, H-1α), 1.69 (1H, t, *J* = 6.8 Hz, H-8α), 1.82 (3H, s, $CH_3$-20), 1.87 (1H, dd, *J* = 11.0 and 3.2 Hz, H-4), 2.02 (1H, m, H-8β), 2.04 (3H, s, 5-OCO$CH_3$), 2.07 (3H, s, 15-OCO$CH_3$), 2.11 (1H, m, H-2), 2.11 (1H, m, H-7β), 2.29 (1H, m, H-17α), 2.29 (2H, d, *J* = 2.7 Hz, 3-OCO$CH_2$CH$_3$), 2.46 (1H, d, *J* = 3.6 Hz, H-17β), 3.39 (1H, dd, *J* = 11.4 and 8.4 Hz, H-1β), 5.48 (1H, t, *J* = 3.2 Hz, H-3), 6.17 (1H, d, *J* = 9.2 Hz, H-5), 6.56 (1H, d, *J* = 11.6 Hz,H-12).

**$^{13}$C NMR (75.45 MHz, $CDCl_3$):** δ 48.1 (C-1), 37.7 (C-2), 80.2 (C-3), 50.1 (C-4), 65.3 (C-5), 59.0 (C-6), 33.7 (C-7), 20.1 (C-8), 34.9 (C-9), 25.7 (C-10), 29.1 (C-11), 143.9 (C-12), 136.1 (C-13), 197.0 (C-14), 91.9 (C-15), 14.1 (C-16), 55.6 (C-17), 29.0 (C-18), 16.8 (C-19), 12.5 (C-20), 173.6 (3-O$C$OCH$_2$CH$_3$), 27.8 (3-OCO$CH_2$CH$_3$), 9.1 (3-OCOCH$_2$$CH_3$), 170.7 (5-O$C$OCH$_3$), 21.1 (5-OCO$CH_3$), 169.8 (15-O$C$OCH$_3$), 21.9 (15-OCO$CH_3$).

#### *2.1.2.3. Study of fraction $D_6$*

Fraction $D_6$ (10.42 g) was chromatographed using reverse-phase $C_{18}$ column (800 g; MeOH/H2O 7:3 to 9:1, 10% gradient). Fractions $D_{6.1}$-$D_{6.3}$ were eluted using MeOH/$H_2O$ (7:3) (Scheme 10).

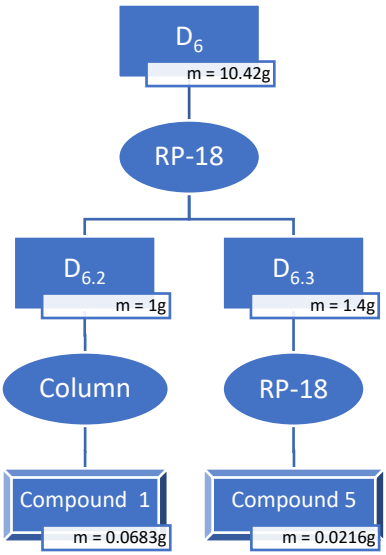


**Scheme 10** General workup of Fraction $D_6$ and isolated compounds.

Fraction $D_{6.2}$ (1 g) was chromatographed over $SiO_2$ (70 g, $CH_2Cl_2$/acetone 1:0 to 97:3, 1% gradient; $CH_2Cl_2$/acetone 19:1, 100 mL; $CH_2Cl_2$/acetone 9:1, 100 mL; EtOAc 100 mL), yielding 0.0683 g of compound **1**.

**Euphomyrsinane A (1)**

**White powder**

**IR, $\nu_{max}$cm$^{-1}$ (KBr):** 3487, 1739, 1700

**ESI-MS, *m/z*:** 657 $[M + H]^+$

**m.p.:** 235 °C

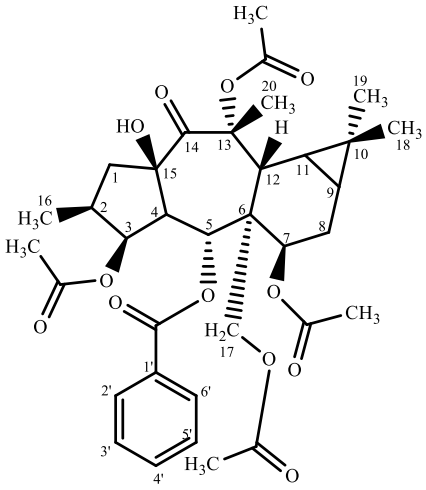

**1**

**$^1$H NMR (300 MHz, $CDCl_3$):** δ 0.72 (1H, d, *J* = 3.3 Hz, H-11), 0.74 (1H, d, *J* = 1.8 Hz, H-9), 0.87 (3H, d, *J* = 6.6 Hz, $CH_3$-16), 0.94 (3H, s, $CH_3$-18), 1.05 (3H, s, $CH_3$-19), 1.46 (3H, s, 13-OCO$\underline{CH_3}$), 1.65 (1H, s, H-1β), 1.71 (3H, s, $CH_3$-20), 1.8 (1H, m, H-8β), 1.84 (1H, m, H-2), 1.95 (3H, s, 7-OCO$\underline{CH_3}$), 2.12 (3H, s, 3-OCO$\underline{CH_3}$), 2.13 (1H, m, H-8α), 2.16 (3H, s, 17-OCO$\underline{CH_3}$), 2.39 (1H, dd, *J* = 11.6 and 3.9 Hz, H-4), 3.14 (1H, dd, *J* = 13.5 and 7.5 Hz, H-1α), 3.51 (1H, d, *J* = 6.3 Hz, H-12), 4.33 (1H, d, *J* = 11.7 Hz, H-17β), 4.71 (1H, d, *J* = 11.7 Hz,

H-17α), 4.8 (1H, d, *J* = 6.3 Hz, H-7), 5.35 (1H, t, *J* = 3.45 Hz, H-3), 6.38 (1H, d, *J* = 11.4 Hz, H-5), 7.38 (2H, t, *J* = 7.65 Hz, H-3' and H-5'), 7.51 (1H, t, *J* = 7.35 Hz, H-4'), 7.88 (2H, d, *J* = 7.8 Hz, H-2' and H-6').

**$^{13}$C NMR (75.45 MHz, $CDCl_3$):** δ 42.9 (C-1), 37.3 (C-2), 78.6 (C-3), 50.3 (C-4), 69.9 (C-5), 47.9 (C-6), 70.7 (C-7), 22.2 (C-8), 19.0 (C-9), 18.4 (C-10), 24.0 (C-11), 35.1 (C-12), 85.8 (C-13), 204.4 (C-14), 84.2 (C-15), 14.0 (C-16), 62.9 (C-17), 15.0 (C-18), 29.6 (C-19), 25.1 (C-20), 170.9 (3-O<u>C</u>O$CH_3$), 21.4 (3-OCO<u>$CH_3$</u>), 165.3 (5-O<u>C</u>OBz), 129.7 (C-1'), 129.9 (C-2' and C-6'), 128.4 (C-3' and C-5'), 133.2 (C-4'), 170.6 (7-O<u>C</u>OCH3), 21.1 (C-7-OCO<u>$CH_3$</u>), 170.9 (13-O<u>C</u>O$CH_3$), 20.6 (13-OCO<u>$CH_3$</u>), 170.4 (17-O<u>C</u>O$CH_3$), 21.5 (17-OCO<u>$CH_3$</u>).

Fraction $D_{6.3}$ (1.4 g) was chromatographed using a reverse-phase $C_{18}$ column (100 g; $CH_2Cl_2$/acetone 1:0 to 24:1, 2% gradient; $CH_2Cl_2$/acetone 19:1, 200 mL; $CH_2Cl_2$/acetone 37:3, 600 mL; $CH_2Cl_2$/acetone 9:1, 200 mL), yielding several subfractions, associated according to their TLC profile. From these, subfraction $D_{6.3.2}$ (0.0722 g) was purified by HPLC (MeOH/$H_2O$ 62:38, 3 mL/min, 254 nm) yielding 0.0216 g of compound **5**.

**Euphoboetirane A (5)**

**White powder**

**IR, $\nu_{max}$cm$^{-1}$ (KBr):** 1736, 1644, 1613, 905 (lit. 3439, 2924, 2856, 1740, 1627, 1453, 1383, 1273, 1254, 1236, 1115, 1059, 1032, 1018, 904, 713, 620, 450 cm$^{-1}$) [93]

**ESI-MS, *m/z*:** 461 $[M + H]^+$ (lit. 483 $[M + Na]^+$) [93]

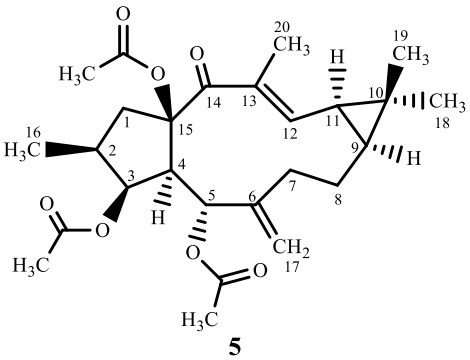


**5**

**$^{1}$H NMR (300 MHz, $CDCl_3$):** δ 0.88 (3H, d, *J* = 5.1 Hz, $CH_3$-16), 1.11 (1H, m, H-7α), 1.12 (3H, s, $CH_3$-18), 1.14 (1H, m, H-9), 1.14 (3H, s, $CH_3$-19), 1.38 (1H, dd, *J* = 8.7 and 6.3 Hz, H-11), 1.56 (1H, dd, *J* = 15.75 and 8.7 Hz, H-1α), 1.66 (3H, m, $CH_3$-20), 1.69 (1H, d, *J* = 5.1 Hz, H-8α), 1.96 (3H, s, 5-OCO<u>$CH_3$</u>), 2.02 (3H, s, 3-OCO<u>$CH_3$</u>), 2.07 (1H, s, H-8β), 2.09 (3H, s, 15-OCO<u>$CH_3$</u>), 2.20 (1H, m, H-7β), 2.24 (1H, m, H-2), 2.72 (1H, dd, *J* = 7.65 and 2.55 Hz, H-4), 3.42 (1H, dd, *J* = 12.3 and 7.8 Hz, H-1β), 4.70 (1H, s, H-17α), 4.97 (1H, s, H-17β),

5.53 (1H, t, *J* = 3.75 Hz, H-3), 6.04 (1H, d, *J* = 7.8 Hz, H-5), 6.49 (1H, dd, *J* = 11.4 and 1.2 Hz, H-12).

**$^{13}$C NMR (75.45 MHz, $CDCl_3$):** δ 48.4 (C-1), 37.3 (C-2), 80.3 (C-3), 52.3 (C-4), 65.9 (C-5), 144.5 (C-6), 35.1 (C-7), 21.7 (C-8), 35.5 (C-9), 25.4 (C-10), 28.5 (C-11), 146.9 (C-12), 134.3 (C-13), 197.0 (C-14), 92.4 (C-15), 14.2 (C-16), 115.7 (C-17), 16.9 (C-18), 29.1 (C-19), 12.6 (C-20), 170.9 (3-O<u>C</u>O$CH_3$), 21.4 (3-OCO<u>$CH_3$</u>), 170.7 (5-O<u>C</u>O$CH_3$), 21.0 (5-OCO<u>$CH_3$</u>), 170.0 (15-O<u>C</u>O$CH_3$), 22.1 (15-OCO<u>$CH_3$</u>).

### 2.1.3. Study of fraction $C_6$

Fraction $C_6$ (18.45 g) was eluted from the main column using *n*-hexane/EtOAc (7:3). This fraction was submitted to a reverse-phase chromatographic column (YMC-GEL ODS-A 12nm S-50µm AA12S50) using MeOH/$H_2O$ 1:1 to MeOH/$H_2O$ (1:0) (Table 24).

**Table 24** Column chromatography of Fraction $C_6$.

| **Solvent** | | | **Fractions** |
|---|---|---|---|
| **Volume** | MeOH/$H_2O$ | $CH_2Cl_2$ | |
| **1 L** | 1:1 | - | 1-2 |
| **1 L** | 3:2 | - | 3-4 |
| **2 L** | 7:3 | - | 5-9 |
| **1 L** | 3:1 | - | 10-12 |
| **1 L** | 4:1 | - | 13-14 |
| **1 L** | 9:1 | - | 15-17 |
| **2.25 L** | 1:0 | - | 18-20 |
| **1 L** | - | 1:0 | Clean-up |

Compound **5** (2.5 g) was obtained from fractions 6-10.

The mother liquors from fractions 8, 9 and fraction 11 were associated for further chromatographic studies. Fractions 12-14 were added for further chromatographic studies. Fraction 15 yielded 0.0182 mg of compound **4**.

**Phorboboetirane B (4)**

**Yellow oil**

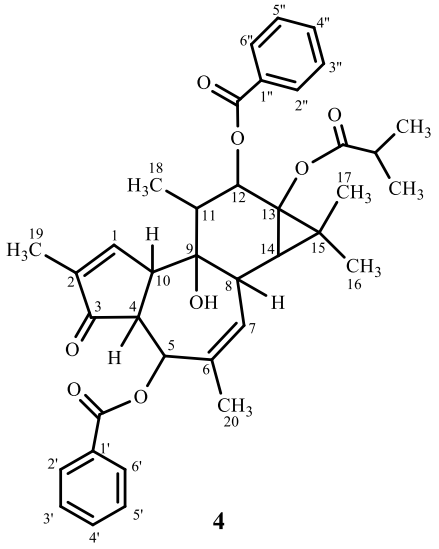

**4**

**$^{1}$H NMR (300 MHz, $CDCl_3$):** δ 1.0 (3H, d, *J* = 6.4 Hz, $CH_3$-18), 1.1 (1H, d, *J* = 1.6 Hz, H-14), 1.18 (3H, s, $CH_3$-1’’’), 1.21 (3H, d, *J* = 3.4 Hz, 2’’’), 1.23 (3H, s, H-16), 1.33 (3H, s, H-17), 1.62 (3H, dd, *J* = 2.5 and 1.3 Hz, H-19), 1.7 (1H, d, *J* = 3.1 Hz, H-11), 1.75 (3H, s, H-20), 2.46 (1H, br s, H-8), 2.63 (1H, m, 13-OCOC<u>H</u>$(CH_3)_2$), 2.81 (1H, t, *J* = 4.4 Hz, H-4), 3.81 (1H, m, H-10), 5.48 (1H, d, *J* = 4.9 Hz, H-7), 5.66 (1H, d, *J* = 9.6 Hz, H-12), 6.48 (1H, d, *J* = 3.7 Hz, H-5), 7.38 (2H, t, *J* = 7.6 Hz, H-3’ and H-5’), 7.48 (2H, m, H-3’’ and H-5’’), 7.52 (1H, t, *J* = 2.0 Hz, H-4’), 7.58 (1H, m, H-4’’), 7.72 (1H, br s, H-1), 7.84 (2H, d, *J* = 1.5 Hz, H-2’ and H-6’), 8.01 (1H, m, H-4’’).

**$^{13}$C NMR (75.45 MHz, $CDCl_3$):** δ 161.0 (C-1), 138.0 (C-2), 205.5 (C-3), 49.3 (C-4), 73.8 (C-5), 138.4 (C-6), 130.0 (C-7), 42.6 (C-8), 78.9 (C-9), 52.6 (C-10), 43.2 (C-11), 77.7 (C-12), 65.2 (C-13), 36.8 (C-14), 26.5 (C-15), 23.8 (C-16), 17.2 (C-17), 15.5 (C-18), 10.2 (C-19), 21.7 (C-20), 165.4 (5-O<u>C</u>OBz), 130.1 (C-1’ and C-1’’), 129.8 (C-2’ and C-6’), 128.4 (C-3’ and C-5’), 133.4 (C-4’), 166.1 (12-O<u>C</u>OBz), 129.8 (C-2’’ and C-6’’), 128.7 (C-3’’ and C-5’’), 133.1 (C-4’’), 179.6 (13-O<u>C</u>OCH$(CH_3)_2$), 34.4 (13-OCO<u>C</u>H$(CH_3)_2$), 18.7 (C-1’’’), 18.8 (C-2’’’).

The mother liquors from fractions 15 and 16 were associated and submitted to further chromatography column and preparative TLC, to yield compound **4** ($m_{total}$ ≈ 50 mg).

#### 2.1.3.1. Study of fraction 8-11

This fraction (2.4 g) was submitted to chromatographic column ($SiO_2$, 120 g) eluted with mixtures of *n*-hexane/$CH_2Cl_2$ of increasing polarity (Table 25).

**Table 25** Solvents used and respective fractions from column 8-11.

| Fraction | Solvent | | Weight (g) |
|---|---|---|---|
| | *n*-hexane/$CH_2Cl_2$ | $CH_2Cl_2$/Acetone | |
| **23-40** | 17:18 | - | 0.054 |
| **41-47** | 9:10 | 1:0 | 0.0613 |
| **48-97** | - | 1:0 | 0.9949 |
| **98-155** | - | 50:1 | 0.46663 |
| **156-158** | - | 50:1 | 0.0069 |
| **159-161** | - | 50:1 | 0.0084 |
| **162-163** | - | 97:3 | 0.0069 |
| **164-174** | - | 97:3 | 0.3373 |
| **175-207** | - | 97:3-3:1 | 0.0586 |
| **208-end** | - | 3:1 | 0.0702 |

Compound **5** (0.467 g) was obtained from fraction 98-155.

### 2.1.4. Study of Fraction E

Fraction E (181 g, eluted with *n*-hexane/EtOAc 9:11-1:3) was fractioned by column chromatography (1.2 Kg, $SiO_2$) and eluted with mixtures of *n*-hexane/EtOAc of increasing polarity Scheme 11). Compound **8** (methyl gallate) was obtained by recrystallization of fraction E (111-132) using EtOAc/*n*-hexane (Scheme 11).

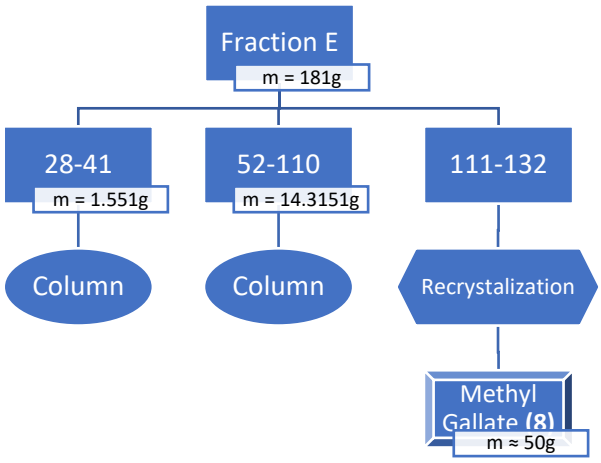


**Scheme 11** Overall workup of fraction E.

**Methyl Gallate (8)**

**White crystals**

**m.p.:** 204 ºC (lit. 201-203 ºC) [105]

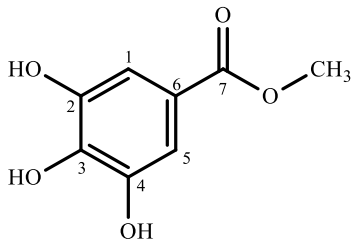


**8**

**$^{1}$H NMR (300 MHz, $CDCl_3$):** δ 3.8 (3H, s, 7-O$\underline{CH_3}$), 7.03 (2H, s, H-2 and H-6).

**$^{13}$C NMR (75.45 MHz, $CDCl_3$):** δ 120.0 (C-1), 108.6 (C-2 and C-6), 145.1 (C-3 and C-5), 138.3 (C-4), 167.6 (C-7), 50.9 (7-O$\underline{CH_3}$).

# 3. PHYTOCHEMICAL STUDY OF *Euphorbia pubescens*

## 3.1. Extraction and isolation

The air-dried powdered plant (7.5 kg) was extracted exhaustively with methanol at room temperature. Evaporation of the solvent (under vacuum, 40 °C) from the crude extract yielded a residue of 1.25 kg. This residue was resuspended in MeOH/$H_2O$ solution (1:2) and extracted with EtOAc. The ethyl acetate-soluble fraction was dried ($Na_2SO_4$) and evaporated under vacuum, yielding a residue (607 g), which was chromatographed over $SiO_2$, using mixtures of *n*-hexane/EtOAc (1:0 to 0:1) and EtOAc/MeOH (9:1 to 3:7), in increasing gradients of 5%. According to differences in composition as indicated by TLC, twelve crude fractions were obtained. Fraction 93-111 (19.15 g, eluted with *n*-hexane/EtOAc 7:3), was submitted to reverse-phase column chromatography (MeOH/$H_2O$ 1:1 to MeOH/$H_20$ 1:0). According to differences in composition as indicated by TLC, seven crude fractions were obtained (Scheme 12). The process of extraction and fractionation were both conducted by other members of our Natural Products group.


**Scheme 12** Partial workup of Fraction 93-111.

### 3.1.1. Study of fraction 60:40-70:30

This fraction (5.27 g) was submitted to column chromatography using *n*-hexane/EtOAc, starting at *n*-hexane/EtOAc 1:0 up to EtOAc/MeOH 4:1. Sub-fraction 61-72 (2.5195 g) was obtained using *n*-hexane/EtOAc 3:2 and submitted to a *combiflash*, yielding two fractions of interest: 27-29 (0.3291 g) and 30-35 (1.6647 g) that were submitted to chromatographic columns (Scheme 13).

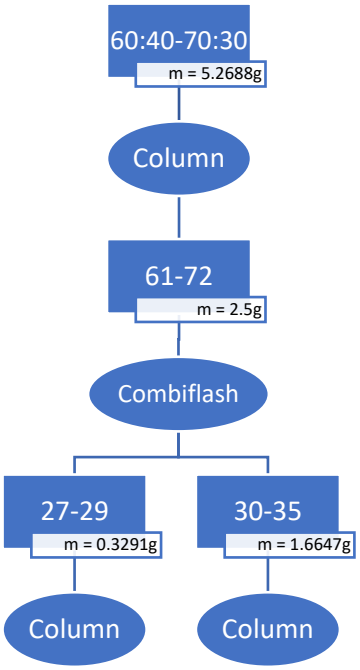


**Scheme 13** Fraction 60:40 and 70:30 - workup.

#### *3.1.1.1. Study of fraction 27-29*

Fraction 27-29 (0.3291 g) was submitted to a chromatographic column using 100 g of $SiO_2$ and eluted with mixtures of $CH_2Cl_2$/MeOH of increasing polarity to give, 11 mg of compound **10** (euphopubescenol).

**Euphopubescenol (10)**

**White amorphous powder**

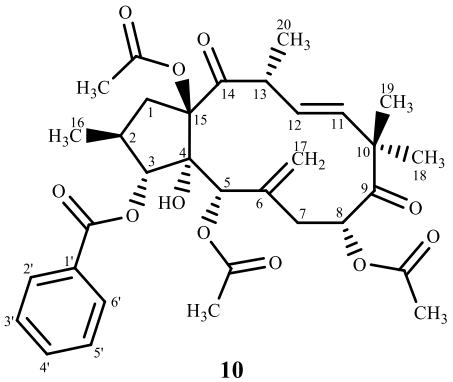

**10**

**$^{1}$H NMR (300 MHz, $CDCl_3$):** δ 1.22 (3H, s, $CH_3$-18), 1.24 (3H, d, *J* = 6.8 Hz, $CH_3$-16), 1.38 (3H, d, *J* = 6.5 Hz, $CH_3$-20), 1.46 (3H, s, $CH_3$-19), 1.71 (1H, dd, *J* = 14.9 and 9.2 Hz, H-7α), 1.91 (3H, s, 8-OCO$\underline{CH_3}$), 2.00 (1H, s, H-7β), 2.08 (3H, s, 5-OCO$\underline{CH_3}$), 2.16 (3H, s, 15-OCO$\underline{CH_3}$), 2.41 (2H, dd, *J* = 10.4 and 1.6 Hz, H-1α and H-1β), 2.91 (1H, m, H-2), 3.84 (1H, m, H-13), 4.85 (1H, s, H-17α), 4.86 (1H, s, H-5), 5.12 (1H, br s, H-17β), 5.61 (1H, d, *J* = 10.5 Hz, H-3), 5.67 (1H, d, *J* = 9.1 Hz, H-8), 5.84 (1H, s, H-12), 5.91 (1H, m, H-11), 7.43 (2H, m, H-3' and H-5'), 7.57 (1H, m, H-4'), 7.97 (2H, m, H-2' and H-6').

**$^{13}$C NMR (75.45 MHz, $CDCl_3$):** δ 38.9 (C-1), 36.9 (C-2), 77.9 (C-3), 82.9 (C-4), 73.3 (C-5), 140.2 (C-6), 36.0 (C-7), 72.4 (C-8), 208.2 (C-9), 50.7 (C-10), 136.9 (C-11), 132.8 (C-12), 46.9 (C-13), 204.6 (C-14), 94.6 (C-15), 17.8 (C-16), 116.9 (C-17), 24.6 (C-18 and C-19), 20.2 (C-20), 166.6 (3-O$\underline{C}$OBz), 129.1 (C-1'), 130.2 (C-2' and C-6'), 128.5 (C-3' and C-5'), 133.7 (C-4'), 168.4 (5-O$\underline{C}$OCH$_3$), 20.7 (5-OCO$\underline{CH_3}$), 169.9 (8-O$\underline{C}$OCH$_3$), 20.4 (8-OCO$\underline{CH_3}$), 168.9 (15-O$\underline{C}$OCH$_3$), 21.1 (15-OCO$\underline{CH_3}$).

### *3.1.1.2. Study of fraction 30-35*

Fraction 30-35 (1.66 g) was submitted to a chromatographic column ($SiO_2$, 70 g) and eluted with a mixture of $CH_2Cl_2$/acetone (1:0 to 4:1, 0.5% gradient) (Scheme 14).

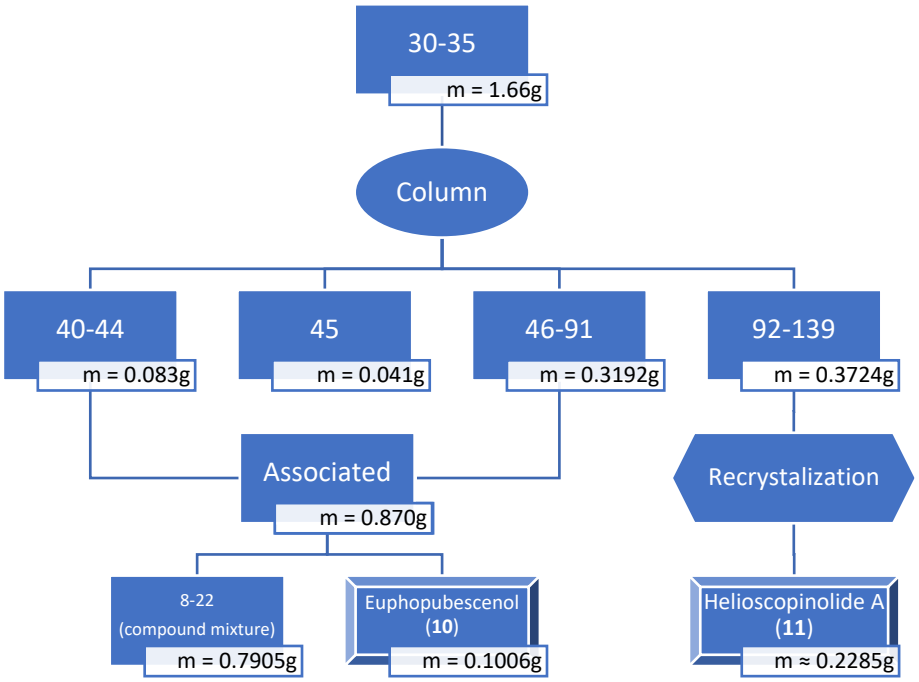


**Scheme 14** Overall workup of fraction 30-35.

Sub-fraction 45 yielded 41mg of compound **10**.

Sub-fraction 40-91 yielded another 100 mg of pure compound **10**.

Sub-fraction 92-139 recrystalized from $CH_2Cl_2$/acetone to give 229 mg of compound **11**.

**Helioscopinolide A (11)**

**White crystals**

**m.p.:** 205 ºC (lit. 208-209 ºC) [106]

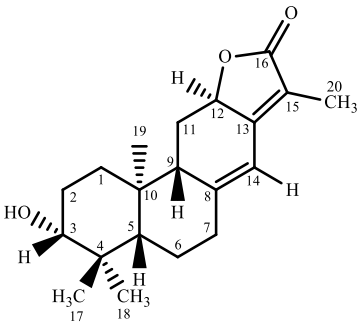

**11**

**$^1$H NMR (300 MHz, $CDCl_3$):** δ 0.81 (3H, s, $CH_3$-18), 0.92 (3H, s, $CH_3$-19), 1.02 (3H, s, $CH_3$-17), 1.14 (1H, dd, *J* = 12.5 and 2.5 Hz, H-5), 1.62 (2H, m, H-2), 1.82 (3H, d, *J* = 1.6 Hz, $CH_3$-20), 1.87 (2H, dt, *J* = 5.2 and 2.5 Hz, H-6), 1.95 (2H, dt, *J* = 13.1 and 3.6 Hz, H-1), 2.16 (1H, d, *J* = 8.9 Hz, H-9), 2.49 (2H, m, H-7), 2.53 (2H, m, H-11), 3.27 (1H, dd, *J* = 11.6 and 4.4 Hz, H-3), 4.85 (1H, ddd, *J* = 13.5 and 6.2 and 1.8 Hz, H-12), 6.27 (1H, s, H-14).

**$^{13}$C NMR (75.45 MHz, $CDCl_3$):** δ 37.5 (C-1), 27.7 (C-2), 78.7 (C-3), 39.2 (C-4), 54.5 (C-5), 23.6 (C-6), 37.1 (C-7), 151.6 (C-8), 51.7 (C-9), 41.3 (C-10), 27.7 (C-11), 76.0 (C-12), 156.2 (C-13), 114.3 (C-14), 116.6 (C-15), 175.4 (C-16), 28.8 (C-17), 15.7 (C-18), 16.8 (C-19), 8.4 (C-20).

# 4. MOLECULAR DERIVATIZATION of Methyl 3,4,5-trihydroxybenzoate (methyl gallate)

## 4.1. Methylation of methyl 3,4,5-trihydroxybenzoate

Methyl 3,4,5-trihydroxybenzoate (**8**, 2 g, 10.9 mmol) was suspended in acetone (30 mL) with dimethylsulfate ($DMSO_4$) (7 mL, 65 mmol) and $K_2CO_3$ (9 g, 65 mmol). The mixture was stirred and refluxed for 20 hours at 90 ˚C until TLC analysis ($CH_2Cl_2$/MeOH, 19:1) showed complete disappearance of the starting material. The mixture was worked up by performing a flash chromatography column using a mixture of *n*-hexane/EtOAc to afford approximately 2.4 g of methyl 3,4,5-trimethoxybenzoate (**8.1**).

**Methyl 3,4,5-trimethoxybenzoate (8.1)**

**White crystals**

**η** = 78.5 %

**m.p.** = 84 ºC

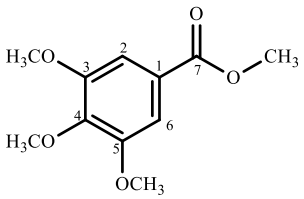


**8.1**

**$^1$H NMR (300 MHz, $CDCl_3$):** δ 3.90 (9H, s, 3-OC<u>H</u>$_3$, 4-OC<u>H</u>$_3$ and 5-OC<u>H</u>$_3$), 3.92 (3H, s, 7-OC<u>H</u>$_3$), 7.30 (2H, s, H-2 and H-6).

**$^{13}$C NMR (75.45 MHz, $CDCl_3$):** δ 126.3 (C-1), 106.8 (C-2 and C-6), 153.0 (C-3 and C-5), 142.2 (C-4), 166.9 (C-7), 56.4 (3-O<u>C</u>H$_3$ and 5-O<u>C</u>H$_3$), 61.1 (4-O<u>C</u>H$_3$), 52.4 (7-O<u>C</u>H$_3$).

## 4.2. Synthesis of 3,4,5-trimethoxybenzohydrazide

Methyl 3,4,5-trimethoxybenzoate (**8.1**, 2 g, 8.855 mmol) was suspended in ethanol (70 mL) and treated with a solution of 20 mL of 64% hydrazine hydrate (34.8 mmol). The mixture was stirred and refluxed for 24 hours at 95 ˚C until TLC analysis showed complete consumption of the starting material. The residue obtained was recrystallized from hot methanol, yielding approximately 1.8 g of 3,4,5-trimethoxybenzohydrazide (**8.2**).

**3,4,5-trimethoxybenzohydrazide (8.2)** [107]

**White crystals**

**η** = 90%

**m.p.:** 75 ºC (lit. 77-78 ºC)

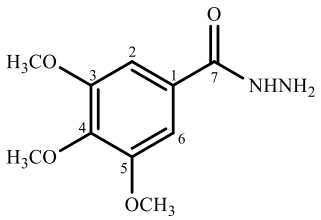


**8.2**

**$^{1}$H NMR (300 MHz, MeOD$_4$):** δ 3.81 (3H, s, 4-OC<u>H$_3$</u>), 3.89 (6H, s, 3- and 5-OC<u>H$_3$</u>), 7.15 (2H, s, H-2 and H-6).

**$^{13}$C NMR (75.45 MHz, MeOD$_4$):** δ 129.5 (C-1), 105.8 (C-2 and C-6), 154.5 (C-3 and C-5), 142.1 (C-4), 169.1 (C-7), 56.7 (3- and 5-O<u>C</u>H$_3$), 61.1 (4-O<u>C</u>H$_3$).

## 4.3. General procedure for the reaction of 3,4,5-trimethoxybenzohydrazide with aromatic aldehydes

3,4,5-trimethoxybenzohydrazide (**8.2**, 20 mg, 88 µmol) was suspended in methanol (15 mL) and treated with suitable aromatic aldehyde (0.66 mmol). The reaction mixture was stirred and refluxed for 2 hours at 75 ˚C until TLC analysis showed complete disappearance of the starting material. The residue was evaporated under vacuum, resuspended in EtOAc and purified by preparative TLC eluted with $CH_2Cl_2$/MeOH 19:1 to give compounds **8.3-8.5**.

**3,4,5-trimethoxy-N'-(4-methoxybenzylidene)benzohydrazide (8.3)**

Obtained from the reaction of compound **8.2** (20 mg, 88 µmol) with *p*-anisaldehyde (0.66 mmol). The reaction mixture was stirred for and refluxed for 2 hours at 75 ºC. The residue was purified by preparative TLC eluted with $CH_2Cl_2$/MeOH (19:1) to afford 19.1 mg (135.03 µmol, 61.74% yield of a white amorphous powder.

**White amorphous solid**

**η** = 61.74%

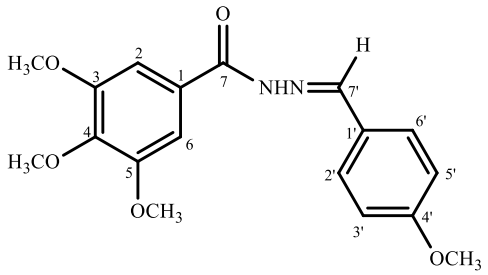

**8.3**

**$^{1}$H NMR (300 MHz, $CDCl_3$):** δ 3.77 (6H, br s, 4-OC<u>H</u>$_3$ and 4'-OC<u>H</u>$_3$), 3.86 (6H, s, 3-OC<u>H</u>$_3$ and 5-OC<u>H</u>$_3$), 6.92 (2H, d, J = 8.3 Hz, H-3' and H-5'), 7.22 (2H, s, H-2 and H-6), 7.72 (2H, d, *J* = 8.3 Hz, H-2' and H-6'), 8.25 (1H, s, H-7').

**$^{13}$C NMR (75.45 MHz, $MeOD_4$):** δ 130.6 (C-1), 106.3 (C-2 and C-6), 154.5 (C-3 and C-5), 141.8 (C-4), 163.2 (C-7), 56.8 (3- and 5-$OCH_3$), 61.2 (4-$OCH_3$), 126.6 (C-1'), 128.0 (C-2' and C-6'), 114.1 (C-3' and C-5'), 163.1 (C-4'), 150.8 (C-7'), 55.9 (4'-$OCH_3$).

**3,4,5-trimethoxy-N'-(4-nitrobenzylidene)benzohydrazide (8.4)**

Obtained from the reaction of compound **8.2** (20 mg, 88 μmol) with 4-nitrobenzaldehyde (0.66 mmol). The reaction mixture was stirred for and refluxed for 2 hours at 75ºC. The residue was purified by preparative TLC eluted with $CH_2Cl_2$/MeOH (19:1) to afford 18.3 mg (50.93 μmol, 57.61% yield) of an amorphous powder.

**Amorphous powder**

**η** = 57.61%

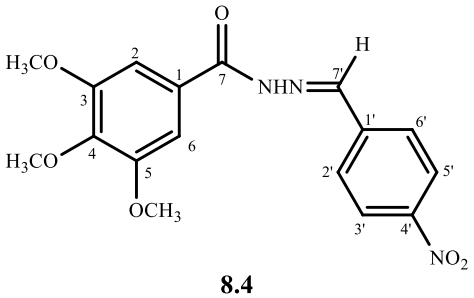

**8.4**

**$^{1}$H NMR (300 MHz, $CDCl_3$):** δ 3.77 (3H, s, 4-OC<u>H</u>$_3$), 3.86 (6H, s, 3- and 5-OC<u>H</u>$_3$), 7.25 (2H, s, H-2 and H-6), 8.01 (2H, d, *J* = 8.8 Hz, H-2' and H-6'), 8.23 (2H, d, *J* = 8.8 Hz, H-3' and H-5'), 8.40 (1H, s, H-7').

**$^{13}$C NMR (75.45 MHz, $MeOD_4$):** δ 129.5 (C-1), 106.5 (C-2 and C-6), 154.6 (C-3 and C-5), 141.6 (C-4), 164.1 (C-7), 56.9 (3- and 5-$OCH_3$), 61.3 (4-$OCH_3$), 122.7 (C-1'), 125.0 (C-2' and C-6'), 125.0 (C-3' and C-6'), 149.8 (C-4' and C-7').

**N'-(4-(dimethylamino)benzylidene)-3,4,5-trimethoxybenzohydrazide (8.5)**

Obtained from the reaction of compound **8.2** (20 mg, 88 µmol) with 4-(Dimethylamino)benzaldehyde (0.66 mmol). The reaction mixture was stirred for and refluxed for 2 hours at 75 ºC. The residue was purified by preparative TLC eluted with $CH_2Cl_2$/MeOH (19:1) to afford 14.20 mg (39.73 µmol, 44.94% yield) of a yellow amorphous powder.

**Yellow amorphous powder**

**η** = 44.94%

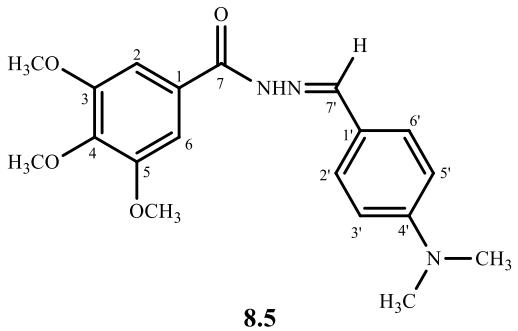


**8.5**

**$^{1}$H NMR (300 MHz, $CDCl_3$):** δ 2.83 (6H, s, N-(C<u>H</u>$_3$)$_2$), 3.75 (6H, s, 3- and 5-OC<u>H</u>$_3$), 3.78 (3H, s, 4-OC<u>H</u>$_3$), 6.42 (2H, d, *J* = 8.47 Hz, H-3' and H-5'), 7.23 (2H, s, H-2 and H-6), 7.38 (2H, d, *J* = 8.5 Hz, H-2' and H-6'), 8.28 (1H, s, H-7').

**$^{13}$C NMR (75.45 MHz, $CDCl_3$):** δ 129.3 (C-1), 104.9 (C-2 and C-6), 151.9 (C-3 and C-5), 140.9 (C-4), 164.1 (C-7), 121.3 (C-1'), 128.9 (C-2' and C-6'), 111.7 (C-3' and C-6'), 153.2 (C-4'), 150.1 (C-7'), 56.3 (3- and 5-$OCH_3$), 61.0 (4-$OCH_3$), 40.2 (4'-$N(CH_3)_2$.

# Chapter IV

## Conclusions

The main goal of this study was to search for bioactive compounds, mainly effective modulators of P-glycoprotein in resistant cancer cells using two main approaches: isolation and molecular derivatization of compounds found in high amounts. In a first stage, the phytochemical study of some fractions of *Euphorbia boetica* and *Euphorbia pubescens* (Euphorbiaceae) methanol extracts were carried out. Several terpenic and phenolic compounds were isolated, using several chromatographic techniques, namely column chromatography, preparative thin layer chromatography and high-performance liquid chromatography. The chemical structures were deduced from their physical and spectroscopic data (IR, MS, $^{1}H$ and $^{13}C$ NMR and also 2D NMR – COSY, HMQC, HMBC and NOESY experiments).

From *Euphorbia boetica* Boiss. (aerial parts), several macrocyclic diterpenes, including one new premyrsinane-type diterpene (**1**), euphomyrsinane A, and one known premyrsinane-type diterpene, premyrsinol-3-propanoate-5-benzoate-7,13,17-triacetate (**2**), two new tigliane-type diterpenes named phorboboetirane A (**3**) and phorboboetirane B (**4**), three macrocyclic lathyrane-type diterpenes, euphoboetirane A (**5**), epoxyboetirane A (**6**) and epoxyboetirane K (**7**), a phenolic compound, methyl gallate (**8**) and a cycloartane-type triterpene, 24-methylenecycloartanol (**9**), were isolated.

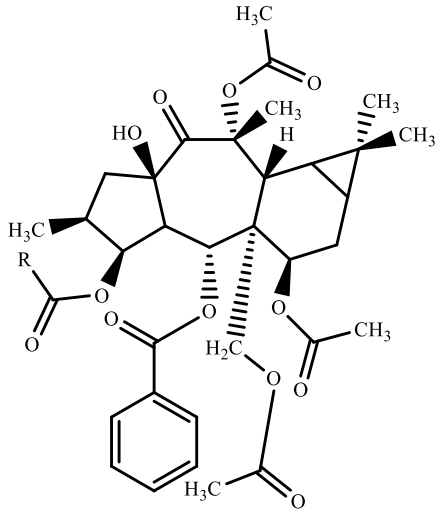

Euphomyrsinane A (**1**) R = Me

Premyrsinol-3-propanoate-5-benzoate-7,13,17-triacetate (**2**) R = Prop

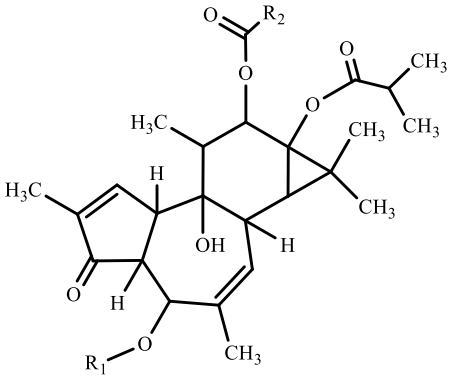

Phorboboetirane A (**3**) $R_1$ = H, $R_2$ = 2,3-dMB

Phorboboetirane B (**4**) $R_1$ = Bz, $R_2$ = Bz

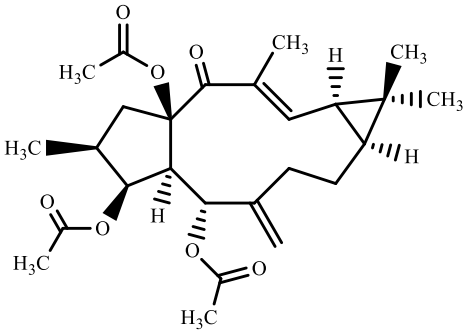

Euphoboetirane A (**5**)

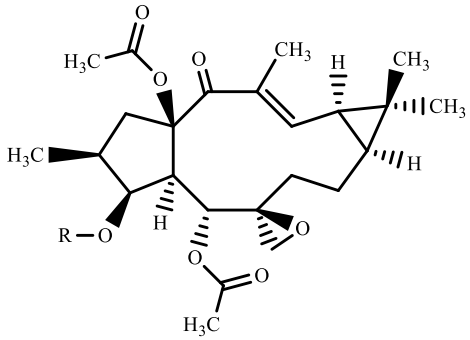

Epoxiboetirano A (**6**) R = Ac

Epoxyboetirane K (**7**) R = Prop

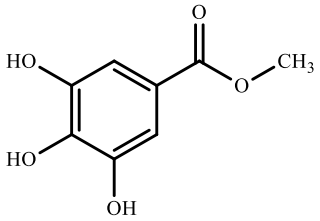

Methyl Gallate (**8**)

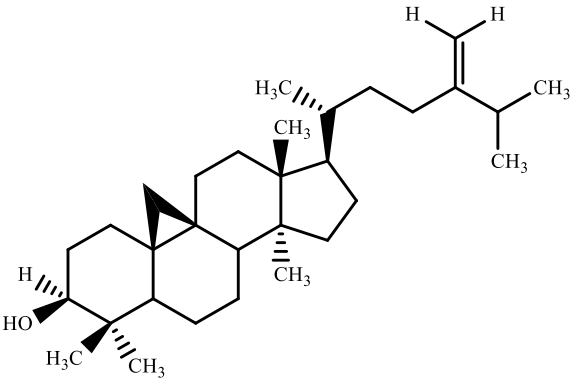

24-methylenecycloartanol (**9**)

Reporting to the various compounds, between family members, their chemical structures were very similar, differing only in unique acylation patterns. Compounds **1** and **2** had different acylation patterns at C-3, while compounds **3** and **4** had different acylation patterns at C-5 and C-12. On the other hand, compounds **5, 6** and **7**, not only had different acylation patterns at C-3 but also at C-6. Compound **5** has an exocyclic double bond at C-6/C-17, while compounds **6** and **7** have an epoxy group at the same location. Other compounds, such as methyl gallate (**8**), which was obtained in large quantities, was methylated and, after reaction with hydrazine, condensed with several aromatic aldehydes affording three derivatives.

From *Euphorbia pubescens* Vahl (aerial parts), one macrocyclic jatrophane diterpene polyester, euphopubescenol (**10**) and a diterpenic lactone, helioscopinolide A (**11**), were isolated.

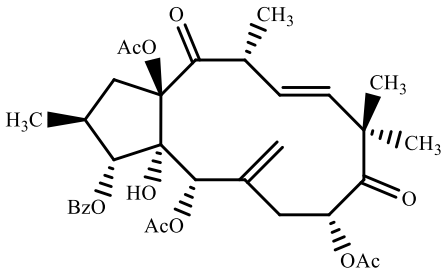


Euphopubescenol (**10**)

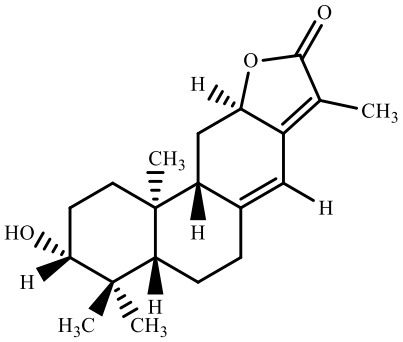


Helioscopinolide A (**11**)

As mentioned above, methyl gallate (**8**) was isolated in large amounts. Therefore, a small set of derivatives was developed through molecular derivatization, taking advantage of its simple structure and chemical reactivity. At first, methyl gallate was methylated, using dimethylsulfate, yielding methyl 3,4,5-trimethoxybenzoate (**8.1**), which was used in a reaction with hydrazine to yield the carbohydrazide, 3,4,5-trimethoxybenzohydrazide (**8.2**). The carbohydrazide was then condensed with several aromatic aldehydes, yielding three derivatives bearing an imine moiety (compounds **8.3**-**8.5**).

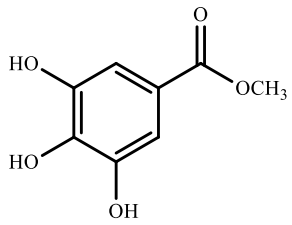


**8**

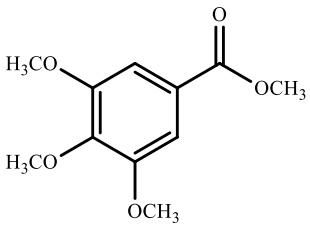


**8.1**

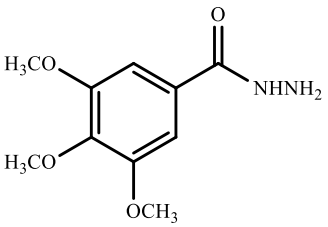


**8.2**

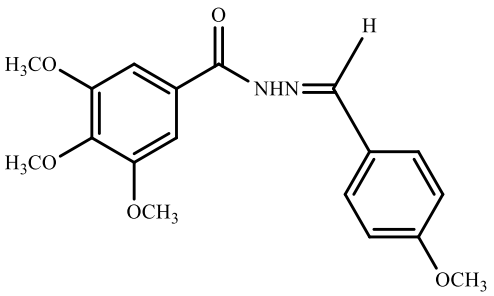


**8.3**

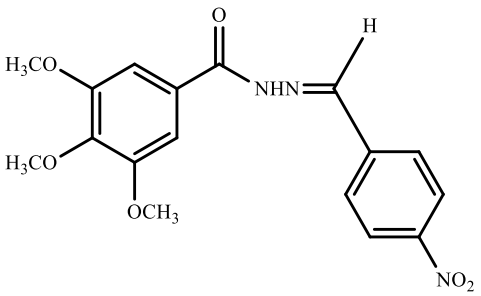


**8.4**

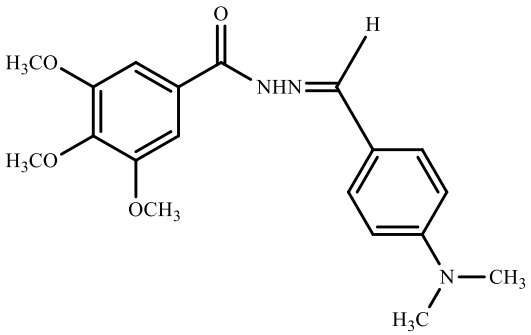


**8.5**

Widely used in traditional medicine to treat warts, skin ulcers and tumours, *Euphorbia* species have been a source of many bioactive compounds. Among these compounds synthesized by *Euphorbia* plants, a wide variety of unique macrocyclic diterpene polyesters have shown promising activity when it comes to multidrug resistance reversal in cancer cells, according to other authors.

This work represents a contribution, not only for the phytochemical studies of *Euphorbia boetica* and *Euphorbia pubescens*, but also corroborates the importance of further research of this genus in order to find new and effective anti-tumour lead compounds.

The isolated compounds and those obtained by derivatization will be evaluated for their ability as P-gp modulators on P-gp-overexpressing cancer cells.

# References

1. Ernst M, Saslis-Lagoudakis CH, Grace OM, Nilsson N, Simonsen HT, Horn JW, et al. Evolutionary prediction of medicinal properties in the genus *Euphorbia* L. Sci Rep. 2016;6:30531.

2. Kinghorn AD, Pan L, Fletcher JN, Chai H. The relevance of higher plants in lead compound discovery programs. J Nat Prod. 2011;74(6):1539-55.

3. Sarker SD, Nahar L. An introduction to natural products isolation. Methods Mol Biol. 2012;864:1-25.

4. Webster GL. Plant dermatitis. Irritant plants in the spurge family (Euphorbiaceae). Clin Dermatol. 1986;4(2):36-45.

5. Vasas A, Hohmann J. *Euphorbia* diterpenes: isolation, structure, biological activity, and synthesis (2008-2012). Chem Rev. 2014;114(17):8579-612.

6. Horn JW, van Ee BW, Morawetz JJ, Riina R, Steinmann VW, Berry PE, et al. Phylogenetics and the evolution of major structural characters in the giant genus *Euphorbia* L. (Euphorbiaceae). Mol Phylogenet Evol. 2012;63(2):305-26.

7. Appendino G, Szallasi A. Euphorbium: modern research on its active principle, resiniferatoxin, revives an ancient medicine. Life Sci. 1997;60(10):681-96.

8. Shi QW, Su XH, Kiyota H. Chemical and pharmacological research of the plants in genus *Euphorbia*. Chem Rev. 2008;108(10):4295-327.

9. Kumar S, Malhotra R, Kumar D. *Euphorbia hirta*: Its chemistry, traditional and medicinal uses, and pharmacological activities. Pharmacogn Rev. 2010;4(7):58-61.

10. Liu Y, Murakami N, Ji H, Abreu P, Zhang S. Antimalarial Flavonol Glycosides from *Euphorbia hirta*. Pharmaceutical Biology. 2007;45(4):278-81.

11. Munro B, Vuong QV, Chalmers AC, Goldsmith CD, Bowyer MC, Scarlett CJ. Phytochemical, Antioxidant and Anti-Cancer Properties of *Euphorbia tirucalli* Methanolic and Aqueous Extracts. Antioxidants (Basel). 2015;4(4):647-61.

12. Ashraf A, Sarfraz RA, Rashid MA, Shahid M. Antioxidant, antimicrobial, antitumor, and cytotoxic activities of an important medicinal plant (*Euphorbia royleana*) from Pakistan. journal of food and drug analysis. 2015;23(1):109-15.

13. Vieira C, Duarte N, Reis MA, Spengler G, Madureira AM, Molnar J, et al. Improving the MDR reversal activity of 6,17-epoxylathyrane diterpenes. Bioorg Med Chem. 2014;22(22):6392-400.

14. Reis MA, Paterna A, Ferreira RJ, Lage H, Ferreira MJ. Macrocyclic diterpenes resensitizing multidrug resistant phenotypes. Bioorg Med Chem. 2014;22(14):3696-702.

15. Ferreira M-JU, Ascenso JR. Steroids and a tetracyclic diterpene from *Euphorbia boetica*. Phytochemistry. 1999;51(3):439-44.

16. Narbona E, Arista M, Ortiz PL, editors. Seed germination ecology of the perennial *Euphorbia boetica*, an endemic spurge of the southern Iberian Peninsula. Annales Botanici Fennici; 2007: JSTOR.

17. Valente C, Ferreira MJ, Abreu PM, Pedro M, Cerqueira F, Nascimento MS. Three new jatrophane-type diterpenes from *Euphorbia pubescens*. Planta medica. 2003;69(4):361-6.

18. Mateos M, Valdés B, Valdés B. Catálogo de la flora vascular del Rif occidental calizo (N de Marueccos). II Caesalpiniaceae-Compositae. Lagascalia. 2010;30(1):47-304.

19. asturnatura.com. "*Euphorbia hirsuta* L.". In: Asturnatura.com, editor. Revista asturnaturacom2016.

20. Roberts SC. Production and engineering of terpenoids in plant cell culture. Nat Chem Biol. 2007;3(7):387-95.

21. Singh B, Sharma RA. Plant terpenes: defense responses, phylogenetic analysis, regulation and clinical applications. 3 Biotech. 2015;5(2):129-51.

22. Wang G, Tang W, Bidigare RR. Terpenoids as therapeutic drugs and pharmaceutical agents. Natural products: Springer; 2005. p. 197-227.

23. Bohlmann J, Meyer-Gauen G, Croteau R. Plant terpenoid synthases: molecular biology and phylogenetic analysis. Proceedings of the National Academy of Sciences. 1998;95(8):4126-33.

24. Tholl D. Biosynthesis and biological functions of terpenoids in plants. Biotechnology of Isoprenoids: Springer; 2015. p. 63-106.

25. Miziorko HM. Enzymes of the mevalonate pathway of isoprenoid biosynthesis. Arch Biochem Biophys. 2011;505(2):131-43.

26. Hunter WN. The non-mevalonate pathway of isoprenoid precursor biosynthesis. J Biol Chem. 2007;282(30):21573-7.

27. Eisenreich W, Bacher A, Arigoni D, Rohdich F. Biosynthesis of isoprenoids via the non-mevalonate pathway. Cell Mol Life Sci. 2004;61(12):1401-26.

28. Lombard J, Moreira D. Origins and early evolution of the mevalonate pathway of isoprenoid biosynthesis in the three domains of life. Mol Biol Evol. 2011;28(1):87-99.

29. Peters RJ. Two rings in them all: the labdane-related diterpenoids. Nat Prod Rep. 2010;27(11):1521-30.

30. Garcia PA, de Oliveira AB, Batista R. Occurrence, biological activities and synthesis of kaurane diterpenes and their glycosides. Molecules. 2007;12(3):455-83.

31. Ghanadian M, Choudhary MI, Ayatollahi AM, Mesaik MA, Abdalla OM, Afsharypour S. New cyclomyrsinol diterpenes from *Euphorbia aellenii* with their immunomodulatory effects. Journal of Asian Natural Products Research. 2013;15(1):22-9.

32. Ghanadian SM, Ayatollahi AM, Afsharypuor S, Javanmard SH, Dana N. New mirsinane-type diterpenes from *Euphorbia microsciadia* Boiss. with inhibitory effect on VEGF-induced angiogenesis. Journal of natural medicines. 2013;67(2):327-32.

33. Zhang Z-X, Qi F-M, Li H-H, Dong L-L, Hai Y, Fan G-X, et al. A New Lathyrane Diterpenoid from the Whole Plant of *Euphorbia altotibetica*. Notes. 2014;35(2):641.

34. Liu C, Liao ZX, Liu SJ, Qu YB, Wang HS. Two new diterpene derivatives from *Euphorbia lunulata* Bge and their anti-proliferative activities. Fitoterapia. 2014;96:33-8.

35. Tian Y, Guo Q, Xu W, Zhu C, Yang Y, Shi J. A minor diterpenoid with a new 6/5/7/3 fused-ring skeleton from *Euphorbia micractina*. Org Lett. 2014;16(15):3950-3.

36. Wang L, Ma Y-T, Sun Q-Y, Zang Z, Yang F-M, Liu J-P, et al. A New Lathyrane Diterpenoid Ester from *Euphorbia Dracunculoides*. Chemistry of Natural Compounds. 2016;52(6):1037-40.

37. Shadi S, Saeidi H, Ghanadian M, Rahimnejad MR, Aghaei M, Ayatollahi SM, et al. New macrocyclic diterpenes from *Euphorbia connata* Boiss. with cytotoxic activities on human breast cancer cell lines. Natural Product Research. 2015;29(7):607-14.

38. Kúsz N, Orvos P, Csorba A, Tálosi L, Chaieb M, Hohmann J, et al. Jatrophane diterpenes from *Euphorbia guyoniana* are new potent inhibitors of atrial GIRK channels. Tetrahedron. 2016;72(37):5724-8.

39. Lanzotti V, Barile E, Scambia G, Ferlini C. Cyparissins A and B, jatrophane diterpenes from *Euphorbia cyparissias* as Pgp inhibitors and cytotoxic agents against ovarian cancer cell lines. Fitoterapia. 2015;104:75-9.

40. Liu T, Liang Q, Xiong N-N, Dai L-F, Wang J-M, Ji X-H, et al. A new ent-kaurane diterpene from *Euphorbia stracheyi* Boiss. Natural Product Research. 2017;31(2):233-8.

41. Yuan W-J, Yang G-P, Zhang J-H, Zhang Y, Chen D-Z, Li S-L, et al. Three new diterpenes with cytotoxic activity from the roots of *Euphorbia ebracteolata* Hayata. Phytochemistry Letters. 2016;18:176-9.

42. Fei D-Q, Dong L-L, Qi F-M, Fan G-X, Li H-H, Li Z-Y, et al. Euphorikanin A, a Diterpenoid Lactone with a Fused 5/6/7/3 Ring System from *Euphorbia kansui*. Organic letters. 2016;18(12):2844-7.

43. Gao J, Chen Q-B, Liu Y-Q, Xin X-L, Yili A, Aisa HA. Diterpenoid constituents of *Euphorbia macrorrhiza*. Phytochemistry. 2016;122:246-53.

44. Wang M, Wang Q, Wei Q, Li J, Guo C, Yang B, et al. Two new ent-atisanes from the root of *Euphorbia fischeriana* Steud. Natural product research. 2016;30(2):144-9.

45. Reis MA, André Vn, Duarte MT, Lage H, Ferreira M-JU. 12, 17-cyclojatrophane and jatrophane constituents of *Euphorbia welwitschii*. Journal of natural products. 2015;78(11):2684-90.

46. Ghanadian M, Saeidi H, Aghaei M, Rahiminejad MR, Ahmadi E, Ayatollahi SM, et al. New jatrophane diterpenes from *Euphorbia osyridea* with proapoptotic effects on ovarian cancer cells. Phytochemistry Letters. 2015;12:302-7.

47. Aichour S, Haba H, Benkhaled M, Harakat D, Lavaud C. Terpenoids and other constituents from *Euphorbia bupleuroides*. Phytochemistry Letters. 2014;10:198-203.

48. Rawal MK, Shokoohinia Y, Chianese G, Zolfaghari B, Appendino G, Taglialatela-Scafati O, et al. Jatrophanes from *Euphorbia squamosa* as potent inhibitors of Candida albicans multidrug transporters. Journal of natural products. 2014;77(12):2700-6.

49. Reis MA, Paterna A, Mónico A, Molnar J, Lage H, Ferreira M-JU. Diterpenes from *Euphorbia piscatoria*: synergistic interaction of Lathyranes with doxorubicin on resistant cancer cells. Planta medica. 2014;80(18):1739-45.

50. Chen R, You C-X, Wang Y, Zhang W-J, Yang K, Geng Z-F, et al. Chemical constituents from the roots of *Euphorbia nematocypha* Hand.-Mazz. Biochemical Systematics and Ecology. 2014;57:1-5.

51. Yang D-S, Peng W-B, Li Z-L, Wang X, Wei J-G, He Q-X, et al. Chemical constituents from *Euphorbia stracheyi* and their biological activities. Fitoterapia. 2014;97:211-8.

52. Nothias-Scaglia L-F, Retailleau P, Paolini J, Pannecouque C, Neyts J, Dumontet V, et al. Jatrophane diterpenes as inhibitors of Chikungunya virus replication: structure–activity relationship and discovery of a potent lead. Journal of natural products. 2014;77(6):1505-12.

53. Chen H, Wang H, Yang B, Jin D-Q, Yang S, Wang M, et al. Diterpenes inhibiting NO production from *Euphorbia helioscopia*. Fitoterapia. 2014;95:133-8.

54. Zarei SM, Ayatollahi AM, Ghanadian M, Aghaei M, Choudhary MI, Fallahian F. Unusual ingenoids from *Euphorbia erythradenia* Bioss. with pro-apoptotic effects. Fitoterapia. 2013;91:87-94.

55. Zhang BB, Jiang Q, Liao ZX, Liu C, Liu SJ, Ji LJ, et al. Norlathyrane Diterpenes from the Root of *Euphorbia kansuensis*. Chemistry & biodiversity. 2013;10(10):1887-93.

56. Xu J, Yang B, Fang L, Wang S, Guo Y, Yamakuni T, et al. Four new myrsinol diterpenes from *Euphorbia prolifera*. Journal of natural medicines. 2013;67(2):333-8.

57. Yang D-S, Zhang Y-L, Peng W-B, Wang L-Y, Li Z-L, Wang X, et al. Jatropholane-type diterpenes from *Euphorbia sikkimensis*. Journal of natural products. 2013;76(2):265-9.

58. Ghanadian SM, Ayatollahi AM, Mesaik MA, Abdalla OM. New immunosuppressive cyclomyrsinol diterpenes from *Euphorbia kopetdaghi* Prokh. Natural product research. 2013;27(3):246-54.

59. Abdel-Monem AR, Abdelrahman EH. New abietane diterpenes from *Euphorbia pseudocactus* berger (Euphorbiaceae) and their antimicrobial activity. Pharmacognosy magazine. 2016;12(Suppl 3):S346.

60. Tian Y, Xu W, Zhu C, Lin S, Guo Y, Shi J. Diterpenoids with diverse skeletons from the roots of *Euphorbia micractina*. Journal of natural products. 2013;76(6):1039-46.

61. Qi W-Y, Zhang W-Y, Shen Y, Leng Y, Gao K, Yue J-M. Ingol-Type Diterpenes from *Euphorbia antiquorum* with Mouse 11β-Hydroxysteroid Dehydrogenase Type 1 Inhibition Activity. Journal of natural products. 2014;77(6):1452-8.

62. Wang S, Liang H, Zhao Y, Wang G, Yao H, Kasimu R, et al. New triterpenoids from the latex of *Euphorbia resinifera* Berg. Fitoterapia. 2016;108:33-40.

63. Giner J-L, Schroeder TN. Polygonifoliol, a New Tirucallane Triterpene from the Latex of the Seaside Sandmat *Euphorbia polygonifolia*. Chemistry & Biodiversity. 2015;12(7):1126-9.

64. Kuang X, Li W, Kanno Y, Mochizuki M, Inouye Y, Koike K. Cycloartane-type triterpenes from *Euphorbia fischeriana* stimulate human CYP3A4 promoter activity. Bioorg Med Chem Lett. 2014;24(23):5423-7.

65. World Health Organization (WHO). Fact Sheet nº 297 [updated February 2017. Available from: http://www.who.int/mediacentre/factsheets/fs297/en/.

66. Saraswathy M, Gong S. Different strategies to overcome multidrug resistance in cancer. Biotechnology advances. 2013;31(8):1397-407.

67. Sausville EA, Longo DL. Principles of Cancer Therapy. Harrison's Principles Of Internal Medicine. 18th ed: McGraw-Hill Professional; 2011. p. 689-711.

68. Mercado-Lubo R, McCormick BA. Can a nanoparticle that mimics Salmonella effectively combat tumor chemotherapy resistance? Nanomedicine. 2017;12(7):705-10.

69. Sharom FJ. Complex interplay between the P-glycoprotein multidrug efflux pump and the membrane: its role in modulating protein function. Frontiers in oncology. 2014;4.

70. Gottesman MM. Mechanisms of cancer drug resistance. Annual review of medicine. 2002;53(1):615-27.

71. Zhang C, Zhai S, Li X, Zhang Q, Wu L, Liu Y, et al. Synergistic action by multi-targeting compounds produces a potent compound combination for human NSCLC both in vitro and in vivo. Cell death & disease. 2014;5(3):e1138.

72. Gottesman MM, Ludwig J, Xia D, Szakacs G. Defeating drug resistance in cancer. Discovery medicine. 2009;6(31):18-23.

73. Becker J-P, Depret G, Van Bambeke F, Tulkens PM, Prévost M. Molecular models of human P-glycoprotein in two different catalytic states. BMC structural biology. 2009;9(1):3.

74. Damas JM, Oliveira ASF, Baptista AM, Soares CM. Structural consequences of ATP hydrolysis on the ABC transporter NBD dimer: molecular dynamics studies of HlyB. Protein Science. 2011;20(7):1220-30.

75. Srivalli KMR, Lakshmi P. Overview of P-glycoprotein inhibitors: a rational outlook. Brazilian Journal of Pharmaceutical Sciences. 2012;48(3):353-67.

76. Bansal T, Jaggi M, Khar R, Talegaonkar S. Emerging significance of flavonoids as P-glycoprotein inhibitors in cancer chemotherapy. Journal of Pharmacy & Pharmaceutical Sciences. 2009;12(1):46-78.

77. Locher KP. Mechanistic diversity in ATP-binding cassette (ABC) transporters. Nature structural & molecular biology. 2016;23(6):487-93.

78. O'Mara ML, Mark AE. Structural characterization of two metastable ATP-bound states of P-glycoprotein. PLoS One. 2014;9(3):e91916.

79. Hodges LM, Markova SM, Chinn LW, Gow JM, Kroetz DL, Klein TE, et al. Very important pharmacogene summary: ABCB1 (MDR1, P-glycoprotein). Pharmacogenet Genomics. 2011;21(3):152-61.

80. Ambudkar SV, Kimchi-Sarfaty C, Sauna ZE, Gottesman MM. P-glycoprotein: from genomics to mechanism. Oncogene. 2003;22(47):7468-85.

81. Fung KL, Gottesman MM. A synonymous polymorphism in a common MDR1 (ABCB1) haplotype shapes protein function. Biochim Biophys Acta. 2009;1794(5):860-71.

82. Lopez D, Martinez-Luis S. Marine natural products with P-glycoprotein inhibitor properties. Mar Drugs. 2014;12(1):525-46.

83. Gonzalez ML, Vera DMA, Laiolo J, Joray MB, Maccioni M, Palacios SM, et al. Mechanism Underlying the Reversal of Drug Resistance in P-Glycoprotein-Expressing Leukemia Cells by Pinoresinol and the Study of a Derivative. Front Pharmacol. 2017;8:205.

84. Basha Syed S, Selvaraj Coumar M. P-glycoprotein mediated multidrug resistance reversal by phytochemicals: a review of SAR & future perspective for drug design. Current topics in medicinal chemistry. 2016;16(22):2484-508.

85. Vasas A, Forgo P, Orvos P, Tálosi L, Csorba A, Pinke G, et al. Myrsinane, Premyrsinane, and Cyclomyrsinane Diterpenes from *Euphorbia falcata* as Potassium Ion Channel Inhibitors with Selective G Protein-Activated Inwardly Rectifying Ion Channel (GIRK) Blocking Effects. Journal of Natural Products. 2016;79(8):1990-2004.

86. Appendino G, Belloro E, Tron GC, Jakupovic J, Ballero M. Diterpenoids from *euphorbia pithyusa* subsp. cupanii. J Nat Prod. 1999;62(10):1399-404.

87. Marco JA, Sanz-Cervera JF, Checa J, Palomares E, Fraga BM. Jatrophane and tigliane diterpenes from the latex of *Euphorbia obtusifolia*. Phytochemistry. 1999;52(3):479-85.

88. Appendino G, Jakupovic S, Tron GC, Jakupovic J, Milon V, Ballero M. Macrocyclic diterpenoids from *Euphorbia semiperfoliata*. J Nat Prod. 1998;61(6):749-56.

89. Ayatollahi AM, Ghanadian M, Mesaik MA, Mohamed Abdella O, Afsharypuor S, Kobarfard F, et al. New myrsinane-type diterpenoids from *Euphorbia aellenii* Rech. f. with their immunomodulatory activity. J Asian Nat Prod Res. 2010;12(12):1020-5.

90. Ren FX, Ren FZ, Yang Y, Yu NJ, Zhang Y, Zhao YM. Tigliane diterpene esters from the leaves of *Croton tiglium*. Helvetica Chimica Acta. 2014;97(7):1014-9.

91. Haba H, Lavaud C, Harkat H, Magid AA, Marcourt L, Benkhaled M. Diterpenoids and triterpenoids from *Euphorbia guyoniana*. Phytochemistry. 2007;68(9):1255-60.

92. Dagang W, Sorg B, Hecker E. Oligo-and macrocyclic diterpenes in thymelaeaceae and Euphorbiaceae occurring and utilized in Yunnan (Southwest China). 6. Tigliane type diterpene esters from latex of *Euphorbia prolifera*. Phytotherapy Research. 1994;8(2):95-9.

93. Lu J, Li G, Huang J, Zhang C, Zhang L, Zhang K, et al. Lathyrane-type diterpenoids from the seeds of *Euphorbia lathyris*. Phytochemistry. 2014;104:79-88.

94. Yazdiniapour Z, Ghanadian M, Zolfaghari B, Lanzotti V. 6(17)-Epoxylathyrane diterpenes from *Euphorbia sogdiana* Popov with cytotoxic activity. Fitoterapia. 2016;108:87-92.

95. Sanchez E, Heredia N, Camacho-Corona Mdel R, Garcia S. Isolation, characterization and mode of antimicrobial action against Vibrio cholerae of methyl gallate isolated from *Acacia farnesiana*. J Appl Microbiol. 2013;115(6):1307-16.

96. Kamatham S, Kumar N, Gudipalli P. Isolation and characterization of gallic acid and methyl gallate from the seed coats of *Givotia rottleriformis* Griff. and their anti-proliferative effect on human epidermoid carcinoma A431 cells. Toxicology Reports. 2015;2:520-9.

97. De PT, Urones J, Marcos I, Basabe P, Cuadrado MS, Moro RF. Triterpenes from *Euphorbia broteri*. Phytochemistry. 1987;26(6):1767-76.

98. Valente C, Pedro M, Ascenso JR, Abreu PM, Nascimento MS, Ferreira MJ. Euphopubescenol and euphopubescene, two new jatrophane polyesters, and lathyrane-type diterpenes from *Euphorbia pubescens*. Planta medica. 2004;70(3):244-9.

99. Borghi D, Baumer L, Ballabio M, Arlandini E, Perellino NC, Minghetti A, et al. Structure elucidation of helioscopinolides D and E from *Euphorbia calyptrata* cell cultures. Journal of Natural Products. 1991;54(6):1503-8.

100. Kasture VS, Katti SA, Mahajan D, Wagh R, Mohan M, Kasture SB. Antioxidant and antiparkinson activity of gallic acid derivatives. Pharmacol Online. 2009;1:385-95.

101. Kane CJ, Menna JH, Yeh Y-C. Methyl gallate, methyl-3, 4, 5-trihydroxy-benzoate, is a potent and highly specific inhibitor of herpes simplex virusin vitro. I. Purification and characterization of methyl gallate fromSapium sebiferum. Bioscience reports. 1988;8(1):85-94.

102. Maximo da Silva M, Comin M, Santos Duarte T, Foglio MA, de Carvalho JE, do Carmo Vieira M, et al. Synthesis, Antiproliferative Activity and Molecular Properties Predictions of Galloyl Derivatives. Molecules. 2015;20(4):5360-73.

103. Borchhardt DM, Mascarello A, Chiaradia LD, Nunes RJ, Oliva G, Yunes RA, et al. Biochemical evaluation of a series of synthetic chalcone and hydrazide derivatives as novel inhibitors of cruzain from Trypanosoma cruzi. Journal of the Brazilian Chemical Society. 2010;21(1):142-50.

104. 24-Methylenecycloartanol. In: Azimova SS, editor. Natural Compounds: Cycloartane Triterpenoids and Glycosides. New York, NY: Springer New York; 2013. p. 138-.

105. Sánchez E, Heredia N, Camacho-Corona MdR, García S. Isolation, characterization and mode of antimicrobial action against Vibrio cholerae of methyl gallate isolated from *Acacia farnesiana*. Journal of applied microbiology. 2013;115(6):1307-16.

106. Shizuri Y, Kosemura S, Yamamura S, Ohba S, Ito M, Saito Y. Isolation and structures of helioscopinolides, new diterpenes from *Euphorbia helioscopia* L. Chemistry Letters. 1983;12(1):65-8.

107. Chida AS, Vani PVSN, Chandrasekharam M, Srinivasan R, Singh AK. Synthesis of 2,3-dimethoxy-5-methyl-1,4-benzoquinone: A key fragment in Coenzyme-Q series*. Synthetic Communications. 2001;31(5):657-60.